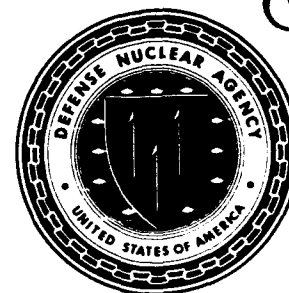


AD-A251 090



Defense Nuclear Agency
Alexandria, VA 22310-3398



DNA-TR-91-189

Theoretical Study of the Radiative and Kinetic Properties of Selected Metal Oxides and Air Molecules

H. Harvey Michels
United Technologies Research Center
400 Main Street
East Hartford, CT 06108

May 1992



Technical Report

CONTRACT No. DNA 001-88-C-0032

Approved for public release;
distribution is unlimited.

92-14638

92 0 03 050

Destroy this report when it is no longer needed. Do not return to sender.

PLEASE NOTIFY THE DEFENSE NUCLEAR AGENCY,
ATTN: CSTI, 6801 TELEGRAPH ROAD, ALEXANDRIA, VA
22310-3398, IF YOUR ADDRESS IS INCORRECT, IF YOU
WISH IT DELETED FROM THE DISTRIBUTION LIST, OR
IF THE ADDRESSEE IS NO LONGER EMPLOYED BY YOUR
ORGANIZATION.



DISTRIBUTION LIST UPDATE

This mailer is provided to enable DNA to maintain current distribution lists for reports. (We would appreciate your providing the requested information.)

- ☐ Add the individual listed to your distribution list.
- ☐ Delete the cited organization/individual.
- ☐ Change of address.

NOTE:

Please return the mailing label from the document so that any additions, changes, corrections or deletions can be made easily.

NAME: _____

ORGANIZATION: _____

OLD ADDRESS

CURRENT ADDRESS

TELEPHONE NUMBER: () _____

DNA PUBLICATION NUMBER/TITLE

CHANGES/DELETIONS/ADDITIONS, etc.) (Attach Sheet if more Space is Required)

DNA OR OTHER GOVERNMENT CONTRACT NUMBER: _____

CERTIFICATION OF NEED-TO-KNOW BY GOVERNMENT SPONSOR (if other than DNA):

SPONSORING ORGANIZATION: _____

CONTRACTING OFFICER OR REPRESENTATIVE: _____

SIGNATURE: _____

CUT HERE AND RETURN

DEFENSE NUCLEAR AGENCY
ATTN: TITL
6801 TELEGRAPH ROAD
ALEXANDRIA, VA 22310-3398

DEFENSE NUCLEAR AGENCY
ATTN: TITL
6801 TELEGRAPH ROAD
ALEXANDRIA, VA 22310-3398

REPORT DOCUMENTATION PAGE			Form Approved OMB No. 0704-0188	
Public reporting burden for this collection of information is estimated to average 1 hour per response, including the time for reviewing instructions, searching existing data sources, gathering and maintaining the data needed, and reviewing the collection of information. Send comments regarding this burden estimate or any other aspect of this collection of information, including suggestions for reducing this burden, to Washington Headquarters Services, Directorate for Information Operations and Reports, 1215 Jefferson Davis Highway, Suite 1204, Arlington, VA 22202-4302, and to the Office of Management and Budget, Paperwork Reduction Project (0704-0188), Washington, DC 20503.				
1. AGENCY USE ONLY (Leave blank)	2. REPORT DATE 920501	3. REPORT TYPE AND DATES COVERED Technical 880415-910930		
4. TITLE AND SUBTITLE Theoretical Study of the Radiative and Kinetic Properties of Selected Metal Oxides and Air Molecules		5. FUNDING NUMBERS C - DNA 001-88-C-0032 PE - 63220C PR - SA TA - SA WU - DH048180		
6. AUTHOR(S) H. Harvey Michels				
7. PERFORMING ORGANIZATION NAME(S) AND ADDRESS(ES) United Technologies Research Center 400 Main Street East Hartford, CT 06108		8. PERFORMING ORGANIZATION REPORT NUMBER R91-927893		
9. SPONSORING/MONITORING AGENCY NAME(S) AND ADDRESS(ES) Defense Nuclear Agency 6801 Telegraph Road Alexandria, VA 22310-3398 RAAE/Berggren		10. SPONSORING/MONITORING AGENCY REPORT NUMBER DNA-TR-91-189		
11. SUPPLEMENTARY NOTES This work was sponsored by the Defense Nuclear Agency under RDT&E RMC Code B7660D SA SA 00186 RAAE 3200A 25904D.				
12a. DISTRIBUTION/AVAILABILITY STATEMENT Approved for public release; distribution is unlimited.			12b. DISTRIBUTION CODE	
13. ABSTRACT (Maximum 200 words) A theoretical research program directed toward the study of the energetics and LWIR radiative properties of selected uranium/oxygen band systems has been undertaken. Included in this research program was the investigation of the strongest electronic and vibrational bands in the LWIR region for the species UO , UO^+ , UO_2 , UO_2^+ , and UO_2^{++} . The program for accomplishing this research effort was formulated into three separate tasks: a) adaption of our electronic structure codes to the DNA CRAY X-MP computer, b) calculation of pertinent electronic wavefunctions and energies, as a function of internuclear separation and within a relativistic framework, for selected species of the uranium/oxygen system which may be important in the LWIR region, and c) calculation of electronic transition moments and transition probabilities between specific vibrational levels of the electronic states corresponding to the strongest radiating band systems belonging to the uranium/oxygen system and prediction of IR and possible optical oscillator strengths. The results obtained to date for the uranium/oxygen system indicate that both UO^+ and UO_2^+ are very strong LWIR radiators in the 10-14 μm region. In addition, UO^+ , which is a potential late time radiator, exhibits strong visible bands and should be efficiently solar pumped. A careful evaluation of the low-lying excited states of UO_2^+ , particularly those charge transfer states that arise by promotion of an electron from (mainly) ligand MO's to a central uranium atom MO, indicates that such transitions lie well outside of the region for efficient solar pumping of UO_2^+ . However, the density of electronic states for UO_2^+ lying below 8 eV is immense, and additional studies are needed for this system.				
14. SUBJECT TERMS UO UO_2 UO_2^{++} $N + O_2$ Potential energy curves UO^+ UO_2^+ $O + N_2$ Dielectronic recombination			15. NUMBER OF PAGES 106	
			16. PRICE CODE	
17. SECURITY CLASSIFICATION OF REPORT UNCLASSIFIED	18. SECURITY CLASSIFICATION OF THIS PAGE UNCLASSIFIED	19. SECURITY CLASSIFICATION OF ABSTRACT UNCLASSIFIED	20. LIMITATION OF ABSTRACT SAR	

UNCLASSIFIED

SECURITY CLASSIFICATION OF THIS PAGE

CLASSIFIED BY:

N/A since Unclassified

DECLASSIFY ON:

N/A since Unclassified

13. ABSTRACT (Continued)

Other studies within DNA chemistry requirements include a preliminary analysis of dielectronic recombination of $e + U^{+9}$ and $e + UO^+$, which are possible charge neutralization processes, and an analysis of the kinetics of the $N + O_2$ and $O + N_2$ reactions in producing vibrationally hot NO molecules radiating in the IR. Our analysis of dielectronic recombination indicates the $e + U^{++}$ and $e + UO^+$ are not rate competitive with possible ion-neutral charge exchange reactions but that $e + U^+$ may exhibit a large kinetic rate for neutralization.

SECURITY CLASSIFICATION OF THIS PAGE

UNCLASSIFIED

PREFACE

This report was prepared by the United Technologies Research Center, East Hartford, Connecticut, under Contract DNA 001-88-C-0032. The research was performed under Program Element 63220C, Project SA, Task Area SA, Work Unit 00186 and was funded by the Defense Nuclear Agency (DNA).

Inclusive dates of research were 1988 April 15 through 1991 August 30. Lt. Col. Stephen Berggren (RAAE) was the Contract Technical Manager (CTM) for this contract.

Very useful discussions with Drs. Russell Armstrong (Mission Research Corporation), Morris Krauss (National Bureau of Standards), Robert Field (MIT), Douglas Archer (Mission Research Corporation), Michael Heaven (Emory University), and Forrest Gilmore (R&D Associates) are also acknowledged.

All aspects of the research work reported herein were aided by the skilled help of Judith B. Addison (UTRC), who carried out much of the computer program development and assisted in the analysis of the calculated data and in the preparation of this final report.



Accession For	
NTIS GRA&I	<input checked="checked" type="checkbox"/>
DTIC TAB	<input type="checkbox"/>
Unannounced	<input type="checkbox"/>
Justification	
By	
Distribution/	
Availability Codes	
Dist	Avail and/or Special
A-1	

Conversion Table

(Conversion factors for U.S. customary to
metric (SI) units of measurement)

To Convert From	To	Multiply By
angstrom	meters (m)	$1.000\ 000 \times E-10$
atmosphere (normal)	kilo pascal (kPa)	$1.013\ 25 \times E+2$
bar	kilo pascal (kPa)	$1.000\ 000 \times E+2$
barn	meter ² (m ²)	$1.000\ 000 \times E-28$
British thermal unit (thermochemical)	joule (J)	$1.054\ 350 \times E+3$
cal (thermochemical)/cm ²	mega joule/m ² (MJ/m ²)	$4.184\ 000 \times E-2$
calorie (thermochemical)	joule (J)	4.184 000
calorie (thermochemical)/g	joule per kilogram (J/kg)	$4.184\ 000 \times E+3$
curie	giga becquerel (GBq)	$3.700\ 000 \times E+1$
degree Celsius	degree kelvin (K)	$t_K = t_C + 273.15$
degree (angle)	radian (rad)	$1.745\ 329 \times E-2$
degree Fahrenheit	degree kelvin (K)	$t_K = (t_F + 459.67)/1.8$
electron volt	joule (J)	$1.602\ 19 \times E-19$
erg	joule (J)	$1.000\ 000 \times E-7$
erg/second	watt (W)	$1.000\ 000 \times E-7$
foot	meter (m)	$3.048\ 000 \times E-1$
foot-pound-force	joule (J)	1.355 818
gallon (U.S. liquid)	meter ³ (m ³)	$3.785\ 412 \times E-3$
inch	meter (m)	$2.540\ 000 \times E-2$
jerk	joule (J)	$1.000\ 000 \times E+9$
joule/kilogram (J/kg) (radiation dose absorbed)	gray (Gy)	1.000 000
kilotons	terajoules	4.183
kip (1000 lbf)	newton (N)	$4.448\ 222 \times E+3$
kip/inch ² (ksi)	kilo pascal (kPa)	$6.894\ 757 \times E+3$
ktap	newton-second/m ² (N-s/m ²)	$1.000\ 000 \times E+2$
micron	meter (m)	$1.000\ 000 \times E-6$

Conversion Table (Concluded)

To Convert From	To	Multiply By
mil	meter (m)	2.540 000 x E-5
mile (international)	meter (m)	1.609 344 x E+3
ounce	kilogram (kg)	2.834 952 x E-2
pound-force (lbf avoirdupois)	newton (N)	4.448 222
pound-force inch	newton-meter (N•m)	1.129 848 x E-1
pound-force/inch	newton/meter (N/m)	1.751 268 x E+2
pound-force/foot ²	kilo pascal (kPa)	4.788 026 x E-2
pound-force/inch ² (psi)	kilo pascal (kPa)	6.894 757
pound-mass (lbm avoirdupois)	kilogram (kg)	4.535 924 x E-1
pound-mass-foot ² (moment of inertia)	kilogram-meter ² (kg•m ²)	4.214 011 x E-2
pound-mass/foot ³	kilogram-meter ³ (kg/m ³)	1.601 846 x E+1
rad (radiation dose absorbed)	gray (Gy)	1.000 000 x E-2
roentgen	coulomb/kilogram (C/kg)	2.579 760 x E-4
shake	second (s)	1.000 000 x E-8
slug	kilogram (kg)	1.459 390 x E+1
torr (mm Hg, 0°C)	kilo pascal (kPa)	1.333 22 x E-1

TABLE OF CONTENTS

Section	Page
PREFACE	iii
CONVERSION TABLE	iv
LIST OF ILLUSTRATIONS	vii
LIST OF TABLES	viii
1 INTRODUCTION	1
2 METHOD OF APPROACH - NON RELATIVISTIC METHODS	3
2.1 Quantum Mechanical Calculations	3
2.2 Transition Probabilities	30
3 DISCUSSION OF RELATIVISTIC METHODS	39
3.1 Breit-Pauli Hamiltonian	41
3.2 Approximate Treatments	43
3.3 Effective Core Models	45
4 DISCUSSION OF RESULTS	48
4.1 UO	48
4.2 UO^+	49
4.3 UO_2^+	50
4.4 Photoelectron Spectra of UO and UO_2^+	52
4.5 $e + \text{U}^+, e + \text{U}^{++}$ Dielectronic Recombination	52
4.6 $\text{N} + \text{O}_2$ Reactions	55
5 RECOMMENDATIONS	58
5.1 Uranium/Oxygen	58
5.2 Dielectronic Recombination	59
5.3 NO/ NO^+ Formation	60
6 LIST OF REFERENCES	87

LIST OF ILLUSTRATIONS

Figure		Page
1	Potential energy curves for UO^+ .	61
2	He I photoelectron spectrum of the vapor above an equimolar $\text{UO}_2(\text{s})/\text{U}(\text{s})$ mixture heated to 2250 ± 30 K.	62
3	Dielectronic recombination.	63
4	Molecular correlation diagram for low-lying states of NO_2 in $C_{\infty v}$ symmetry.	64
5	Molecular correlation diagram for low-lying states of NO_2 in C_s symmetry.	65
6	Molecular correlation diagram for low-lying doublet states of NO_2 in C_s symmetry.	66
7	Molecular correlation diagram for low-lying quartet states of NO_2 in C_s symmetry.	67

LIST OF TABLES

Table		Page
1	Calculated oscillator strengths $f_{(v'v'')}$ for the $1^4\text{I} - 1^4\text{K}$ transition of UO^+ .	68
2	Calculated oscillator strengths $f_{(v'v'')}$ for the $1^4\text{I} - 3^4\text{H}$ transition of UO^+ .	69
3	Calculated oscillator strengths $f_{(v'v'')}$ for the $1^4\text{I} - 2^4\text{H}$ transition of UO^+ .	70
4	Calculated oscillator strengths $f_{(v'v'')}$ for the $1^4\text{I} - 1^4\text{H}$ transition of UO^+ .	71
5	Calculated oscillator strengths $f_{(v'v'')}$ for the $1^4\text{I} - 2^4\text{I}$ transition of UO^+ .	72
6	Calculated oscillator strengths $f_{(v'v'')}$ for the $1^4\text{I} - 1^6\text{H}$ transition of UO^+ .	73
7	Calculated oscillator strengths $f_{(v'v'')}$ for the $1^4\text{I} - 3^4\text{I}$ transition of UO^+ .	74
8	Calculated oscillator strengths $f_{(v'v'')}$ for the $1^4\text{H} - 2^4\text{I}$ transition of UO^+ .	75
9	Calculated oscillator strengths $f_{(v'v'')}$ for the $1^4\text{H} - 2^4\text{H}$ transition of UO^+ .	76
10	Calculated oscillator strengths $f_{(v'v'')}$ for the $1^4\text{H} - 1^4\text{K}$ transition of UO^+ .	77
11	Calculated oscillator strengths $f_{(v'v'')}$ for the $1^4\text{H} - 1^6\text{H}$ transition of UO^+ .	78
12	Calculated oscillator strengths $f_{(v'v'')}$ for the $1^4\text{H} - 3^4\text{H}$ transition of UO^+ .	79
13	Calculated oscillator strengths $f_{(v'v'')}$ for the $1^4\text{H} - 3^4\text{I}$ transition of UO^+ .	80
14	Energetics of dielectronic recombination.	81
15	$e + \text{U}^+$ dielectronic recombination rate (preliminary data).	82
16	Molecular correlation diagram for $\text{N} + \text{O}_2$.	83
17	Adiabatic reaction surfaces arising from $\text{N}[^2\text{P}] + \text{O}_2$.	85
18	Adiabatic reaction surfaces arising from $\text{N}[^2\text{D}] + \text{O}_2$.	85
19	Minimum energy long range interaction potentials for $\text{N} + \text{O}_2$ in C_s symmetry.	86

SECTION 1

INTRODUCTION

The release of certain chemical species into the upper atmosphere results in luminous clouds that display the resonance electronic-vibration-rotation spectra of the chemically reacting species. Such spectra are seen in rocket releases of chemicals for upper atmospheric studies, upon re-entry into the atmosphere of artificial satellites and missiles, and as a result of energy deposition in the atmosphere caused by nuclear weapons effects. Of particular interest in this connection is the observed spectra of certain metallic oxides. From band intensity distributions of the spectra, and knowledge of the f -values for electronic and vibrational transitions, the local conditions of the atmosphere can be determined (Reference 1). Such data are fundamental for the analysis of detection and discrimination problems.

Present theoretical efforts, which are directed toward a more complete and realistic analysis of the transport equations governing atmospheric relaxation and the propagation of artificial disturbances, require detailed information of thermal opacities and LWIR absorption in region of temperature and pressure where both atomic and molecular effects are important (References 2 and 3). Although various experimental techniques have been employed for both atomic and molecular systems, theoretical studies have been largely confined to an analysis of the properties (bound-bound, bound-free and free-free) of atomic systems (References 4 and 5). This has been due in large part to the unavailability of reliable wavefunctions for diatomic molecular systems, and particularly for excited states or states of open-shell structure. Only recently (References 6-8) have reliable procedures been prescribed for such systems which have resulted in the development of practical computational programs.

The application of these computational methods to studies of the electronic structure and radiation characteristics of metal oxides has been reported for several of the lighter systems (References 9-11). A preliminary study of the uranium/oxygen system has been reported by Michels (Reference 12) which identified a large number of low-lying molecular states for both the UO and UO^+ systems. Of particular interest was the discovery of two structures for UO^+ that resulted from two different spin-couplings of the uranium valence electrons. These results suggested strong LWIR radiation in UO^+ arising from different electronic state transitions.

An inherent uncertainty in these preliminary calculations was present, owing to the neglect of relativistic effects that were much too difficult to include in molecular calculations at that period of time. The 7s valence electron of uranium, and its corresponding σ -bonding molecular orbital, are highly relativistic in nature which results in a contracted charge density relative to that which would occur in lighter molecular systems. The effect of this contraction on the relative

positions of the low-lying electronic states of the uranium/oxygen system can now be calculated with some degree of confidence using newly developed relativistic computer codes.

Because of inherent difficulties in the experimental determination of the spectroscopy, transition probabilities and LWIR radiation for metal oxide systems and in light of the aforementioned recent progress in the calculation of relativistic electronic wavefunctions, especially for diatomic systems, a technical program for calculating these properties was undertaken for the Defense Nuclear Agency under Contracts DNA001-88-C-0032, DNA001-85-C-0120, DNA001-83-C-0044 and DNA001-82-C-0015. The emphasis in this work was on the ions of uranium and uranium oxide since these species have been determined to be important radiators in the LWIR region. These studies indicated that, in addition to UO^+ and UO_2^+ , the doubly ionized species, U^{++} , UO^{++} and UO_2^{++} , should also be considered because of their role in charge neutralization processes and their potential as early-time radiators.

A summary of the results obtained to date for the uranium/oxygen system indicates that both UO^+ and UO_2^+ are very strong LWIR radiators in the 10-14 μm region. In addition, UO^+ , which is a potential late time radiator exhibits strong visible bands and should be efficiently solar pumped. A careful evaluation of the low-lying excited states of UO_2^+ , particularly those charge transfer states that arise by promotion of an electron from (mainly) ligand MO's to a central uranium atom MO, indicates that such transitions lie well outside of the region for efficient solar pumping. However, the density of electronic states for UO_2^+ lying below 8 eV is immense, and additional studies are needed for this system.

Other studies within DNA chemistry requirements include an analysis of dielectronic recombination of $e + \text{U}^+$ and $e + \text{UO}^+$ which, are possible charge neutralization processes, and an analysis of the kinetics of the $\text{N} + \text{O}_2$ and $\text{O} + \text{N}_2$ reactions in producing vibrationally hot NO molecules radiating in the IR. This report addresses theoretical studies in all of the areas described above.

The general composition of this report is as follows. In Section 2, we present a description of the mathematical methods which were employed in this research. Included in Section 2 are sub-sections which deal with the construction of electronic wavefunctions, the calculations of expectation properties, the evaluation of molecular transition probabilities, and the calculation of electronic wavefunctions using both the *ab initio* and density functional methods. This is followed by Section 3 which describes the inclusion of relativistic effects into the density functional (X_α) method. The calculated results and pertinent discussion are presented in Section 4. Recommendations are presented in Section 5.

SECTION 2

METHOD OF APPROACH - NON RELATIVISTIC METHODS

2.1 QUANTUM MECHANICAL CALCULATIONS.

Central to these theoretical studies are the actual quantum-mechanical calculations which must be carried out for the atomic and molecular species. In particular, the methodology for computing the minimum energy reaction pathways and testing for vibrational stability must be carefully analyzed. For added clarity, various aspects of these calculations are discussed below.

Much evidence on diatomic and polyatomic systems indicates the inadequacy of minimum basis sets for constructing quantitatively correct molecular wavefunctions (References 13 and 14). This means inner-shell and valence-shell orbitals of quantum numbers appropriate to the atoms (1s, 2s, 2p, for C, N, O; etc.). The main deficiency of the minimum basis set is its inability to properly describe polarization and the change of orbital shape for systems which exhibit large charge transfer effects. Values of the screening parameters for each orbital can either be set from atomic studies or optimized in the molecule; the latter approach is indicated for studies of higher precision. When high chemical accuracy is required, as for detailed studies of the ground or a particular excited state of a system, a more extended basis must be used. Double-zeta plus polarization functions or optimized MO's are usually required as a minimum representation for reliable calculated results of chemical accuracy.

The chosen basis sets give good results only when used in a *maximally flexible manner*. This implies the construction of perturbation expansions or the use of CI wavefunctions with all kinds of possible orbital occupancies, so that the correlation of electrons into overall states can adjust to an optimum form at each geometrical conformation and for each state. Except when well-defined pairings exist, as for closed shell and exchange dominated systems, a single-configuration study (even of Hartree-Fock quality) will be inadequate.

Proper electronic states for systems composed of light atoms should possess definite eigenvalues of the spin operator S^2 as well as an appropriate geometrical symmetry. The geometrical symmetry can be controlled by the assignment of orbitals to each configuration, but the spin state must be obtained by a constructive or projective technique. Formulas have been developed (Reference 15) for projected construction of spin states from orthogonal orbitals, and programs implementing these formulas have been in routine use at UTRC for several years. One of the least widely appreciated aspects of the spin-projection problem is that the same set of occupied spatial orbitals can sometimes be coupled to give more than one overall state of a given spin quantum number. It is necessary to include in calculations all such spin couplings, as the optimum coupling will continuously change with changes in the molecular conformation. This is especially important in describing degenerate or near-degenerate excited electronic states.

In the sections below, we describe the several mathematical approaches that are applicable to calculation of the electronic structure of molecules, to the calculation of potential energy surfaces for chemically reacting systems, and to the subsequent calculation of radiation and collisional processes. Since several different approaches are indicated, we describe their expected areas of applicability.

2.1.1 Method of *Ab Initio* Calculation.

2.1.1.1 Born–Oppenheimer Separation. For a system of n electrons and N nuclei, and considering only electrostatic interactions between the particles, we have for the total Hamiltonian

$$\mathcal{H} = \mathcal{H}_{\text{el}} - \sum \frac{\hbar^2}{2m_a} \nabla_a^2 + \frac{\hbar^2}{2M_T} \left[\sum_{\beta=1}^N \sum_{\alpha=1}^N \nabla_\alpha \cdot \nabla_\beta + 2 \sum_{\alpha=1}^N \sum_{i=1}^n \nabla_\alpha \cdot \nabla_i + \sum_{i=1}^n \sum_{j=1}^n \nabla_i \cdot \nabla_j \right] \quad (1)$$

where

$$\mathcal{H}_{\text{el}} = - \frac{\hbar^2}{2m_e} \sum_{i=1}^n \nabla_i^2 + V^{\text{el}}(\vec{r}_n, \vec{R}_N) \quad (2)$$

and where m_e , m_a , M_T , are the masses of the electron, atom and combined system mass, respectively. Now since the ratios m_e/m_a , and m_e/M_T are both small, ($2 \cdot 10^{-6} - 5 \cdot 10^{-4}$) we can effect a separation of the electronic and nuclear coordinates treating the total wavefunction as a product of a nuclear and an electronic part. We have

$$\psi(\vec{r}_n, \vec{R}_N) = \sum_k \chi_k(\vec{R}_N) \psi_k(\vec{r}_n, \vec{R}_N) \quad (3)$$

where $\psi_k(\vec{r}_n, \vec{R}_N)$ is an electronic wavefunction parametric in the nuclear coordinates as given in Equation (3) and $\chi_k(\vec{R}_N)$ are nuclear motion wavefunctions which satisfy (neglecting terms of the order of m_e/m_a)

$$\left[- \sum_{\alpha=1}^N \frac{\hbar^2}{2m_a} \nabla_\alpha^2 + \frac{\hbar^2}{2M_T} \sum_{\alpha=1}^N \sum_{\beta=1}^N \nabla_\alpha \cdot \nabla_\beta + V^{\text{el}}(\vec{r}_n, \vec{R}_N) \right] \chi_k = i\hbar \frac{\partial \chi_k}{\partial t} \quad (4)$$

The cross term in $\nabla_\alpha \cdot \nabla_\beta$ can be eliminated by a proper change of variables and Equation (4) then reduces to a 3N-3 dimensional Schrödinger equation.

For most systems, where the velocity of motion of the nuclei is slow relative to the electron velocity, this decoupling of electron and nuclear motion is valid and is referred to as the adiabatic approximation. Equation (3) thus defines an electronic eigenstate $\psi_k(\vec{r}_n, \vec{R}_N)$, parametric in the nuclear coordinates, and a corresponding eigenvalue $E_k(\vec{R}_N)$ which is taken to represent the potential energy curve or surface corresponding to state k.

2.1.1.2 Variational Methods. By an *ab initio* method is meant one that starts from a zero-order Hamiltonian which is exact except for relativistic and magnetic effects, and which involves the evaluation of electronic energies and other relevant quantities for wavefunctions which are properly antisymmetrized in the coordinates of all the electrons. For a system containing n electrons and M nuclei, the zero-order Hamiltonian depends parametrically on the nuclear positions and is of the form

$$\mathcal{H} = -\frac{1}{2} \sum_{i=1}^N \nabla_i^2 - \sum_{i=1}^n \sum_{j=1}^M \frac{Z_j}{|\vec{r}_i - \vec{R}_j|} + \sum_{1 \leq i < j}^M \frac{Z_i Z_j}{|\vec{R}_i - \vec{R}_j|} + \sum_{1 \leq i < j} \frac{1}{|\vec{r}_i - \vec{r}_j|} \quad (5)$$

where Z_i and \vec{R}_i are the charge and position of nucleus i, \vec{r}_j is the position of electron j, and ∇_j^2 is the Laplacian operator for electron j. All quantities are in atomic units, i.e. lengths in bohrs, energies in hartrees (1 hartree = 2 Rydbergs). The many-electron wavefunction consists of one, or a linear combination, $\psi = \sum_{\mu} c_{\mu} \psi_{\mu}$ of terms of the form

$$\Psi_{\mu}(R) = \mathcal{A} \mathcal{O}_S \prod_{i=1}^n \phi_{\mu i}(\vec{r}_i, R) \theta_{\mu M} \quad (6)$$

where each $\phi_{\mu i}$ is a spatial orbital, \mathcal{A} is the antisymmetrizing operator, \mathcal{O}_S is the spin-projection operator for spin quantum number S, and $\theta_{\mu M}$ is a product of α and β one-electron spin functions of magnetic quantum number M_S . No requirement is imposed as to the double occupancy of the spatial orbital, so linear combinations of the form given by Equation (6) can describe a completely general wavefunction. The spatial orbitals $\phi_{\mu i}$ may be whatever basis orbitals have been introduced, arbitrary linear combinations thereof, or specific linear combinations determined pursuant to the particular calculational method in use.

The spatial orbitals $\phi_{\mu i}$, the spin functions $\theta_{\mu m}$ and the coefficients of different ψ_{μ} , if a linear combination of ψ_{μ} is used, may be explicitly determined by invoking the variational principle. Various specific methods are described below for determining wavefunctions. However, we should first observe that the adequacy of an *ab initio* calculation, or for that matter any energy calculation, will depend crucially upon the extent to which the wavefunction can be qualitatively appropriate. Some of the considerations surrounding the choice of a wavefunction are the following:

- (i) necessity that the wavefunction possess sufficient flexibility to be able to describe dissociation to the correct atomic and molecular fragments as various internuclear separations are increased;
- (ii) maintenance of equivalent quality of calculation for nuclear geometries differing in the nature or number of chemical bonds;
- (iii) ability to describe degenerate or near-degenerate electronic states when they are pertinent;
- (iv) ability to describe different electronic states to equivalent accuracy when their interrelation (e.g., crossing) is relevant, in particular, ability to describe ionic-valence state mixing;
- (v) ability to represent changes in the coupling of electron spins as bonds are broken or reformed.

The foregoing considerations indicate that it will often be necessary to consider wavefunctions with more than a minimum number of singly-occupied spatial orbitals, and that there will be many potential curves or surfaces for which a wavefunction consisting of a single ψ_{μ} cannot suffice. It will then be necessary to allow mixing of ψ_{μ} with different degrees of orbital spatial occupancy so as to obtain smooth transitions from the occupancies characteristic of separated atoms or molecules (or ions) to those characteristic of a compound system or a different fragmentation.

Another implication of the considerations surrounding the choice of a wavefunction is related to the treatment of electron spin. Not only is it necessary to require that the wavefunction be an eigenfunction of S^2 and S_z but it is also necessary to take account of the fact that under many conditions, there will be more than one spin eigenfunction of given S and m_s . The different spin eigenfunctions correspond to different couplings among the individual spins. Since reactive processes involve the breaking and forming of electron-pair bonds, they must necessarily be accompanied by reorganizations of the spin coupling. A failure to take account of this will lead to qualitatively inappropriate wavefunctions.

In Hartree-Fock calculations $\psi(R)$ is restricted to a single ψ_μ which is assumed to consist as nearly as possible of doubly-occupied orbitals. The orbitals $\phi_{\mu i}$ are then selected to be the linear combinations of basis orbitals best satisfying the variational principle. Writing $\phi_{\mu i} = \sum_\nu a_{\nu i} \chi_\nu$, the $a_{\nu i}$ are determined by solving the matrix Hartree-Fock equation

$$\sum_\nu F_{\lambda\nu} a_{\nu i} = \epsilon_i \sum_\nu S_{\lambda\nu} a_{\nu i} \quad (\text{each } \lambda) \quad (7)$$

where ϵ_i is the orbital energy of $\phi_{\mu i}$.

The Fock operator $F_{\lambda\nu}$ has been thoroughly discussed in the literature (Reference 16) and depends upon one- and two-electron molecular integrals and upon the $a_{\nu i}$. This makes Equation (7) nonlinear and it is therefore solved iteratively. UTRC has developed programs for solving Equation (7) for both closed and open-shell systems, using basis sets consisting of either Slater-type or Gaussian-type atomic orbitals. Examples of their use are in the literature (Reference 7).

In configuration interaction calculations, the overall wavefunction has more than one term, ψ_μ , and the c_μ are determined by invoking the variational principle to obtain the secular equation

$$\sum_\nu (H_{\mu\nu} - \epsilon S_{\mu\nu}) c_\nu = 0 \quad (\text{each } \mu) \quad (8)$$

where

$$H_{\mu\nu} = \int \Psi_\mu^*(R) \mathcal{H}(R) \Psi_\nu(R) d\tau \quad S_{\mu\nu} = \int \Psi_\mu^*(R) \Psi_\nu(R) d\tau \quad (9)$$

Equation (8) is solved by matrix diagonalization using either a modified Givens method (Reference 17) or a method due to Shavitt (Reference 18) or Raffanetti (Reference 19).

The matrix elements $H_{\mu\nu}$ and $S_{\mu\nu}$ may be reduced by appropriate operator algebra to the forms

$$H_{\mu\nu} = \sum_P \epsilon_P \langle \theta_M | O_S P | \theta_M \rangle \left(\prod_{i=1}^n \Psi_{\mu i}(\vec{r}_i, \vec{R}_N) | \mathcal{H}(\vec{R}_N) P | \prod_{i=1}^n \Psi_{\nu i}(\vec{r}_i, \vec{R}_N) \right) \quad (10)$$

$$S_{\mu\nu} = \sum_P \epsilon_P \langle \theta_M | O_S P | \theta_M \rangle \left(\prod_{i=1}^n \Psi_{\mu i}(\vec{r}_i, \vec{R}_N) | P | \prod_{i=1}^n \Psi_{\nu i}(\vec{r}_i, \vec{R}_N) \right) \quad (11)$$

where P is a permutation and ϵ_P its parity. The sum is over all permutations. $\langle \theta_M | O_S P | \theta_M \rangle$ is a "Sanibel coefficient" and the remaining factors are spatial integrals which can be factored into one- and two-electron integrals. If the $\phi_{\mu i}$ are orthonormal, Equations (10) and (11) become more tractable and the $H_{\mu\nu}$ and $S_{\mu\nu}$ may be evaluated by explicit methods given in the literature (Reference 15). Computer programs have been developed for carrying out this procedure, and they have been used for problems containing up to 106 total electrons, 10 unpaired electrons, and several thousand configurations.

The CI studies described above can be carried out for any orthonormal set of $\phi_{\mu i}$ for which the molecular integrals can be calculated. Programs developed by UTRC make specific provision for the choice of the $\phi_{\mu i}$ as Slater-type atomic orbitals, as Gaussian-type orbitals, as symmetry molecular orbitals, as Hartree-Fock orbitals, or as more arbitrary combinations of atomic orbitals.

The one- and two-electron integrals needed for the above described method of calculation are evaluated for STO's by methods developed by this Center (Reference 20). For Gaussian orbitals, either the Carnegie-Mellon integral package (Reference 21) or the integral routines incorporated in the HONDO or GAMESS programs (Reference 22) can be employed.

2.1.1.3 Configuration Selection. Using a double-zeta plus polarization basis set of one-electron functions, a typical system can easily have of the order of 10^6 configurations in full CI (that resulting from all possible orbital occupancies). It is therefore essential to identify and use the configurations describing the significant part of the wavefunction. There are several ways to accomplish this objective. First, one may screen atomic-orbital occupancies to eliminate configurations with excessive formal charge. Alternatively, in a molecular-orbital framework, one may eliminate configurations with excessive numbers of anti-bonding orbitals. A third possibility is to carry out an initial screening of configurations, rejecting those whose diagonal energies and interaction matrix elements do not satisfy energy significance criteria.

Another common method of classifying configurations is to examine the total number of orbitals in the wavefunction that differ from the SCF reference wavefunction. We write the CI wavefunction as

$$\psi_{CI} = C_0\psi_0 + \sum_i C_i\phi_i^S + \sum_j C_j\phi_j^D + \dots \quad (12)$$

where a single excitation function, ϕ_i^S differs from the SCF reference ψ_0 by one orbital and the double excitation function ϕ_j^D by two, and so on. The CI coefficients, C_i , are then determined variationally to yield the lowest possible total energy. In the limit of a complete basis set ($N \rightarrow \infty$), and where all possible substitutions are included in ψ_{CI} , the variational energy approaches the correct nonrelativistic Born-Oppenheimer result. Errors arise from a truncation of the functions used to determine the SCF reference wavefunction and from the truncation of the excitation functions series in ψ_{CI} . The reference wavefunction ψ_0 will typically be the same for a CI or Many Body Perturbation Theory (MBPT) calculation; however, for a molecule even as small as water, ψ_{CI} becomes a function of a very large number of basis functions. Additionally, the reference state itself may be multi-dimensional in order to describe systems such as diradicals or systems with orbital degeneracy. Because of this, one must truncate the expansion and eliminate unimportant configurations. In general one can show that

$$\langle \psi_0 | \mathcal{H} | \phi^T \rangle = \langle \psi_0 | \mathcal{H} | \phi^Q \rangle = 0 \quad (13)$$

In words, the matrix elements between the reference wavefunction and triple and quadruple excitations is zero. Thus to first order, only single and double excitations contribute. Because of this, many CI calculations attempt to include all single and double excitations in the expressions for ψ_{CI} . To go beyond this, generally more than one reference wavefunction is used. Programs to handle configurations on all the above criteria are available at UTRC.

Other, potentially more elegant methods of configuration choice involve formal approaches based on natural orbital (Reference 23) or multiconfiguration SCF (Reference 24) concepts. To implement the natural-orbital approach, an initial limited CI wavefunction is transformed to natural orbital form, and the resulting natural orbitals are used to form a new CI. The desired result is a concentration of the bulk of the CI wavefunction into a smaller number of significant terms. The multiconfiguration SCF approach is more cumbersome, but in principle more effective. It yields the optimum orbital choice for a preselected set of configurations. This

approach works well when a small number of dominant configurations can be readily identified. The method is described briefly below.

2.1.1.4 Multiconfiguration – Self Consistent Field Method (MC-SCF). The Hartree-Fock self consistent field method has been proven to be a powerful tool for the calculation and understanding of many ground state properties of molecules in the vicinity of their equilibrium structure. However, in most cases the one configuration Hartree-Fock approximation is not adequate to properly describe the dissociation of molecular bonds. Also, many excited states cannot be represented by a single configuration wave function. In order to calculate properties for such states, or to investigate the formation of molecular bonds, one often needs multiconfiguration wave functions for which both the linear coefficients, C_i of the configuration expansion

$$\psi = \sum_i C_i \psi_i \quad (14)$$

as well as the set of orthonormal molecular orbitals $\{\phi_j\}$, from which the configurations ψ_i are constructed, are optimized according to the variational principle. As is well known, this "MC-SCF" problem presents many more difficulties than the simple one configuration Hartree-Fock case and much work has been devoted to obtaining convergent solutions during the last decade.

The difficulties mainly arise from the fact that for general MC-SCF wave functions the energy is not invariant with respect to rotations between occupied orbitals. Hence, instead of a relatively simple pseudo-eigenvalue equation in the one determinant case, the set of coupled Fock equations

$$\sum_j F_{ij} |\phi_j\rangle = \sum_j \epsilon_{ij} |\phi_j\rangle, \quad (15)$$

with the hermiticity conditions

$$\epsilon_{ij} = \epsilon_{ji}^* \quad (16)$$

has to be solved. ϵ_{ij} are Lagrange multipliers which account for the orthonormality constraints imposed on the orbitals. The Fock operators F_{ij} depend on the orbitals $\{\phi_i\}$ and the set of CI

coefficients $[C_i]$. In analogy to the one determinant case many attempts have been made to solve these equations iteratively by keeping the Fock operators fixed in each iteration step. Then the Lagrange multipliers can be expressed by coupling operators constructed such that the Fock equations are transformed into pseudo-eigenvalue equations yielding the improved orbitals. These are used in a second step to determine new CI coefficients by diagonalizing the CI matrix $\langle \psi_i | \mathcal{H} | \psi_j \rangle$. The convergence of these algorithms, however, has often been found to be poor.

A second group of MC-SCF methods is based on the generalized Brillouin theorem. In these methods, the orbital changes are derived from the coefficients of a CI expansion consisting of the MC-SCF wavefunction and all one-electron singly excited configurations. A computer program (ALIS) implementing this method has been developed by Ruedenberg, et al. (Reference 25). A somewhat more elegant program (GAMESS) which also incorporates analytical gradients is also available (Reference 22). More recently, various methods have been proposed which are based on direct minimization of the energy, avoiding the Fock operators altogether. Such methods are now being studied in our laboratory and will be incorporated into our existing computer programs if they prove to be highly efficient.

2.1.1.5 Many-Body Perturbation Theory (MBPT). In MBPT we again begin with the SCF wavefunction (ψ_0) as our reference and attempt to account for E_c , the correlation energy. The concept of excitation functions described in the above section on CI calculations carries over to MBPT calculations. In MBPT one can write the wavefunction, ψ_p , as

$$\psi_p = e^T |\phi_0\rangle \quad (17)$$

where T is an excitation operator defined as

$$T = T_S + T_D + T_T + T_Q \dots \quad (18)$$

where S, D, T, and Q refer to single, double, triple, and quadruple substitutions respectively. One can write T_n in general, where n refers to the number of excitations as

$$T_n = \frac{1}{n!} \sum_{\substack{ijk\dots \\ abc\dots}} t_{ijk\dots}^{abc\dots} \chi_a^+ \chi_b^+ \chi_c^+ \dots \chi_i \chi_j \chi_k \dots \quad (19)$$

where a,b,c,... are excited orbitals and i,j,k,... are orbitals occupied in ϕ_0 . The total energy is now given by

$$E_{\text{MBPT}} = \langle \phi_0 | \mathcal{H} e^T | \phi_0 \rangle \quad (20)$$

To evaluate E_{MBPT} , the $t_{i,j,k,\dots}^{a,b,c,\dots}$ from above must be determined. An equivalent expression that makes the perturbation expansion clearer is

$$E_{\text{MBPT}} = \sum_{k=0}^{\infty} \langle \phi_0 | \mathcal{H} [(E_0 - \mathcal{H}_0)^{-1} \mathcal{H}]^k | \phi_0 \rangle \quad (21)$$

where the sum is over only so-called linked diagrams, \mathcal{H}_0 has eigenfunctions ϕ_0 , and the expansion is of orders in the perturbation, $V = (\mathcal{H} - \mathcal{H}_0)$. The $k = 0$ term gives the reference energy and for $k > 0$ correlation corrections are included. In practice the MBPT total energy is calculated by truncating the T operator expansion and projecting $\mathcal{H} e^T |\phi_0\rangle$ onto the appropriate n-space. This leads to a set of nonlinear coupled equations for the $t_{i,j,k,\dots}^{a,b,c,\dots}$ coefficients which correspond to the CI expansion coefficients. The equations are solved iteratively and E_{MBPT} evaluated. In practice T_4 is an upper limit that corresponds to quadruple substitutions. The series is an oscillatory convergent sum, which in practice has proven to be at least as accurate as E_{CI} with single and double excitations included.

The best possible method to use would be a full CI (all possible configurations) with a complete basis set. However, since the number of configurations is proportional to $\langle n \rangle^l$, where n is the number of basis functions and l is the level of excitation, it would be prohibitive to even include all single and double excitations. This truncation causes the loss of size consistency, which implies that the energy calculated for A and B as a molecular system, but dimensionally far apart, is the sum of the energy calculated for A and B separately. In a size extensive calculation the energy is proportional to the size of the system. These properties are very important if one wishes to compute correct relative energies on a potential energy surface, a necessary criteria for defining the reactive pathways of interest in this research program. MBPT, on the other hand, is guaranteed to have the correct size-dependence because the expansions contain only the so-called linked diagrams. In addition, because of the computational efficiency of MBPT, calculations can be performed up to fourth order in the perturbation expansion and include single, double, triple, and quadruple excitations in the calculation of the correlation energy. Such calculations are usually performed with at least a split valence plus polarization basis set. For the light element

compounds which exhibit ionic bonding, the inclusion of diffuse basis functions and possibly higher polarization d or f-functions may be required for a more quantitative treatment.

2.1.2 Density Functional Approach.

The X_α method (Reference 26) for the electronic structure of atoms, molecules, clusters and solids is a local potential model obtained by making a simple approximation to the exchange - correlation energy. Although this method, as currently implemented, is less accurate than standard *ab initio* approaches, it is very useful for heavy-atom molecular systems. For such system ($Z \geq 30$), relativistic effects become increasingly important and their incorporation into density functional methods is much easier than into *ab initio* methods. If we assume a nonrelativistic Hamiltonian with only electrostatic interactions, it can be shown that the total energy E of a system can be written exactly (Reference 27) (in atomic units) as

$$E = \sum_i n_i \left\langle u_i \left| -\frac{1}{2} \nabla^2 + \sum_\mu \frac{Z_\mu}{r_{1\mu}} \right| u_i \right\rangle + \frac{1}{2} \sum_\mu \sum_{\mu \neq \nu} \frac{Z_\mu Z_\nu}{r_{\mu\nu}} \quad (22)$$

$$+ \frac{1}{2} \sum_{ij} n_i n_j \left\langle u_i u_j \left| \frac{1}{r_{12}} \right| u_i u_j \right\rangle + E_{xc}$$

This expression is exact provided the u_i are natural orbitals and n_i are their occupation number (i.e., eigenfunctions and eigenvalues of the first order density matrix). The first term in Equation (22) represents the kinetic and electron-nuclear energies. The second term is the nuclear repulsion energy. The sums (μ, ν) are over all the nuclear charges in the system. The third term is the electron-electron repulsion term, which represents the classical electrostatic energy of the charge density ρ interacting with itself, where

$$\rho(1) = \sum_i n_i u_i^*(1) u_i(1) \quad (23)$$

The last term E_{xc} represents the exchange correlation energy and can be expressed formally as

$$E_{xc} = \frac{1}{2} \int \rho(1) d\vec{r}_1 \int \frac{\rho_{xc}(1, 2)}{r_{12}} d\vec{r}_2, \quad (24)$$

where $\rho_{xc}(1, 2)$ represents the exchange-correlation hole around an electron at position 1. In the exact expression ρ_{xc} is dependent on the second-order density matrix. In the Hartree-Fock approximation E_{xc} is the exchange energy, ρ_{xc} represents the Fermi hole due to the exclusion principle and depends only on the first-order density matrix. In the X_α method, we make a simpler assumption about ρ_{xc} . If we assume that the exchange-correlation hole is centered on the electron and is spherically symmetric, it can be shown that the exchange-correlation potential

$$U_{xc} = \int \frac{\rho_{xc}(1, 2)}{r_{12}} d\vec{r}_2 \quad (25)$$

is inversely proportional to the range of the hole, r_s , where r_s is defined by

$$\frac{4\pi}{3} r_s^3 \rho(1) = 1 \quad (26)$$

Therefore, in the X_α model, the potential U_{xc} is proportional to $\rho^{1/3}(\vec{r})$. We define a scaling parameter α such that

$$U_{xc}(1) = -\frac{9\alpha}{2} (3\rho(1)/8\pi)^{1/3} \quad (27)$$

The expression in Equation (27) is defined so that $\alpha = 2/3$ for the case of a free electron gas in the Hartree-Fock model (Reference 28) and $\alpha = 1$ for the potential originally suggested by Slater (Reference 29). A convenient way to choose this parameter for molecular and solid state applications is to optimize the solutions to the X_α equations in the atomic limit. Schwartz (Reference 30) has done this for atoms from $z = 1$ to $z = 41$ and found values between $2/3$ and 1 .

In the "spin polarized" version of the X_α theory, it is assumed (as in the spin-unrestricted Hartree-Fock model) that electrons interact only with a potential determined by the charge

density of the same spin. In this case the contribution to the total energy is summed over the two spins, $s = \pm 1/2$.

$$E_{xc} = \frac{1}{2} \sum_s \int \rho_s(1) U_{x_{\alpha,s}}(1) d\vec{r}_1 \quad (28)$$

where the potential is spin-dependent

$$U_{x_{\alpha,s}}(1) = -\frac{9\alpha}{2} (3\rho_s(1)/4\pi)^{1/3} \quad (29)$$

and ρ_s is the charge density corresponding to electrons of spin s . The spin polarized X_α model is useful for describing atoms and molecules with open-shell configurations and crystals which are ferromagnetic or anti-ferromagnetic.

Once one has made the X_α approximation to the total energy functional E in Equation (1), then the rest of the theory follows from the application of the variational principle. The orbitals u_i are determined by demanding that E be stationary with respect to variations in u_i . This leads to the set of one-electron X_α equations

$$\left[-\frac{1}{2} \nabla_1^2 + \sum_\mu \frac{Z_\mu}{r_{1\mu}} + \int \frac{\rho(2)}{r_{12}} d\vec{r}_2 + \frac{2}{3} U_{x_\alpha} \right] u_i = \epsilon_i u_i \quad (30)$$

where ϵ_i is the one-electron eigenvalue associated with u_i . Since $\rho(\vec{r})$ is defined in terms of the orbitals u_i , Equation (30) must be solved iteratively, until self-consistency is achieved. Empirically, if one takes as an initial guess that ρ is approximately a sum of superimposed atomic charge densities, then the convergence of this procedure is fairly rapid. The factor of 2/3 multiplying the potential is a result of the linear dependence of E_{xc} on ρ . This also has a consequence that the X_α eigenvalues ϵ_i do not satisfy Koopman's theorem, i.e., they cannot be interpreted as

ionization energies. However, it can be shown that the ϵ_i are partial derivatives of the total expression of Equation (22) with respect to the occupation number,

$$\epsilon_i = \frac{\delta E}{\delta n_i} \quad (31)$$

If E were a linear function of n_i , then Koopmans' theorem would hold. However, because of the dominant Coulomb term, E is better approximated by a quadratic function in n_i . This leads to the "transition state" approximation which allows one to equate the difference in total energy between the state (n_i, n_j) and $(n_i - 1, n_j + 1)$ to the difference in the one-electron energies $\epsilon_j - \epsilon_i$ calculated in the state $(n_i - 1/2, n_j + 1/2)$. The error in this approximation is proportional to third-order derivatives of E with respect to n_i and n_j , which are usually small (Reference 31). The main advantage of using the transition state rather than directly comparing the total energy values is computational convenience, especially if the total energies are large numbers and the difference is small.

The relationship of Equation (31) also implies the existence of a "Fermi level" for the ground state. This can be seen by varying E with respect to n_i under the condition that the sum $\sum_i n_i$ is a constant, i.e.,

$$\delta \left[E - \lambda \sum_i n_i \right] = 0 \quad (32)$$

implies $\delta E / \delta n_i = \lambda$, where λ is a Lagrangian multiplier. This implies that the total energy is stationary when all the one-electron energies are equal. However, the occupation numbers are also subject to the restriction $0 \leq n_i \leq 1$. This leads to the following conditions on the ground state occupation numbers:

$$\epsilon_i < \lambda \cdot n_i = 1 \quad (33)$$

$$\epsilon_i > \lambda \cdot n_i = 0 \quad (34)$$

$$\epsilon_i = \lambda \cdot 0 \leq n_i \leq 1 \quad (35)$$

In other words, the ground state eigenvalues obey Fermi statistics with λ representing the Fermi energy. It should be noted that, in contrast to the Hartree-Fock theory, where all the n_i are either 0 or 1, the X_α model predicts, in some cases, fractional occupation numbers at the Fermi

level. In particular, this will occur in a system (such as transition metal or actinide atom) which has more than one open shell.

The X_α model differs in other significant ways from the Hartree-Fock method. In fact, the simplification introduced in approximating the total energy expression introduces several distinct advantages over Hartree-Fock:

1. The primary advantage is purely computational. The one-electron potential in Equation (30) is orbital-independent and local, i.e., it is the same for all electrons (except in the spin-polarized X_α theory) and is a multiplicative operator. On the other hand, the Hartree-Fock potential is nonlocal, or equivalently, there is a different local potential for each orbital. This involves a great deal more computational effort, especially for systems described by a large number of orbitals. It has been shown (Reference 32) that the X_α orbitals for the first and second row atoms are at least as accurate as a double-zeta basis set, and are probably better for larger atoms which involve electrons with $l \geq 2$.
2. The orbital-independent X_α potential leads to a better one-electron description of electronic excitations of a system. Both the unoccupied ($n_i = 0$) and occupied ($n_i = 1$) eigenfunctions are under the influence of the same potential resulting from the other $N-1$ electrons. The Hartree-Fock virtual orbitals see a potential characteristic of the N occupied orbitals, and therefore are not as suitable for describing the excited states. Actually, although the ground state virtual eigenvalues are usually a good description of the one-electron excitations, the virtual spectrum of the transition state potential where one-half an electron has been removed from the system gives a much better first-order picture of these levels (Reference 33).
3. As has been shown by Slater (Reference 34), the X_α model rigorously satisfies both the virial and Hellman-Feynman theorems, independent of the value of the parameter α . This is convenient for calculating the force on a nucleus directly in terms of a three-dimensional integral, rather than the six-dimensional integrals in the expression for the total energy of Equation (22).

2.1.2.1 Computational Aspects of the X_α Method. In application of the X_α model to finite molecular systems, there are two practical aspects of the calculations which must be considered. The first concerns the choice of the integration framework for describing the molecular wavefunctions and the second deals with the choice of the exchange parameter, α , in different regions of space.

In computations with heteronuclear molecules, there are several free parameters that must be chosen: the ratio of sphere radii for the atomic spheres of integration at a given internuclear separation, the degree of sphere overlap, and the value of the exchange parameter in the atomic spheres and the intersphere region.

It has been found that changing the ratio of the sphere radii for the two atoms in a heteronuclear diatomic molecule introduces changes in the total energy that can be large on a chemical scale ($\sim 1\text{eV}$). A choice for sphere radii based on covalent bonding radii does not necessarily provide a good estimate for these calculations. The value of the exchange parameter, α , and the sphere radii and/or sphere overlap is normally fixed in X_α calculations for crystals where the geometry is fixed. However, to develop a potential curve, the molecule description needs to change substantially as the internuclear separation varies and the changing sphere radii include varying fractions of the total molecular charge (Reference 35). Studies made at UTRC have shown that at any given separation the total energy calculated from the X_α model is a minimum at the radii ratio where the spherically averaged potentials from the two atomic centers is equal at the sphere radius.

$$V_1(r_{s_1}) = V_2(r_{s_2}) \quad (36)$$

This relationship between the potential match at the sphere boundary and the minimum in the total energy appears to hold exactly for "neutral" atoms and holds well for ionic molecular constituents. In the case of two ionic species, the long range tail of the potential must go like $+2/R$ for one ion and $-2/R$ (in Rydbergs) for the other ion and so at large internuclear separations, the tails of the potential cannot match well. However, at reasonable separations, the $1/R$ character of the potential does not invalidate the potential match criterion for radii selection. This match for the atomic potentials is applied to the self-consistent potentials.

In molecules with significant charge sharing in the bonds, the radii of the atomic spheres is frequently increased in X_α calculations so that an overlap region appears in the vicinity of the bond (Reference 36). Studies made at UTRC show that the contribution to the total molecular energy from the exchange integral shows a minimum at the optimum sphere radius or sphere overlap. This provides a sensitive criterion for selecting these parameters.

The values of the exchange parameters in the spherical integration region around each atomic center are frequently set at the atomic values both for neutral and for ionic molecular constituents. However, for light atoms, the value of α which best reproduces Hartree-Fock results varies substantially with ionicity. In argon, the following table compares, for the neutral atom and the positive ion, the HF energy and the X_α energy calculated for several values of α .

	α	X α Energy	HF Energy
Ar ⁰	.72177	526.8176	526.8173
Ar ^{+ 1/2}	.72177	526.5857	-
	.72213	526.6007	-
Ar ^{+ 1}	.72177	526.2447	-
	.72213	526.2596	-
	.72249	526.2745	526.2743

The optimum value of α changes even more rapidly in the fluorine atom going from 0.73732 for F⁰ to 0.72991 for F⁻¹. Since the total energy depends linearly on α , this parameter must be chosen carefully.

The intersphere exchange coefficient is chosen to be a weighted average of the atomic exchange parameters from the two constituents. At small internuclear separations, the optimum radius for an atomic sphere frequently places significant amounts of charge outside that atomic sphere – charge that is still strongly associated with its original center rather than being transferred to the other center or associated with the molecular binding region. To best account for these cases the weighting coefficients are chosen to reflect the origin of the charge in the intersphere (or outersphere region),

$$\alpha_{\text{intersphere}} = \frac{\alpha_{s_1}(Q_{s_1} - Q_1^0) + \alpha_{s_2}(Q_{s_2} - Q_2^0)}{(Q_{s_1} - Q_1^0) + (Q_{s_2} - Q_2^0)} \quad (37)$$

where $(Q_{s_i} - Q_i^0)$ is the charge lost from sphere i relative to its atomic value (or ionic value) Q_i^0 and α_{s_i} is the atomic exchange parameter for sphere i . This value for $\alpha_{\text{intersphere}}$ is calculated dynamically – it is updated after each iteration in the self-consistent calculation.

While for heavy atoms, these changes in the exchange parameter would be small, the α 's for small atoms vary rapidly with z (and with ionicity). The correct choice of the exchange parameters influences not only the total energy calculated for the molecule but also in some cases affects the distribution of charge between the atomic spheres and the intersphere region.

2.1.3 *Ab Initio* Gaussian Wavefunction Electronic Structure Codes.

Owing to the complexity of evaluating multicenter electron repulsion integrals over Slater-type (exponential) orbitals, various groups have adopted a computational approach to electronic structure calculations based on gaussian orbitals. A highly developed series of

programs, named GAUSSIAN 8X ($X = 2, 6, 8$), is available from Carnegie-Mellon University (Reference 21). A second series of programs has evolved from the original version of Dupuis and King's (Reference 37) HONDO code. This code has been further developed by separate groups as GAMESS (Reference 22), CADPAC (References 38) and HONDO 7 (Reference 39). Finally a new code named COLUMBUS (Reference 40 and 41) has been developed by the Ohio State/Argonne/Battelle group. UTRC has been designated as a beta test site for this new development. A brief description of the features of these codes follows.

2.1.3.1 GAUSSIAN 88/90. GAUSSIAN 88/90 is a connected system of programs for performing *ab initio* molecular orbital (MO) calculations. It represents further development of the GAUSSIAN 70/76/80/82/86 systems already published. The contributors to this program include: M. J. Frisch, J. S. Binkley, H. B. Schlegel, K. Raghavachari, C. F. Melius, R. L. Martin, J. J. P. Stewart, F. W. Bobrowicz, C. M. Rohlfing, L. R. Kahn, D. J. Defrees, R. Seeger, R. A. Whiteside, D. J. Fox, E. M. Fleuder, and J. A. Pople. GAUSSIAN 8X was originally implemented on the chemistry department DEC VAX 11/780 computer at Carnegie-Mellon University. Since then this program has been installed on a number of different computers.

GAUSSIAN 88/90 was designed with a transparent input data stream, making this program very user friendly. All of the standard input is free-format and mnemonic. Reasonable defaults for input data have been provided, and the output is intended to be self-explanatory. Mechanisms are available for the sophisticated user to override defaults or interface their own code to the GAUSSIAN system. In this respect, we have utilized GAUSSIAN 88/90 as a fundamental framework for several applications. Options are being incorporated into this code to provide capabilities beyond Hartree-Fock and various perturbation theory options.

The capabilities of the GAUSSIAN 88/90 system include:

- a) Calculation of one- and two-electron integrals over s, p, d, and f contracted gaussian functions. The basis functions can either be cartesian gaussians or pure angular momentum functions and a variety of basis sets are stored in the program and can be requested by name.
- b) Self-consistent field calculations for restricted closed-shell (RHF), unrestricted open-shell (UHF), and open-shell restricted (ROHF) Hartree-Fock wavefunctions as well as those types of multiconfigurational wavefunctions that fall within the Generalized Valence Bond-Perfect Pairing (GVB-PP) formalism.
- c) Evaluation of various one-electron properties of the Hartree-Fock wavefunction, including Mulliken population analysis, multipole moments, and electrostatic fields.
- d) Automated geometry optimization to either minima or saddle points, and analytical or numerical differentiation to produce force constants, polarizabilities, and dipole

derivatives. This feature can be used to develop minimum energy reaction paths along a complicated many dimensional potential energy surface.

- e) Correlation energy calculations using Møller–Plesset perturbation theory carried to second, third, or fourth order.
- f) Correlation energy calculations using configuration interaction (CI) with either all double excitations (CID) or all single and double excitations (CISD).
- g) Correlation energy calculations using coupled cluster theory with double substitutions (CCD).
- h) Correlation energy calculations using quadratic convergence SCF (QCSCF). This is a new highly efficient size-consistent method recently developed by Pople.
- i) Analytic computation of the nuclear coordinate gradient of the RHF, UHF, ROHF, GVB-PP, MP2, CID and RCISD energies.
- j) Computation of force constants (nuclear coordinate second derivatives), polarizabilities, hyperpolarizabilities, dipole derivatives, and polarizability derivatives either analytically or numerically.
- k) Harmonic vibrational analysis.
- l) Determination of intensities for vibrational transitions at the HF, MP2, and CI levels.
- m) Testing the SCF wavefunctions for stability under release of constraints.
- n) Correlated electron densities and properties.
- o) Minimum-energy pathway following from products to reactants through a transition state-intrinsic reaction coordinate finder.

2.1.3.2 GAMESS. A wide range of quantum chemical computations are possible using GAMESS (Reference 22), a refinement by M. Schmidt and S. Elbert of the original HONDO code (Reference 37).

The capabilities of this code include:

- a) Calculations of RHF/UHF/ROHF/GVB-SCF molecular wavefunctions.
- b) Calculations of multiconfiguration SCF (MCSCF) wavefunctions.
- c) Calculations of CI wavefunctions using the unitary group method.
- d) Optimization of molecular geometries using an energy gradient in terms of Cartesian or internal coordinates.

- e) Searches for potential energy surface saddle points.
- f) Tracing the intrinsic reaction path from a saddle point to reactants or products.
- g) Computation of normal modes and vibrational frequencies.
- h) Calculation of the following properties:
 1. dipole, quadrupole, and octupole moments
 2. electrostatic potentials
 3. electric field and electric field gradients
 4. electron density and spin density
 5. Mulliken and Löwdin population analysis
 6. localized orbitals by the Boys method
 7. virial theorem and energy components.

GAMESS is a synthesis, with many major modifications, of several programs. A large part of the program is from HONDO. For pure sp basis sets, the HONDO symmetry and supermatrix procedure has been adapted from GAUSSIAN 76 and GRADSCF integrals, both for the SCF and gradient parts. The GVB section is a heavily modified version of GVBONE. A Boys localization algorithm is implemented from a heavily modified version of Streitweiser's QCPE program.

The CI module is based on Brooks and Schaefer's unitary group program which was modified to run within GAMESS, using a Davidson eigenvector method written by S. T. Elbert. The MCSCF module is a Newton-Raphson procedure, developed at NRCC, based on the unitary group CI package. The intrinsic reaction coordinate pathfinder was written at North Dakota State University.

2.1.3.3 CADPAC. The Cambridge Analytic Derivatives Package (CADPAC) (Reference 38) is a group of programs which has been under development at Cambridge University, UK. It originated as a version of Dupuis and King's HONDO program. From its initial state as an SCF gradient package for closed-shell and UHF wavefunctions, this program has been extensively modified with many of the old features being enhanced and many new features being added. The input data is now in free format with a 'keyword' system, to make the program easier to use. The integral routines use essentially the same methods as those in HONDO, being based on the Rys polynomial method, but have been extended to cover f-functions. These routines have also been vectorized to take advantage of the much greater availability of supercomputers such as the Cray in recent years. The SCF programs are by now a blend of techniques, but still contain a few

features from the initial HONDO program, particularly in the way symmetry is handled. There have been many modifications to improve efficiency and the addition of level-shifting and damping techniques and the implementation of the DIIS method to aid convergence. A high-spin open-shell SCF program, and a completely general open-shell SCF program have also been included.

The gradient routines have been considerably altered from those in the original HONDO, the method having been changed to one which is more efficient and easier to extend to higher-order derivatives. These routines also work for f-functions. The original program's capabilities for the calculation of force-constants by numerical differentiation of gradients and for the optimization of geometries remain essentially intact. However there is now a choice of two optimization algorithms with the inclusion of Schlegel's method.

In addition to the above modifications a range of extra facilities were developed. These included a more powerful method of calculating one-electron properties and analyzing molecular charge distributions, and various 'post-SCF' stages, beginning with a 4-index transformation. These new sections include Møller-Plesset perturbation theory for total energies and molecular properties, and coupled Hartree-Fock calculations of molecular polarizabilities. The polarizability routines can calculate dynamic properties at real or imaginary frequencies, and obtain dispersion coefficients. It is also possible to use CHF theory to obtain the perturbations due to nuclear displacements. These can be used to obtain, analytically, all the dipole and quadrupole moment derivatives of a molecule. They also form part of the most important addition to the package, the section which calculates analytic second derivatives of the energy. This is a powerful technique whose speed and accuracy represents a considerable improvement over numerical differentiation.

The capabilities of the latest CADPAC code (Version 4) include:

- a) the evaluation of one- and two-electron integrals over contracted cartesian gaussian basis functions of type s, p, d, or f.
- b) SCF calculations for closed shell, open-shell, UHF and generalized open-shell techniques.
- c) calculation of one-electron properties for these types of wavefunction, including a distributed multipole analysis.
- d) calculation of the gradients of the SCF energy.
- e) use of the gradients for automatic geometry optimization, and for the calculation of force constants by numerical differentiation. There is a choice of two optimization algorithms.
- f) transformation of the integrals from the atomic orbital to the molecular orbital basis.

- g) Møller-Plesset perturbation theory calculations to third order in the energy and second order in the one-electron properties.
- h) coupled Hartree-Fock calculations of polarizabilities, including frequency dependence, and magnetizabilities.
- i) coupled Hartree-Fock calculations of the perturbation due to nuclear displacements.
- j) calculation of the dipole and quadrupole moment derivatives.
- k) calculation of the second derivatives (force constants) of the energy by analytic methods.
- l) analytic calculations of polarizability derivatives.
- m) calculation of infrared and Raman intensities, and the study of vibrational circular dichroism.
- n) calculation of MP2 gradients, dipole moment derivatives, polarizabilities and force constants using analytic algorithms.
- o) spin-projected UHF MP2 energies

2.1.3.4 HONDO. The HONDO program, (Reference 37) originally developed by Dupuis and King at NRCC has recently been refined and updated by M. Dupuis at IBM-Kingston (Reference 39).

The following features are available in the present version (HONDO 7) of the program:

- a) Single configuration self-consistent-field wavefunctions (closed shell RHF, spin unrestricted UHF, restricted open shell ROHF), generalized valence bond GVB and general multiconfiguration self-consistent-field MCSCF wavefunctions, and configuration interaction CI wavefunctions can be calculated.
- b) The electron correlation correction to the energy of closed shell RHF wavefunctions can be calculated by means of Møller-Plesset (MP) perturbation theory applied to second-, third-, and fourth-order (with or without the effects of triple excitations).
- c) The effective core potential approximation can be used.
- d) Optimization of molecular geometries using the gradient of the energy with respect to nuclear coordinates is possible with all but the CI and MP wavefunctions. Optimization can be carried out in the cartesian space or in the internal coordinate space with the possibility of freezing some cartesian or internal coordinates.

- e) The force constant matrix in the cartesian space, and the vibrational spectrum, including infrared and Raman intensities, can be calculated with all but the CI and MP wavefunctions.
- f) Calculation of the dipole moment and polarizability derivatives with respect to the nuclear coordinates is possible, for use with a previously calculated force constant matrix. The force constant matrix can be transformed to the internal coordinate basis.
- g) Transition state structures can be determined with all but the CI and MP wavefunctions by taking advantage of the energy gradients.
- h) The 'Intrinsic Reaction Coordinate' (IRC) pathway can be determined with all but the CI and MP wavefunctions by taking advantage of the energy gradients.
- i) Molecular energies for several points on a potential energy surface can be calculated in a single run.
- j) Non-gradient optimization of basis function exponents is possible. The source code can be modified to carry out optimization of other non-linear parameters, for example, contraction coefficients and geometrical parameters.
- k) The following electronic properties can be extracted from the wavefunction:
 - 1. dipole moment
 - 2. quadrupole moment
 - 3. Mulliken population, bond order and valency analyses
 - 4. spin density maps
 - 5. electron density maps
 - 6. electrostatic potential maps
 - 7. localized orbitals via Boys' method
 - 8. static dipole polarizability
 - 9. static first and second hyperpolarizabilities.
- l) The potential due to finite point charges for a classical representation of an environment, or a uniform electric field can be incorporated into the one-electron Hamiltonian.

2.1.3.5 COLUMBUS. The COLUMBUS code (Reference 40 and 41) is a continuing development based on a joint project at Ohio State University (I. Shavitt), University of Karlsruhe

(R. Ahlrichs), and Argonne National Laboratory (R. Shepard). The unique features of this code are the incorporation of relativistic or non-relativistic core potentials to permit analysis of heavy atom molecular systems and the inclusion of a sophisticated CI package based on the unitary group approach of Shavitt (Reference 42). The basic programs included in the COLUMBUS code are as follows.

1. AO Integrals

This is R. Pitzer's version of the integral package from HONDO with partial vectorization of auxiliary integral routines. This package can handle up to g-functions.

2. Integral Transformation

The transformation algorithm is written over all the orbitals which constitute a shell, using contraction coefficients defined over the primitive basis functions. Limited vectorization is possible over the innermost loops for dyadic operations.

3. SCF Gradients

These routines are based on the HONDO version but include checks on integral symmetry to avoid operations over zero or near zero elements. At this time, only a first derivative analysis has been included.

4. SCF Energy

The SCF routines are typical of those found in the molecular structure codes. They incorporate level shifting, damping and the incorporation of Pulay's DIIS convergence acceleration procedure.

5. MCSCF Analysis

The MCSCF package is due to R. Shepard and incorporates extensive vectorization. The output vectors can be taken directly from this package and transferred to the CI program.

6. Multireference Direct CI

This set of routines is based on the graphical representation of the unitary group approach (GUGA) for constructing a CI wavefunction. This code differs from conventional CI in that a matrix representation of the hamiltonian is not explicitly computed. The unitary group approach can be much more efficient in most applications since ~80% of the hamiltonian matrix elements are usually zero but must still be included. This leads to the storage and diagonalization problems associated with large, sparse matrices. However, little work has been done on analysis of excited states with the same molecular symmetry as the ground state. An approach that looks promising is to define an approximate vector corresponding to the excited state wavefunction and to iteratively improve upon this solution using the direct CI contraction. The uncertainties in the procedure are applications to situations where degeneracies or near-degeneracies arise. Further studies of this case are in progress.

2.1.4 Spin-Projected Unrestricted Hartree-Fock Method.

The unrestricted Hartree-Fock (UHF) method developed by Pople and Nesbet (References 43 and 44) yields the best single-determinant approximation to the exact wavefunction for an atomic or molecular system. Such a wavefunction incorporates correlation by allowing orbitals of different spin to adjust to spatially different forms, thus breaking the symmetry restrictions of the conventional (RHF) method (References 45 and 46). It is necessary, however, to project from such a wavefunction, a properly antisymmetrized spin and angular momentum state in order to define eigenstates and eigenenergies corresponding to observable spectroscopic states.

Let $|\alpha\rangle, |\beta\rangle$ refer to the doubly-occupied molecular orbitals (MO's), ϕ_α, ϕ_β . Let $|\gamma\rangle, |\delta\rangle, |\tau\rangle$ refer to the singly occupied MO's. We assume that all MO's have been subjected to a transformation to orthogonal form. Let $C_{\gamma\delta}$ be the coefficient associated with the permutation $\gamma \longleftrightarrow \delta$ (this permutation is (-1) times the overlap of the permuted spin eigenfunction with the original spin eigenfunction), and adopt the convention $C_{\gamma\gamma} = -1$. Then the expectation value of the nonrelativistic Hamiltonian

$$\mathcal{H} = \sum_i U(i) + \sum_{i<j} V(i,j) \quad (38)$$

is given by

$$\begin{aligned} \langle \mathcal{H} \rangle = & 2 \sum_\alpha \langle \alpha | U | \alpha \rangle + \sum_\gamma \langle \gamma | U | \gamma \rangle + 2 \sum_{\alpha\beta} \langle \alpha\beta | V | \alpha\beta \rangle \\ & - \sum_{\alpha\beta} \langle \alpha\beta | V | \beta\alpha \rangle + 2 \sum_{\alpha\gamma} \langle \alpha\gamma | V | \alpha\gamma \rangle - \sum_{\alpha\gamma} \langle \alpha\gamma | V | \gamma\alpha \rangle \\ & - \frac{1}{2} \sum_{\gamma\delta} \langle \gamma\delta | V | \gamma\delta \rangle + \frac{1}{2} \sum_{\gamma\delta} C_{\gamma\delta} \langle \gamma\delta | V | \delta\gamma \rangle \end{aligned} \quad (39)$$

where i, j refer to electron numbers, $\alpha, \beta, \gamma, \delta$ etc., refer to MO's and the sums run over all α, β, \dots

The equations for determining the optimum MO's can be derived from the following variational form

$$\delta \left[\langle \mathcal{H} \rangle - 2 \sum_{\alpha\beta} \epsilon_{\alpha\beta} \langle \alpha | \beta \rangle - \sum_{\alpha\beta} (\epsilon_{\gamma\alpha} \langle \alpha | \gamma \rangle + \epsilon_{\alpha\gamma} \langle \gamma | \alpha \rangle) - \sum_{\gamma\delta} \epsilon_{\gamma\delta} \langle \gamma | \delta \rangle \right] = 0 \quad (40)$$

These equations are

$$(U + 2J_c - K_c + J_o - \frac{1}{2}K_o) | \alpha \rangle = \sum_{\beta} \epsilon_{\beta\gamma} | \beta \rangle + \frac{1}{2} \sum_{\delta} \epsilon_{\delta\alpha} | \delta \rangle \quad (41)$$

$$(U + 2J_c - K_c + J_o) | \gamma \rangle + \sum_{\delta} C_{\gamma\delta} | \langle \delta | V | \gamma \rangle \delta \rangle = \sum_{\beta} \epsilon_{\beta\gamma} | \beta \rangle + \sum_{\delta} \epsilon_{\delta\gamma} | \delta \rangle \quad (42)$$

where

$$| \langle \delta | V | \gamma \rangle \delta \rangle = \int d\vec{r} \phi_{\delta}^*(\vec{r}) V(\vec{r}, \vec{r}) \phi_{\gamma}(\vec{r}) \phi_{\delta}(\vec{r})$$

$$\langle W | V | W' \rangle = \int d\vec{r} W^+(\vec{r}) V(\vec{r}, \vec{r}) W'(\vec{r}) \quad (43)$$

$$J_c = \sum_{\beta} \langle \beta | V | \beta \rangle \quad J_o = \sum_{\delta} \langle \delta | V | \delta \rangle$$

$$K_c | W \rangle = \sum_{\beta} | \langle \beta | V | W \rangle \beta \rangle \quad K_o | W \rangle = \sum_{\delta} | \langle \delta | V | W \rangle \delta \rangle$$

Left-multiplying Equation (41) by $\langle \gamma |$ and Equation (42) by $\langle \alpha |$, these equations can be combined to yield

$$\epsilon_{\gamma\alpha} = \sum_{\delta} (2C_{\gamma\delta} + 1) \langle \gamma\delta | V | \delta\alpha \rangle \quad (44)$$

Noting that

$$\sum_{\gamma} C_{\gamma\tau} \langle \delta\tau | V | \tau\gamma \rangle = \sum_{\tau} C_{\delta\tau} \langle \delta\tau | V | \tau\gamma \rangle, \quad (45)$$

Equations (41) and (42) can be recast as follows. From Equation (41),

$$\frac{1}{2} \sum_{\delta} \epsilon_{\delta\alpha} | \delta \rangle = \frac{1}{2} M | \alpha \rangle \quad (46)$$

with

$$M = \sum_{\delta\tau} (2C_{\delta\tau} + 1) | \delta \rangle \langle \tau | \langle \delta | V | \tau \rangle |$$

From Equation (42),

$$\sum_{\beta} \epsilon_{\beta\gamma} | \beta \rangle = \sum_{\beta\tau} (2C_{\gamma\tau} + 1) | \beta \rangle \langle \beta\tau | V | \delta\gamma \rangle = o_c M^{\dagger} | \gamma \rangle \quad (47)$$

with

$$o_c = \sum_{\beta} | \beta \rangle \langle \beta |; \quad o_o = \sum_{\delta} | \delta \rangle \langle \delta | \quad (48)$$

Using Equations (47) and (48) in (41) and (42), we find

$$(U + 2J_c - K_c + J_o - \frac{1}{2}K_o - \frac{1}{2}M)|\alpha\rangle = \sum_{\beta} \epsilon_{\beta\alpha}|\beta\rangle \quad (49)$$

$$(U + 2J_c - K_c + J_o - \frac{1}{2}K_o + \frac{1}{2}M^\dagger - \alpha_c M^\dagger)|\gamma\rangle = \sum_{\delta} \epsilon_{\delta\gamma}|\delta\rangle \quad (50)$$

Finally, Equations (49) and (50) can be rearranged to yield the same Hermitian operator on the left-hand side with the resulting definition of the one-electron eigenenergies for the closed and open-shell eigenstates:

$$\epsilon_{\alpha'} = \langle \alpha | U + 2J_c - K_c + J_o - \frac{1}{2}K_o | \alpha \rangle \quad (51)$$

$$\epsilon_{\gamma'} = \langle \gamma | U + 2J_c - K_c + J_o - \frac{1}{2}K_o + \frac{1}{2}M^\dagger | \gamma \rangle \quad (52)$$

Equations (51) and (52) represent the correct one-electron energy expressions for the spin-projected eigenstate.

This formalism has been developed to extend the conventional HF method to include split-shell correlation and proper spin and symmetry projections. It is being incorporated into a computer program using gaussian-type orbitals (GTO's) as the elementary basis functions. A crucial feature of this method is that dissociation always follows the lowest energy pathway thereby permitting a proper description of bond formation and breakage. In contrast, RHF or MC-SCF methods often exhibit improper dissociation character or exhibit size inconsistencies owing to correlation energy changes in going from molecular geometries to separated atom-molecule or atom-atom dimensions.

2.2 TRANSITION PROBABILITIES.

The electronic and vibrational-rotational wavefunctions of a pair of states can be used to calculate transition probabilities. If two molecular states are separated in energy by an amount

$\Delta E_{nm} = hc\nu$ (h = Planck's constant, c = velocity of light, ν = frequency in wave numbers), the semi-classical theory of radiation (References 47 and 48) yields for the probability of a spontaneous transition from an upper state n to a lower state m

$$A_{nm} = \frac{4}{3} \frac{\Delta E_{nm}^3}{\hbar^4 c^3} \frac{S_{nm}}{g_n} \quad (53)$$

Here A_{nm} is the Einstein coefficient for spontaneous transition from level $n \rightarrow m$, g_n is the total degeneracy factor for the upper state

$$g_n = (2 - \delta_{\sigma, \Lambda'}) (2S' + 1) (2J' + 1) \quad (54)$$

and S_{nm} is the total strength of a component line in a specific state of polarization and propagated in a fixed direction. A related quantity is the mean radiative lifetime of state n defined by

$$\frac{1}{\tau_n} = \sum_{m < n} A_{nm} \quad (55)$$

the summation being over all lower levels which offer allowed connections. The intensity of the emitted radiation is

$$I_{nm} = \Delta E_{nm} N_n A_{nm} \quad (56)$$

where N_n is the number density in the upper state n . This analysis assumes that all degenerate states at the same level n are equally populated, which will be true for isotropic excitation. The total line strength S_{nm} can be written as the square of the transition moment summed over all

degenerate components of the molecular states n and m :

$$S_{nm} = \sum_{i,j} |M_{ji}|^2 \quad (57)$$

where j and i refer to all quantum numbers associated collectively with upper and lower electronic states, respectively.

In the Born-Oppenheimer approximation, assuming the separability of electronic and nuclear motion, the wavefunction for a diatomic molecule can be written as

$$\psi'_{vJM\Lambda} = \psi'_{el}(\vec{r}, R) \psi_v(R) \psi_{JM\Lambda}(\theta, \chi, \phi) \quad (58)$$

where $\psi'_{el}(\vec{r}, R)$ is an electronic wavefunction for state i at fixed internuclear separation R , $\psi_v(R)$ is a vibrational wavefunction for level v , and $\psi_{JM\Lambda}(\theta, \chi, \phi)$ refers to the rotational state specified by electronic angular momentum Λ , total angular momentum J and magnetic quantum number M . The representation is in a coordinate system related to a space-fixed system by the Eulerian angles (θ, χ, ϕ) . The transition moment M_{ji} can be written, using the wavefunction given by Equation (58), as

$$M_{ji} = \int \psi_{v'J'\Lambda'M'}^j \{ \vec{M}^e + \vec{M}^n \} \psi_{v''J''\Lambda''M''} \psi_{JM\Lambda} d\tau_e d\tau_v d\tau_r \quad (59)$$

The subscripts e , v and r refer to the electronic, vibrational and rotational wavefunctions and \vec{M}^e and \vec{M}^n are the electronic and nuclear electric dipole moments, respectively. Integration over the electronic wavefunction, in the Born-Oppenheimer approximation, causes the contribution of the nuclear moment \vec{M}^n to vanish for $i \neq j$. The electronic dipole moment can be written (References 48 and 49) in the form

$$\vec{M}^e = - \sum_k e \vec{r}_k' = - \left\{ \sum_k e \vec{r}_k \right\} \cdot \vec{\mathfrak{D}}(\theta, \chi, \phi) \quad (60)$$

where the primed coordinates refer to the space fixed system, the coordinates \vec{r}_k refer to a molecule-fixed system and $\vec{\mathfrak{D}}(\theta, \chi, \phi)$ is a group rotation tensor whose elements are the direction

cosines related to the Eulerian rotation angles (θ, χ, ϕ) . Using bracket notation, Equations (59) and (60) can be combined to yield for the transition moment

$$M_{ji} = M_{iv''J''\Lambda''M''}^{jv'J'\Lambda'M'} = \langle j|v'| - \sum_k e\tilde{r}_k |iv'' \rangle \cdot \langle J'\Lambda'M' | \mathfrak{D}(\theta, \chi, \phi) | J''\Lambda''M'' \rangle \quad (61)$$

The matrix elements $\langle J'\Lambda'M' | \mathfrak{D}(\theta, \chi, \phi) | J''\Lambda''M'' \rangle$ determine the group selection rules for an allowed transition and have been evaluated for many types of transitions (References 50-52). Summing Equation (61) over the degenerate magnetic quantum numbers M' and M'' we have from Equation (57)

$$S_{nm} = S_{mv''J''\Lambda''}^{nv'J'\Lambda'} = \mathfrak{F}_{J''\Lambda''}^{J'\Lambda'} p_{mv''}^{nv'} \quad (62)$$

where $\mathfrak{F}_{J''\Lambda''}^{J'\Lambda'}$ is the Hönl - London factor (References 53 and 54) and

$$p_{mv''}^{nv'} = \sum_{ij} |\langle jv'| - \sum_k e\tilde{r}_k |iv'' \rangle|^2 \quad (63)$$

is the band strength for the transition. Combining Equations (54), (56) and (62), we have for the intensity of a single emitting line from upper level n :

$$I_{nm} = i_{mv''J''}^{nv'J'} = \frac{4}{3} N_{J'} \frac{[\Delta E_{mv''J''}^{nv'J'}]^4 S_{mv''J''\Lambda''}^{nv'J'\Lambda'}}{\hbar^4 c^3 \omega_n (2J' + 1)} \quad (64)$$

where $N_{J'}$ is the number density in the upper rotational state J' and $\omega_n = (2 - \delta_{o\Lambda}) (2S' + 1)$ is the electronic degeneracy. Taking an average value of $\Delta E_{mv''J''}^{nv'J'}$ for the whole band, Equation (64) can be summed to yield the total intensity in the (v', v'') band:

$$I_{mv''}^{nv'} = \sum_{J'J''} I_{mv''J''}^{nv'J'} = \frac{4}{3} N_{v'} \frac{[\Delta E_{mv''}^{nv'}]^4 p_{mv''}^{nv'}}{\hbar^4 c^3 \omega_n} \quad (65)$$

where $N_{v'} = \sum_{J'} N_{J'}$ is the total number density in the upper vibrational level v' and where we make use of the group summation property

$$\sum_{J''} J_{J''}^{J' \Lambda'} = (2J' + 1) \quad (66)$$

Comparing Equations (56) and (65) we have for the Einstein spontaneous transition coefficient of the band (v', v'')

$$A_{mv''}^{nv'} = \frac{4}{3} \frac{[\Delta E_{mv''}^{nv'}]^3 p_{mv''}^{nv'}}{\hbar^4 c^3 \omega_n} \quad (67)$$

Similarly, the lifetime of an upper vibrational level v' of state n can be written

$$\frac{1}{\tau_n} = \sum_{m < n} \sum_{v''} A_{mv''}^{nv'} \quad (68)$$

where the summation runs over all v'' for each lower state m . Equation (67) can be cast in the computational form

$$A_{mv''}^{nv'} (\text{sec}^{-1}) = \frac{(21.41759 \times 10^9)}{\omega_n} [\Delta E_{mv''}^{nv'} (\text{a.u.})]^3 p_{mv''}^{nv'} (\text{a.u.}) \quad (69)$$

where $\Delta E_{mv''}^{nv'}$ and $p_{mv''}^{nv'}$ are in atomic units. It is also often convenient to relate the transition probability to the number of dispersion electrons needed to explain the emission strength classically. This number, the f -number or oscillator strength for emission, is given by

$$f_{nm, v'v''} = \frac{mc^3 \hbar^2}{2e^2 [\Delta E_{mv''}^{nv'}]^2} A_{mv''}^{nv'} \quad (70)$$

The inverse process of absorption is related to the above development through the Einstein B coefficient. Corresponding to Equation (56), we have for a single line in absorption

$$\frac{I_{mn}}{I_0 \Delta x} = \int_{\text{line}(v'v''J''J')} K(\nu) d\nu = h\nu_{mn} N_m B_{mn} \quad (71)$$

where $K(\nu)$ is the absorption coefficient of a beam of photons of frequency ν and

$$B_{mn} = B_{mn}^{nv', J', \Lambda'} = \frac{2\pi}{3\hbar^2 c} \frac{S_{mn}^{nv', J', \Lambda'}}{\omega_m (2J'' + 1)} \quad (72)$$

is the Einstein absorption coefficient for a single line. Summing over all lines in the band (v'', v') , assuming an average band frequency, we obtain

$$\frac{I_{mn}^{nv''}}{I_v^0 \Delta x} = N_{v''} \frac{2\pi}{3\hbar^2 c \omega_m} p_{mn}^{nv''} \overline{\Delta E_{mn}^{nv''}} \quad (73)$$

where $N_{v''} = \sum_{J''} N_{J''}$ is the total number density in the lower vibrational state v'' . Corresponding to Equations (69) and (70) we can define an f-number or oscillator strength for absorption as

$$f_{mn, v'' v'} = \frac{2m \overline{\Delta E_{mn}^{nv'}}}{3\hbar^2 e^2 \omega_m} p_{mn}^{nv'} \quad (74)$$

In computational form, Equation (74) becomes

$$f_{mn, v'' v'} = \frac{2}{3} \cdot \frac{\overline{\Delta E_{mn}^{nv'}} (\text{a.u.})}{\omega_m} p_{mn}^{nv'} (\text{a.u.}) \quad (75)$$

where $\overline{\Delta E_{mn}^{nv'}}$ and $p_{mn}^{nv'}$ are in atomic units. Combining Equations (67) and (70) and comparing with Equation (74), we see that the absorption and emission f-numbers are related by

$$f_{mn, v'' v'} = \left(\frac{\omega_n}{\omega_m} \right) f_{nm, v' v''} \quad (76)$$

Some caution must be observed in the use of f-numbers given either by Equations (70) or (74) since both band f-numbers and system f-numbers are defined in the literature. The confusion arises from the several possible band averaging schemes that can be identified.

An integrated absorption coefficient (density corrected) can be defined from Equation (73) as

$$S_{v'',v'} = \frac{1}{P_c} I_{mv''}^{nv''} = N_{v''} B_{v'',v'} (1 - \exp \frac{-hc\nu_{v'',v'}}{kT}) h \frac{\nu_{v'',v'}}{P_c^2} \quad (77)$$

where the exponential factor corrects for stimulated emission. Equation (77) can be written in terms of the absorption f-number as

$$S_{v'',v'} = \frac{\pi e^2}{mc^2} \frac{N_{v''}}{P} (1 - \exp \frac{-hc\nu_{v'',v'}}{kT}) f_{mn,v''v'} \quad (78)$$

Using $hc/k = 1.43880 \text{ cm-K}$, we obtain a computational formula for the integrated absorption coefficient as $S_{v'',v'} (\text{cm}^{-2} \text{atm}^{-1}) =$

$$2.3795 \times 10^7 \left(\frac{273.15}{T(\text{K}^\circ)} \right) \left(\frac{N_{v''}}{N_T} \right) \left(1 - \exp \frac{1.43880 \nu_{v'',v'} (\text{cm}^{-1})}{T} \right) \cdot f_{mn,v''v'} \quad (79)$$

The total integrated absorption is found from

$$S_{\text{TOTAL}} = \sum_{v''} \sum_{v'} S_{v'',v'} \quad (80)$$

where, under normal temperature conditions, only the first few fundamentals and overtones contribute to the summations.

The developments given above are rigorous for band systems where an average band frequency can be meaningfully defined. Further approximations, however, are often made. For example, the electronic component of the dipole transition moment can be defined as

$$\mathfrak{D}_{ji}(R) = \langle j | - \sum_k e \vec{r}_k | i \rangle \quad (81)$$

This quantity is often a slowly varying function of R and an average value can sometimes be chosen. Equation (63) can then be written approximately in factored form as

$$P_{mv''}^{nv''} \approx q_{v''v'} \sum_{ij} |\overline{\mathfrak{D}_{ji}(R)}|^2 \quad (82)$$

where $q_{v''v'}$, the square of the vibrational overlap integral, is called the Franck-Condon factor. \mathfrak{D}_{ji} is evaluated at some mean value of the internuclear separation R . In addition, it is sometimes

possible to account for a weak R-dependence in \bar{M}^e by a Taylor series expansion of this quantity about some reference value, $R_{a\beta}$ usually referred to the (0, 0) band. We have,

$$\mathfrak{R}_{ji} \approx \mathfrak{R}_{ji}^{a\beta} \left[1 + a(R - R_{a\beta}) + b(R - R_{a\beta})^2 + \dots \right] \quad (83)$$

Substituting into Equation (83) and integrating yields

$$p_{mv'}^{nv'} \approx q_{v'v''} \sum_{ij} |\mathfrak{R}_{ji}^{a\beta} [1 + a(\overline{R_{v'v''}} - R_{a\beta}) + b(\overline{R_{v'v''}} - R_{a\beta})^2 + \dots]|^2 \quad (84)$$

where

$$\overline{(R_{v'v''} - R_{a\beta})} = \frac{\langle v' | (R - R_{a\beta}) | v'' \rangle}{\langle v' | v'' \rangle} \quad (85)$$

is the R-centroid for the transition and

$$\overline{(R_{v'v''} - R_{a\beta})^2} = \frac{\langle v' | (R - R_{a\beta})^2 | v'' \rangle}{\langle v' | v'' \rangle} \quad (86)$$

is the R^2 -centroid. Note that this last term differs (to second order) from the square of the R-centroid. An alternate procedure can be developed by evaluating Equation (81) at each R-centroid, $\bar{R}_{v'v''}$. Then

$$p_{mv'}^{nv'} \approx q_{v'v''} \sum_{ij} |\mathfrak{R}_{ji}(\bar{R}_{v'v''})|^2 \quad (87)$$

Equation (87) assumes that the vibrational wavefunction product $\psi_{v'}\psi_{v''}$, behaves like a delta function upon integration,

$$\psi_{v'}\psi_{v''} = \delta(R - \bar{R}_{v'v''})\langle v' | v'' \rangle \quad (88)$$

The range of validity of Equation (87) is therefore questionable, particularly for band systems with bad overlap conditions such as oxygen Schumann-Runge. The range of validity of the R-centroid approximation has been examined by Frazer (Reference 55).

The final step in calculating transition probabilities is the determination of $\mathfrak{R}_{ji}(R)$, the electronic dipole transition moment, for the entire range of internuclear separations, R , reached in the vibrational levels to be considered. This can be expressed in terms of a CI expansion as

$$\mathfrak{R}_{ji}(R) = \sum_{\mu\nu} c_{\mu}^j * c_{\nu}^i \langle \psi_{\mu}(R) | \tilde{M}^e | \psi_{\nu}(R) \rangle \quad (89)$$

where c_{μ}^j and c_{ν}^i are coefficients for ψ_{e1}^j and ψ_{e1}^i , respectively.

An analysis similar to that yielding Equations (10) and (11) gives

$$\langle \psi_{\mu}(R) | \tilde{M}^e | \psi_{\nu}(R) \rangle = \sum_p \epsilon_p \langle \theta_{Ms} | O_{SP} | \theta_{Ms} \rangle \langle \prod_{k=1}^n \psi_{\mu k}(\tilde{r}_k, R) | \tilde{M}^e P | \prod_{k=1}^n \psi_{\nu k}(\tilde{r}_k, R) \rangle \quad (90)$$

The spatial integral in Equation (90) reduces to one-electron integrals equivalent to overlap integrals, and the evaluation of Equation (90) can be carried out with any of the standard *ab initio* programs such as DIATOM or GAMESS. Programs for evaluating $\mathfrak{R}_{ji}(R)$ in Equation (89) have been developed at UTRC and examples of their application have appeared in the literature (Reference 8).

For perturbed electronic systems, the transition dipole moment will have a strong R -dependence and R -centroid or other approximations will be invalid. A direct evaluation of Equation (63) would therefore be required using the fully-coupled system of electronic and vibrational wavefunctions to properly account for the source of the band perturbations.

SECTION 3

DISCUSSION OF RELATIVISTIC METHODS

For heavy atoms ($Z \geq 30$), and molecular systems built from heavy atoms, relativistic effects become increasingly important and should be taken into account in the calculation of the radial wavefunctions. The implementation of relativistic effects into atomic and molecular computer codes is only fairly recent owing to the increased complexities introduced in the self-consistent field (SCF) procedure and the greatly increased computer time required for such calculations. Compared with the non-relativistic case, the Dirac-Hartree-Fock (DHF) method requires that two radial functions, G_{nlj} , corresponding to the large component and F_{nlj} , corresponding to the small component must be calculated for each of the two possible j values. Thus, the numerical work of a DHF relativistic treatment is increased by nearly a factor of four over the nonrelativistic case, exclusive of increased complexities in evaluation of the terms of the Hamiltonian. In view of this, methods that have been developed to date for molecular systems have involved the use of model potentials to represent relativistic effects.

In the calculation of the internal energy of a molecular system comprised of n electrons and N nuclei, and considering only electrostatic interactions between the particles, we have for the total Hamiltonian

$$\begin{aligned} \mathcal{H} = \mathcal{H}_{el} - \sum \frac{\hbar^2}{2m_\alpha} \nabla_\alpha^2 + \frac{\hbar^2}{2M_T} \left[\sum_{\substack{\beta=1 \\ \alpha \neq \beta}}^N \sum_{\alpha=1}^N \nabla_\alpha \cdot \nabla_\beta \right. \\ \left. + 2 \sum_{\alpha=1}^N \sum_{i=1}^n \nabla_\alpha \cdot \nabla_i + \sum_{i=1}^n \sum_{\substack{j=1 \\ i \neq j}}^n \nabla_i \cdot \nabla_j \right] \end{aligned} \quad (91)$$

where

$$\mathcal{H}_{el} = - \frac{\hbar^2}{2m_e} \sum_{i=1}^n \nabla_i^2 + V^{el}(\vec{r}_n, \vec{R}_N) \quad (92)$$

where m_e , m_α , M_T , are the masses of the electron, atom α and combined system mass, respectively. Now since the ratios m_e/m_α and M_T are both small, ($2 \times 10^{-6} - 5 \times 10^{-4}$) we can

effect a separation of the electronic and nuclear coordinates treating the total wavefunction as a product of a nuclear and an electronic part. We have

$$\psi(\vec{r}_n, \vec{R}_N) = \sum_k \chi_k(\vec{R}_N) \psi_k(\vec{r}_n, \vec{R}_N) \quad (93)$$

where $\psi_k(\vec{r}_n, \vec{R}_N)$ is an electronic wavefunction parametric in the nuclear coordinates as given in Equation (93) and $\chi_k(\vec{R}_N)$ are nuclear motion wavefunctions which satisfy (neglecting terms of the order of m_e/m_a)

$$\left[- \sum_{a=1}^N \frac{\hbar^2}{2m_a} \nabla_a^2 + \frac{\hbar^2}{2M_T} \sum_{a=1}^N \sum_{\substack{\beta=1 \\ a \neq \beta}}^N \nabla_a \cdot \nabla_\beta + V^{el}(\vec{r}_n, \vec{R}_N) \right] \chi_k = i\hbar \frac{\partial \chi_k}{\partial t} \quad (94)$$

The cross term in $\nabla_a \cdot \nabla_\beta$ can be eliminated by a proper change of variables and Equation (94) then reduces to a $3N-3$ dimensional Schrödinger equation.

For most systems, where the velocity of motion of the nuclei is slow relative to the electron velocity, this decoupling of electronic and nuclear motion is valid and is referred to as the adiabatic approximation. Equation (93) thus defines an electronic eigenstate $\psi_k(\vec{r}_n, \vec{R}_N)$, parametric in the nuclear coordinates, and a corresponding eigenvalue $E_k(\vec{R}_N)$ which is taken to represent the potential energy curve or surface corresponding to state k .

In the usual *ab initio* method for calculating the electronic properties of a molecular system, one starts from a zero-order Hamiltonian that is exact except for relativistic and magnetic effects, and which involves the evaluation of electronic energies and other relevant quantities for wavefunctions that are properly antisymmetrized in the coordinates of all the electrons. For a system containing n electrons and M nuclei, the zero-order Hamiltonian depends parametrically on the nuclear positions and is of the form

$$\mathcal{H}_e = -\frac{1}{2} \sum_{i=1}^n \nabla_i^2 - \sum_{i=1}^n \sum_{j=1}^M \frac{z_i}{|\vec{r}_i - \vec{R}_j|} + \sum_{1 \leq i < j}^M \frac{z_i z_j}{|\vec{R}_i - \vec{R}_j|} + \sum_{1 \leq i < j} \frac{1}{|\vec{r}_i - \vec{r}_j|} \quad (95)$$

where z_i and \vec{R}_i are the charge and position of nucleus i , \vec{r}_j is the position of electron j , and ∇_j^2 is the Laplacian operator for electron j . All quantities are in atomic units, i.e. lengths in bohrs, energies in hartrees (1 hartree = 2 Rydbergs).

In addition to the electrostatic contribution, \mathcal{H}_e , the complete Hamiltonian should contain additional terms which correct for magnetic interactions and relativistic effects. These correction terms may be of importance in several applications. These include:

- (1) calculation of the probability of making a transition from one quantum state to another in high-momentum collisions such as those that can occur in hot atom or heavy atom chemical dynamics experiments;
- (2) determination of the interaction energy in heavy nuclei systems such as Cs_2 and UO^+ , which exhibit open-shell structure on both nuclei at infinite internuclear separations;
- (3) calculation of the intermolecular forces between free radicals, electronically excited states of molecules with open-shell structure, and long molecular conformations of possible biological interest.

3.1 BREIT-PAULI HAMILTONIAN.

The relativistic correction terms to the usual electrostatic Hamiltonian have been derived through order α^2 , where α is the fine structure constant, and are often referred to as the Breit-Pauli (Reference 56) Hamiltonian terms. This Hamiltonian has been derived by Bethe and Salpeter (Reference 57) for a two-electron system and has been generalized to the many-electron system by Hirschfelder, et. al (Reference 58) and Itoh (Reference 59). In the absence of external electric or magnetic fields we can represent these correction terms as follows. Let \vec{s}_j and $\vec{p}_j = \frac{1}{i} \Delta_j$ denote the operators for the spin and linear moment of electron j , respectively. Then the generalized Breit-Pauli Hamiltonian, correct to terms of $\mathcal{O}(\alpha^2/M)$, can be written as:

$$\mathcal{H}_{BP} = \mathcal{H}_e + \mathcal{H}_{LL} + \mathcal{H}_{SS} + \mathcal{H}_{LS} + \mathcal{H}_p + \mathcal{H}_D \quad (96)$$

where \mathcal{H}_e is given by Equation (95) and the correction terms can be expressed as follows:

$$\mathcal{H}_{LL} = -\frac{1}{2} \sum_{1 \leq k \leq j} \frac{1}{r_{jk}^3} \left[r_{jk}^2 \vec{p}_j \cdot \vec{p}_k + \vec{r}_{jk} \cdot (\vec{r}_{jk} \times \vec{p}_j) \vec{p}_k \right] \quad (97)$$

$$\mathcal{H}_{SS} = \sum_{1 \leq k < j} \left\{ - \left(\frac{8\pi}{3} \right) \tilde{s}_j \cdot \tilde{s}_k \delta(\tilde{r}_{jk}) + \frac{1}{r_{jk}^5} \left[r_{jk}^2 (\tilde{s}_j \cdot \tilde{s}_k) - 3(\tilde{s}_j \cdot \tilde{r}_{jk})(\tilde{s}_k \cdot \tilde{r}_{jk}) \right] \right\} \quad (98)$$

$$\mathcal{H}_{LS} = \frac{1}{2} \sum_a \sum_j \left(\frac{z_a}{r_{ja}^3} \right) (\tilde{r}_{ja} \cdot \tilde{p}_j) \cdot \tilde{s}_j - \frac{1}{2} \sum_{1 \leq k < j} \frac{1}{r_{jk}^3} [(\tilde{r}_{jk} \times \tilde{p}_j) \cdot \tilde{s}_j - 2(\tilde{r}_{jk} \times \tilde{p}_k) \cdot \tilde{s}_j] \quad (99)$$

$$\mathcal{H}_p = -\frac{1}{8} \sum_j p_j^4 \quad (100)$$

$$\mathcal{H}_D = \frac{\pi}{2} \left[\sum_a \sum_j z_a \delta(\tilde{r}_{ja}) - 2 \sum_{1 \leq k < j} \delta(\tilde{r}_{jk}) \right] \quad (101)$$

The first correction term, \mathcal{H}_{LL} , represents the magnetic orbit-orbit coupling terms of the electrons arising from the interaction of the magnetic fields created by their motion. The second term, \mathcal{H}_{SS} , gives the spin-spin magnetic coupling terms which are often quite appreciable. For $r_{jk} = 0$, only the delta-function contribution survives which represents the Fermi-contact spin interaction. The third term, \mathcal{H}_{LS} , is usually the largest in magnitude and represents the spin-orbit interaction between the spin and magnetic moment of each electron and the spin-other orbit interaction, which represents the coupling of the spin of one electron with the magnetic moment of a different electron. The term, \mathcal{H}_p , corrects for variation of the electron mass with velocity and the term, \mathcal{H}_D , represents electron spin terms identified by Dirac which appear to have no classical analogue.

Aside from the spin-orbit term, \mathcal{H}_{LS} , usually only the last term, \mathcal{H}_D , (often called the Darwin correction term) and \mathcal{H}_p , the mass-velocity term, are retained in the Hamiltonian, yielding the so-called Pauli approximation (Reference 57).

The eigenfunctions of the Hamiltonian represented by Equation (96) are four-component Dirac spinors which may be expressed as:

$$r\psi_{nkm} = \begin{pmatrix} P_{nk}(r) \chi_{km}(\theta, \phi) \\ iQ_{nk}(r) \chi_{-km}(\theta, \phi) \end{pmatrix} \quad (102)$$

where $\chi_{km}(\theta, \phi)$ are products of spherical harmonics and Pauli spinors and $P_{nk}(r), Q_{nk}(r)$ represent, respectively, the large and small components of the radial wave equation. The exact solution of the Breit-Pauli Hamiltonian has only been given for one- and two-electron atomic systems (Reference 57) owing to the complexity of the operators for the general n -electron case. For a molecular system, Kolos and Wolniewicz (Reference 60) have calculated the relativistic corrections to H_2 using Equation (96) to $O(\alpha^2)$. No heavier molecular systems have been treated using the full Breit-Pauli Hamiltonian.

3.2 APPROXIMATE TREATMENTS.

Although the Breit-Pauli Hamiltonian given in Equation (96) can formally be employed in a molecular system, both the multiplicity of terms and the difficulty of evaluation of the resultant molecular integrals has precluded its general use to date. For atomic systems, various approximate methods of solution, within a Hartree-Fock or multiconfiguration Hartree-Fock framework, have been proposed for atoms (References 61-65). In most of these methods, a restricted Hamiltonian which includes only the one-electron Dirac terms is usually employed. The contributions of the Breit operators for spin-magnetic interactions and velocity retardation are then calculated as first-order perturbations using the zeroth-order Dirac relativistic wavefunctions.

An even more approximate method for incorporating the major relativistic effects has been proposed by Cowan and Griffin (Reference 66). In this method, the mass-velocity (\mathcal{H}_p) and Darwin (\mathcal{H}_D) terms, written in terms of the Pauli equation for one-electron atoms, are simply added to the usual nonrelativistic Hamiltonian operator. In addition, the spin-orbit terms, v , are omitted, thereby reducing the system of equations to a single form representing the description of the major component wavefunction, $P_{nk}(r)$, evaluated at the center-of-gravity of the spin-orbit states. The rationale for this approximation lies in the observation that detailed atomic calculations using the complete DHF method have indicated that, even for an atom as heavy as

uranium, less than 1 percent of the total charge is described by the small component radial wavefunctions.

The resulting equations have the form:

$$\left[-\frac{d^2}{dr^2} + \frac{\ell_i(\ell_i + 1)}{r^2} + v^i(r) + H_m^i(r) + H_D^i(r) \right] G_{n\ell}^i(r) = \epsilon_{n\ell}^i G_{n\ell}^i(r) \quad (103)$$

where the mass-velocity and Darwin terms take the form

$$H_m^i(r) = -\frac{\alpha^2}{4} [\epsilon^i - v^i(r)]^2 \quad (104)$$

$$H_D^i(r) = -\delta_{\ell_i 0} \frac{\alpha^2}{4} \left[1 + \frac{\alpha^2}{4} (\epsilon^i - v^i(r)) \right]^{-1} \left[\frac{dv^i(r)}{dr} \left(\frac{d}{dr} - \frac{1}{r} \right) \right] \quad (105)$$

and $\alpha \approx 1/137.036$ is the fine structure constant. The spin-orbit term is omitted in Equation (103) and thus these equations represent center of gravity radial functions averaged over the two possible total angular momentum quantum numbers. Equation (103) represents (apart from the neglect of spin-orbit effects) the relativistic corrections to first order in α^2 . A more accurate analysis of heavy atom energy levels and spectra is available through the use of the radial functions, $G_{n\ell}^i(r)$, found from Equation (103), and a first-order perturbation calculation. Cowan and Griffin (Reference 66) have illustrated the utility and accuracy of such an approach.

Recently, Wood and Boring (Reference 67) have adapted this approximate relativistic method to the local exchange problem and have implemented the solution of Equation (103) within the context of the multiple scattering X_α method (Reference 22). The central field Hamiltonian is modified to include mass-velocity and Darwin terms, given by Equations (104) and (105), in the sphere surrounding each atomic center. The intersphere region in the multiple scattering approach (constant potential region) is treated nonrelativistically since charge in this region is far from a nucleus and is screened by the charge concentrated around the atomic centers. The matching conditions for continuity of the wavefunction at the sphere boundaries permits any necessary charge transfer between the relativistic intra-atomic regions and the nonrelativistic interatomic constant potential regions. For an atom, the Wood-Boring treatment reduces to the Dirac-Slater local exchange method, but with the neglect of spin-orbit terms.

The implementation of Equation (103) into existing nonrelativistic multiple scattering molecular codes is facilitated by a change in the dependent variable, $G_n^i(r)$, to eliminate the first derivative of the wavefunction, illustrated in Equation (105). The usual Numerov method of solution can then be applied to the central field problem; the only new requirement being the numerical tabulation of the first and second derivatives of the potential at each grid point in the integrations. These derivatives are computed only once for each complete SCF cycle and thus the total required computer time for a typical problem is not significantly increased as compared with a nonrelativistic calculation. A complete self-consistent program incorporating this method has been developed at UTRC. Our code has been tested by repeating calculations for the U and Pu atoms (Reference 66), where we find excellent agreement with the more exact, but cumbersome, Dirac-Slater calculations. Results for molecular calculations have recently been reported by Boring and Wood for UF_6 and UO_2^{++} (References 68 and 69). These calculations were carried out to illustrate the shifts in the valence levels for such systems resulting from relativistic effects. The total energy was not of principal concern.

We have recently reported (Reference 70) the first all-electron calculation of the potential energy curves for a molecule (Hg_2^+) built from atoms which exhibit significant relativistic effects. This study illustrated that reliable total energies are obtainable through a relativistic multiple scattering density functional treatment, provided care is taken to optimize potential match and overlap criteria for such systems. This study formed the basis of the computational scheme that we have employed here for the uranium/oxygen system.

3.3 EFFECTIVE CORE MODELS.

It is well known from chemical experience that the outermost valence electrons contribute most to be determining the chemical properties, especially spectroscopic properties, of molecules. The core electrons remain essentially unchanged from their atomic form except for internuclear separations of the order of the charge radii of the outer core region or less, wherein core polarization effects may become important. Since the computational time required for *ab initio* calculations of electronic structure goes up at least quadratically with the number of electrons in the system, there have been many attempts to replace the more tightly bound core electrons with simple one-electron effective potentials (References 71-79). Concurrent with elimination of an explicit treatment of the core electrons, a transformation of the valence orbital basis is required to insure that the lowest valence orbital of each symmetry has a nodeless radial form, since it is well known that the lowest energy eigenfunction for a local potential must be nodeless (Reference 80).

Typical of the several effective core models that have been reported is that due to Kahn, et al. (Reference 78) whereby an effective core potential is described in terms of angularly dependent projection operators as

$$U^{\text{core}} = U_L^{\text{core}}(r) + \sum_{\ell} \sum_m |\ell m\rangle [U_{\ell}^{\text{core}}(r) - U_L^{\text{core}}(r)] \langle \ell m| \quad (106)$$

where L is taken at least as large as the highest angular momentum orbital occupied in the core. The term $U_L^{\text{core}}(r)$ represents the effective Coulomb and exchange potential felt by the valence electrons. The second term essentially accounts for the repulsive potential between valence and core electrons for each symmetry ℓ . The only non-local character exhibited by a potential of the form of Equation (32) arises from the ℓ -dependence which can be cast in terms of one-electron integrals between the core and valence orbitals. Explicit two-electron terms connecting core and valence orbitals are thus avoided which greatly simplifies the calculation of matrix elements of the effective Hamiltonian. The potential given by Equation (106) can be compared with the generalized Phillips-Kleinman pseudo-potential (Reference 73).

$$U^{\text{core}} = \sum_C (2J_C - K_C) + V^{\text{CO}} \quad (107)$$

where J_C and K_C represent the core orbital Coulomb and exchange operators and V^{CO} is a complicated non-local operator which guarantees core-valence orthogonality. Since the P-K core orbitals must simultaneously be eigenfunctions of both the core and valence Hartree-Fock Hamiltonians, V^{CO} , in general, contains complicated two-electron terms and limits the usefulness of Equation (107) over a full *ab initio* treatment.

The prescription of Kahn can be implemented by analytically fitting a nodeless pseudo-orbital, χ_{nl} , to a linear combination of numerical or analytic Hartree-Fock orbitals determined from a full self-consistent treatment of the core electrons, using, for example, the multiconfiguration Hartree-Fock code of Froese-Fischer (Reference 81). The components, $U_{\ell}^{\text{core}}(r)$, of Equation (106) are then defined implicitly from the Schrödinger equation

$$\left[-\frac{\nabla^2}{2} - \frac{Z}{r} + U_{\ell}^{\text{core}}(r) + 2J_{\text{val}} - K_{\text{val}} \right] \chi_{nl} = \epsilon_{nl} \chi_{nl} \quad (108)$$

whereby

$$U_l^{\text{core}}(r) = \epsilon_{nl} + \frac{Z}{r} + \frac{1}{\chi_{nl}} \left[\frac{\nabla^2}{2} - 2J_{\text{val}} + K_{\text{val}} \right] \chi_{nl} \quad (109)$$

Equation (108) can be extended to relativistic systems in several ways. Kahn, et al. (Reference 82) suggest an approximate treatment of adding only the mass-velocity and Darwin terms to the usual electrostatic Hamiltonian and to determine approximate HF orbitals in the manner prescribed by Cowan and Griffin (Reference 66). Equation (108) is then used to determine an effective $U_l^{\text{core}}(r)$ such that ϵ_{nl} are the eigenvalues of the CG approximate relativistic solution and χ_{nl} are curve-fitted to the CG-HF orbitals. In this treatment, the χ_{nl} represent approximate solutions to the major component wavefunction, P_{nl} , determined at the center-of-gravity of the spin-orbit states.

Lee, et al. (Reference 79) adopt a somewhat more complicated treatment in which the spin-orbit operator is added to the usual electrostatic Hamiltonian, in addition to the mass-velocity and Darwin terms retained in the Cowan-Griffin treatment. The large component eigenfunctions of a full Dirac-Hartree-Fock treatment of the atom, as given, for example, by Desclaux (Reference 83) are then curve-fitted in a manner similar to the Kahn treatment but include the additional index for the particular spin-orbit state, $\chi_{n\ell j}$. Use of these eigenfunctions in a molecular system fits more naturally into a (J-J) coupling scheme whereas the χ_{nl} determined using the Kahn method are more easily represented using $\Lambda - s$ coupling.

Although these effective core models can often accurately describe an atomic eigenvalue sequence, including even high-lying electronically excited states (Reference 84), there are inherent difficulties in their application to molecular environments, where the maximum angular momentum component of the valence shell orbitals may often exceed the highest ℓ -value component retained in Equation (109). This is particularly true for valence orbitals which exhibit strong changes from atomic form through hybridization with higher angular momentum orbitals or through the addition of more compact polarization terms. In either case, since the relativistic terms are now all buried in a fixed rather than a dynamic relativistic operator, only static core effects are imposed in determining the shape of the valence molecular orbitals. Relativistic effects between valence electrons and shielding effects of the core by the valence electrons are therefore neglected in these effective core treatments. In addition, the models obviously break down completely when the nuclei are brought together to dimensions such that core overlap and polarization effects become significant. Unfortunately, calculations to date seem to indicate that such effects begin to set in for internuclear separations of the order of equilibrium bond lengths.

SECTION 4

DISCUSSION OF RESULTS

An analysis of the electronic structure of UO and UO^+ using a relativistic formulation has been undertaken (References 85 and 86). Preliminary calculations were performed for several states of UO and UO^+ and for the ground and excited states of UO_2^+ . An analysis of the IR/visible/UV radiation characteristics of selected band systems in these uranium/oxygen systems has been carried out. Finally, a data base for U^0 , U^{+1} and U^{+2} has been collected for examining the role of dielectronic recombination as a charge neutralization mechanism in the uranium/oxygen system (Reference 87) and a preliminary analysis of the kinetic branchings ratios on $\text{N} + \text{O}_2$ reactions has been performed. A brief summary of the results of these calculations follows.

4.1 UO.

Electronic structure calculations were carried out for this system using a relativistic density functional formalism. Only a selected group of symmetries was studied. Our calculations indicate that the lowest symmetry of UO is derived from the (Λ , S) coupled ^5I state. A vibrational analysis of the $\Omega = 5$ ground state of UO was carried out using a Hulbert-Hirschfelder (Reference 88) fit to our calculated potential curves. This fit yields an equilibrium internuclear distance of 1.89 \AA and a fundamental vibrational constant (ω_e) of 859 cm^{-1} . The spin-orbit interaction was calculated using U^{+2} atomic splitting parameters. No explicit two-center effects are included. Our calculated spectroscopic data are compared with the theoretical work of Krauss and Stevens (Reference 89), the recent rotationally resolved experimental studies of Heaven and Nicolai (Reference 90), the recent rotational analysis reported by Kaledin, et al (Reference 91), and estimates based on experimental data for similar systems. The agreement is well within the uncertainty of the calculations or experimental estimates. The theoretical studies predict a $^5\text{I}_5$ or $^5\text{I}_4$ ground state for UO whereas the experimental data of Heaven and Nicolai (Reference 90) and Kaledin (Reference 91) suggest a $^5\text{I}_4$ ground state. Recent ligand field model calculations by Dulick (Reference 92) predict a $^5\text{I}_1$ ground state for UO, in substantial disagreement with previous theory and experiments. The crystal field model neglects overlap and back charge transfer effects within its $\text{U}^{+2}\text{O}^{2-}$ model, both of which have been found to be of importance in more exact studies carried out within a full molecular framework. The character of all of the low-lying multiplets of UO is similar however, and this apparent discrepancy should not affect our conclusions about optical or LWIR absorptions.

An analysis of the LWIR emission from UO was carried out based on a ground ^5I electronic state. These calculations should also be representative of the LWIR emission from other

low-lying electronic states since they exhibit similar ionicities. Our calculated f-numbers, including fundamentals and overtones, were reported in DNA-TR-82-159. These data ($v' > v''$) were given for the lowest 30 vibrational levels. For UO, our calculated f-number for the 1-0 transition is 4.86×10^{-5} at $\lambda = 12.04 \mu$.

4.2 UO⁺.

Detailed searches of several symmetries of UO⁺ were carried out to determine the ground molecular state of this system. Our calculations indicate that the lowest symmetry of UO⁺ is derived from the (Λ, S) coupled ⁴I state. A vibrational analysis of the $\Omega = 9/2$ ground state of UO⁺ was carried out using a Hulbert-Hirschfelder (Reference 88) fit to our calculated potential curves. The spin-orbit splittings were derived from atomic parameters for the U⁺³ ion. This fit yields an equilibrium internuclear distance of 1.84 Å and a fundamental vibrational constant of 890 cm⁻¹. These data are compared with other calculated estimates, since there are no experimental data available. The agreement between our work and that of Krauss and Stevens (Reference 89) is less satisfactory than in the case of UO, but still well within the uncertainty of the several calculations.

A perturbative treatment for calculating the density of states in uranium molecules is available through the use of ligand field theory. Recent studies by Dulick (Reference 92) predict that the ground state of UO⁺ has $\Omega = 3/2$ in contrast to the effective core hamiltonian calculations of Krauss and Stevens (Reference 89) and our relativistic density functional calculations, both of which predict that the ground state has $\Omega = 9/2$. The neglect of important molecular effects in the ligand field model apparently results in a bias toward lower Ω values.

An analysis of the emission characteristics for the ground state of UO⁺ indicates an oscillator strength for emission (f_{10}) of 5.17×10^{-5} at $\lambda = 11.3 \mu$. A complete analysis of our calculated LWIR emission for UO⁺ was given in DNA-TR-82-159. Our calculated LWIR emission for UO⁺ is typical of that for a highly ionic metal oxide. We predict strong emission from the fundamentals of UO⁺ in the wavelength region 11 – 14 μ . Since this system exhibits weak anharmonicity, we find the overtones down in intensity by several orders of magnitude. However, the first excited state of UO⁺ (⁴H) lies at ~ 1200 cm⁻¹ in our calculations with a predicted electronic oscillator strength of $\sim 1 \times 10^{-5}$ for the ⁴I – ⁴H transition. The electronic and vibrational manifolds for UO⁺ are thus highly overlapped above the second vibrational level of the ground ⁵I_{9/2} state.

A summary of the electronic states of UO⁺ that have been studied, both at NBS (Krauss and Stevens) and at UTRC, is shown in Figure 1. We find (to date) nine electronic states lying in the region .4–.8 μ that are strongly connected to either the ground ⁴I manifold or to the low-lying ⁴H manifold of UO⁺. The calculated f-numbers for the bands ⁴I → ⁴K, ⁴I → ³⁴H,

$1^4\text{I} \rightarrow 2^4\text{H}$ and $1^4\text{I} \rightarrow 1^4\text{H}$ are given in Tables 1, 2, 3 and 4 respectively. We find a considerable shift in R_e for the 3^4H state which offers a route for solar excitation followed by IR radiation. We also show in Table 4 the IR absorption corresponding to the $1^4\text{I} \rightarrow 1^4\text{H}$ transition. Owing to the vertical nature of the potential curves, this behaves similar to a weak vibrational transition.

The photoabsorption strengths for the $1^4\text{I} \rightarrow 2^4\text{I}$, $1^4\text{I} \rightarrow 1^6\text{H}$, and $1^4\text{I} \rightarrow 3^4\text{I}$ transitions are presented in Tables 5-7 respectively. We find that the $1^4\text{I} \rightarrow 2^4\text{I}$ oscillator strengths are large but that most of the absorbed energy will be reradiated in the visible since the transition is nearly vertical. In contrast, the $1^4\text{I} \rightarrow 1^6\text{H}$ transition (Table 6) is an important route for conversion of solar to IR photons, since the oscillator strength is large and the R_e of the excited state is shifted. This transition is not as strong as the $1^4\text{I} \rightarrow 3^4\text{H}$ transition, but is a contributing factor in the total photoabsorption profile. The $1^4\text{I} \rightarrow 3^4\text{I}$ (Table 7) transition reflects the large shift in R_e for the excited state, but the transition moment is weak since this is an $f \rightarrow s$ excitation on uranium.

In both the UTRC and NBS studies, a very low-lying ^4H excited state is found at $T_e \sim 1200 \text{ cm}^{-1}$. Since this state may be thermally populated at short time conditions, the oscillator strengths coupling this 1^4H state to the known six low-lying excited states of UO^+ have been examined. The calculated oscillator strengths are given in Tables 8-13 respectively, for the transitions: $1^4\text{H} \rightarrow 2^4\text{I}$, $1^4\text{H} \rightarrow 2^4\text{H}$, $1^4\text{H} \rightarrow 1^4\text{K}$, $1^4\text{H} \rightarrow 1^6\text{H}$, $1^4\text{H} \rightarrow 3^4\text{H}$ and $1^4\text{H} \rightarrow 3^4\text{I}$. The transitions to 1^4K , 1^6H and 3^4I , show strong oscillator strengths owing to the shifted R_e for the excited states. The overall pattern of solar pumping from the 1^4H state is thus very similar to that from the ground 1^4I state.

Since the density of electronic states of UO^+ is large above $\sim 2.0 \text{ eV}$, we predict that relatively strong solar pumping, followed by both LWIR and visible radiation should occur for this system. This conclusion is similar to that reached by Krauss and Stevens (Reference 89) based on their MCSCF analysis of the UO^+ system. Since several excited electronic states of UO^+ lying in the region of strong solar flux ($.4-.8 \mu$), exhibit shifted equilibrium internuclear separation from that of the ground ^4I state, efficient conversion of solar photons to IR photons is found for this system. At our present level of understanding of the density of low-lying states in UO^+ , we predict that solar pumping of LWIR radiation should be approximately three times the earthshine contribution.

4.3 UO_2^+ .

An analysis of UO_2^+ has been carried out in $D_{\infty h}$ symmetry. McGlynn and Smith (Reference 93) have proposed a $2\Phi_u$ ground state for this ion based on simple molecular orbital arguments. Their set of one-electron orbital energies is based on a maximum overlap criterion

that is empirical in character. More modern calculations of the actinide series atoms suggest that a $U^{+5}[O^{-2}]_2$ or $U^{+3}[O^{-1}]_2$ structure should be the most stable configuration. An extensive series of calculations of the possible low-lying symmetries of UO_2^+ now definitely establish that the symmetry of the ground state is $^2\Phi_u$, but also predict a very low-lying $^2\Delta_u$ state.

A series of calculations of the low-lying electronic states of U^{+3} , U^{+4} and U^{+5} was first undertaken to determine the approximate location of the electronic states of the central ion which corresponded to $f \rightarrow d$ transitions. Strong absorption (dipole-allowed), corresponding to central ion promotion, is predicted to occur only for wavelengths shorter than ~ 300 nm for UO_2^+ . A spin orbit analysis of these calculated levels yields the splittings in J-J coupling. The $^2\Phi_{5/2u}$ state is the predicted ground state multiplet.

In order to establish that $f \rightarrow d$ transitions in UO_2^+ lie at these short wavelengths, a series of molecular calculations of the low-lying electronic states was undertaken. The lowest dipole-allowed $f \rightarrow d$ transitions on the central uranium atom corresponds to the $^2\Phi_u(5f_u) \rightarrow ^2\Delta_g(6d_g)$ excitation at $\lambda \sim 300$ nm. This transition lies beyond the region of efficient solar pumping of UO_2^+ . Hay (Reference 94) reports a similar transition in his effective potential studies of UO_2^+ , but at a somewhat shorter wavelength (~ 250 nm).

A separate molecular spectra for UO_2^+ arises from charge transfer states formed by promotion of an electron from (mainly) ligand MOs to a central uranium atom MO. Careful convergence studies and the employment of a new integration scheme give an equilibrium U-O bond length in UO_2^+ of 1.73 \AA . This value, coupled with a fundamental ν_3 vibrational frequency of 880 cm^{-1} , is in good agreement with Badger's rule (Reference 95) correlating bond lengths and force constants for actinide salts and oxo-ions.

Using these more reliable integration methods, the low-lying charge transfer states of UO_2^+ were re-examined. These charge transfer states, some of which would exhibit very strong absorption, begin at $\sim 47,000 \text{ cm}^{-1}$ [$^4\Pi_u$], with the first strong dipole allowed transitions corresponding to the excitation $1\pi g^4 1\phi u \rightarrow 1\pi g^3 1\phi u^2$. These transitions lie at $53,000 \rightarrow 57,000 \text{ cm}^{-1}$, which correspond to absorption wavelengths in the VUV, well outside of the region for efficient solar pumping. An analysis of the LWIR emission from UO_2^+ has been carried out based on the ground $^2\Phi_{5/2u}$ electronic state. These calculations should also be representative of the LWIR emission from other low-lying electronic states since they all exhibit similar ionicities. For UO_2^+ , our calculated f-number for the 1-0 transition is 1.2×10^{-4} at $\lambda = 11.43 \mu$. This can be compared with a calculated f-number of 5.2×10^{-5} at $\lambda = 11.3 \mu$ for UO^+ . Relatively strong LWIR is therefore predicted for UO_2^+ .

4.4 PHOTOELECTRON SPECTRA OF UO AND UO_2^+ .

A high temperature (2200–2400 K) photoelectron spectrum of UO and UO_2 has recently been reported by Allen, et al. (Reference 96). Although these data are of much lower resolution than those reported for UO by Heaven (Reference 97) and by Kaledin (Reference 98), they represent the first attempt to measure the excitation spectra for UO_2^+ in the gas phase. The measured spectrum is shown in Figure 2 along with tentative assignments of several bands. Allen finds a broad band (F') in the 6–8 eV region, corresponding to low-lying excitation in UO^+ beginning at about 1.2 eV. This agrees nicely with the predicted location by NBS and UTRC of several strong UO^+ band systems as illustrated in Figure 1.

The bands labeled B' and C' can be assigned to excitations in UO_2 beginning at about 4.3 eV. Allen, et al. have assigned these bands to O_{2p} ionization, which would represent charge transfer states in UO_2^+ . These bands should be very strong if they correspond to such charge transfer transitions. We have previously calculated that the $f \rightarrow d$ transition in UO_2^+ should begin at ~ 4 eV and that the charge transfer states should lie above 5.8 eV. Allowing for a possible spin-orbit splitting of ~ 1 eV in UO_2^+ states, our predicted charge transfer states could lie as low as ~ 4.8 eV, thus permitting Allen's B' and C' bands assignments as charge transfer states. However, the $f \rightarrow d$ transitions predicted at 4.0 eV then cannot be assigned to the A' band since this feature should appear at ~ 7.6 eV in the photoelectron spectrum.

A more logical assignment is that the A', B' and C' bands all belong to $f \rightarrow d$ transitions in UO_2^+ and that the (stronger) charge transfer bands appear as the unassigned D' system. The location of this band is in good agreement with our calculations which predict the onset of charge transfer states at ~ 5.8 eV. Further studies of these band assignments in UO_2^+ are in progress but these data of Allen, et al support our conclusion that there are only weak absorptions in UO_2^+ below $0.3 \mu\text{m}$.

4.5 $e + \text{U}^+, e + \text{U}^{++}$ DIELECTRONIC RECOMBINATION.

In addition to our calculations of the structure and radiative properties of metal/oxygen species, an analysis of the importance of dielectronic recombination processes was undertaken. Dielectronic recombination (DR) is the process by which electron capture from the continuum to

a bound state is facilitated by collisional excitation of a previously bound target electron. The process can be represented by:



where $[U^{+q-1}]^{**}$ is a doubly excited state of the system at ionization level $(+q-1)$ and $[U^{+q-1}]^{*}$ is a stabilized excited state lying below the U^{+q-1} ionization threshold. The process is shown schematically in Figure 3. In the case of recombination unperturbed by external fields or the plasma density, the rate coefficient can be calculated as:

$$\sigma_{ij,k}(\epsilon) = \frac{2}{g_i} \left[\frac{\pi a_0^2}{T} \right]^{3/2} \frac{\mathcal{A}_{ji}(\epsilon) A_{jk}}{\sum_{i',k'} \mathcal{A}_{ji'}(\epsilon) + A_{jk}} e^{-\epsilon_j/kT} \quad (112)$$

where $\mathcal{A}_{ji}(\epsilon)$ is the rate of autoionization from state $|j\rangle$ into the continuum state $|i\rangle$, A_{jk} is the radiative rate from state $|j\rangle$ into the final bound state $|k\rangle$ and the sum is over all possible open channels.

An analysis of the low-lying electronic states of U^0 , U^{+1} and U^{+2} has been carried out to establish a data base for examining the role of DR in uranium. The states examined include all one-electron promotions of U^{+q} , followed by one electron capture final configurations which correspond either to high-lying Rydberg states or bound valence excited states of the U^{+q-1} system. Table 14 summarizes the low-lying states which are important for DR of $e + U^{+}$ and $e + U^{++}$. There are two low-lying configurations for U^{++} which have the J-J coupled representations, $[5f_{5/2}^3 7s]$ and $[5f_{5/2}^3 6d_{3/2}]$. These two configurations are separated by only 4117 cm^{-1} and both can be formed by successively removing two electrons from the ground state neutral U^0 configuration, $[5f_{5/2}^3 7s^2 6d_{3/2}]$. Two other U^{++} representations are also possible, $[5f_{5/2}^2 7s^2]$ and $[5f_{5/2}^2 7s 6d_{3/2}]$, but these states lie much higher in energy and would have negligible population, even in a 10,000 K plasma.

In the case of $e + U^+ DR$, at least two channels are accessible for low-energy electron attachment. Since the Rydberg structure lies $\leq 2000 \text{ cm}^{-1}$ from the U^+ ionization limit, several more states are open DR channels for electrons with $T_e = 2000\text{--}5000 \text{ K}$.

The low-lying excited DR electronic states of U^{++} are shown in Table 14, relative to both the $e + U^{++} [5f_{5/2}^3 7s]$ and $e + U^{++} [5f_{5/2}^2 6d_{3/2}]$ reactant channels. These data indicate that the first open attachment channel for dielectronic recombination $e + U^{++} [5f_{5/2}^3 7s]$ occurs at $T_e \sim 4000 \text{ K}$. However, the cross-section for capture into this channel is very low since it involves a $5f_{5/2} \rightarrow 7p_{3/2}$ promotion which has a low transition probability. The first reaction channel for DR of $e + U^{++}$ with a significant cross-section results from the $7s \rightarrow 6d_{3/2}$ transition. This channel opens for electron collision energies, $T_e > 5000 \text{ K}$, where electron capture into a high lying Rydberg orbital can occur. However, the probability of subsequent autoionization is now competitive with radiative stabilization and the dielectronic recombination rate coefficient is of the order of $10^{-13} \text{ cm}^3/\text{sec}$ or less. We conclude that dielectronic recombination of $e + U^{++}$ is a low probability process and not rate competitive with possible ion-neutral charge exchange reactions.

In contrast, dielectronic recombination of $e + U^+$ has a much higher probability. As shown in Table 14, there are two important low-lying recombination channels. A preliminary estimate of recombination into the two lowest lying channels yields the rates given in Table 15. The lowest channel has a significant DR rate ($10^{-10} - 10^{-11} \text{ cm}^3/\text{sec}$) for low temperature recombination. This rate falls off rapidly at higher temperature owing to the $T^{-3/2}$ dependence. The second channel appears to peak at $\sim 25000 \text{ K}$ with an indicated DR rate of $\sim 5 \times 10^{-13} \text{ cm}^3/\text{sec}$. Thus, there may be some atmospheric conditions where $e + U^+ DR$ should be considered.

A corresponding DR process is possible for $e + UO^+$. At the present time, only the optically connected excited states of UO^+ have been studied. The ground molecular orbital configuration for UO^+ is:

$$^4 I [1\sigma^2 2\sigma^2 3\sigma^2 4\sigma^2 1\pi^4 2\pi^4 | 3\pi 1\phi 1\delta] \quad (113)$$

where the last three molecular orbitals are nearly pure f-orbitals centered on uranium. Excitation processes that need to be examined, all in a molecular framework, are: $f^2 \rightarrow d^2$, $f^2 \rightarrow s^2$, $f^2 \rightarrow sd$, $f^2 \rightarrow p^2$, $f^2 \rightarrow sp$, and $f^2 \rightarrow pd$. Additional excitations from the core 2p level will be examined but it is expected that these levels are too tightly bound for the electron energy range of interest.

4.6 N + O₂ REACTIONS.

A study of the atmospheric reactions $O + N_2$ and $N + O_2$ which yield vibrationally excited NO molecules has been initiated. The sources of NO emission in the IR are not fully understood and the detailed kinetic branching of these reactions is being studied (References 99 and 100). In particular the role of the $N[{}^2P] + O_2[X^3\Sigma_g^-]$ reaction in the production of vibrationally excited NO molecules is being examined. The current NORSE code assumes that all the exothermicity of this reaction goes into vibrational excitation of the NO product molecule, with all levels being equally populated up to $v = 26$. The examination, in detail, of the kinetic routes of the $N + O_2$ reaction, including those which lead to electronic as well as vibrationally excited products is described below. A preliminary *ab initio* study of the reaction has been carried out which suggests that only a fraction of the collisions result in vibrational excitation in the product channels.

The molecular correlation diagram for the $N + O_2$ reaction is given in Table 16 for C_s , C_{2v} and $C_{\infty v}$ symmetry. This corresponds, respectively, to oblique, perpendicular and linear collisions of the N atom with the O₂ target molecule. The adiabatic molecular correlations for $C_{\infty v}$ and C_s symmetry are shown in Figures 4 and 5, respectively. These diagrams represent a more complete version of those given by Donovan and Husain (Reference 101) and by Schofield (Reference 102).

Since the kinetic behavior is governed by an average over all collisional trajectories, we illustrate the adiabatic correlations in C_s symmetry for the doublet surfaces in Figure 6, and for the quartet surfaces in Figure 7. In particular, we illustrate the adiabatic connections from $N[{}^2P] + O_2[X^3\Sigma_g^-]$ in bold lines on these figures. The energetics of the adiabatic reaction surfaces arising from $N[{}^2P] + O_2$ and $N[{}^2D] + O_2$ are shown in Tables 17 and 18, respectively. For $N[{}^2P] + O_2$, only the third reaction [yielding $NO[X^2\Pi] + O^*({}^1D)$] is exothermic enough to yield NO with a significant degree of vibrational excitation, provided that this reaction proceeds along an adiabatic pathway. However, there is spectroscopic evidence that curve-crossing and non-adiabatic behavior may occur for this system. The ground 2A_1 state of NO₂ adiabatically correlates to the reactants: $N[{}^4S] + O_2[X^3\Sigma_g^-]$, whereas the first excited 2B_1 state correlates to excited state reactants, $N[{}^2D] + O_2[X^3\Sigma_g^-]$. However, the 2B_1 state lies lower as we connect to the $NO[X^2\Pi] + O[{}^3P]$ dissociation limit. In addition, Gilmore (Reference 103) has pointed out that NO quenching of both $O^*[{}^1S]$ and $O^*[{}^1D]$ proceeds very rapidly, further indicating curve-crossings in the doublet surfaces.

In order to clarify the branching kinetics of the $N^*[{}^2P] + O_2[X^3\Sigma_g^-]$ reaction, we have initiated an extensive series of calculations of the potential energy reaction surfaces for NO₂ in the following symmetries: ${}^2A'$, ${}^2A''$, ${}^4A'$, ${}^4A''$. Preliminary CI calculations, using the GAMESS code

(Reference 104), were carried out in C_s symmetry assuming a frozen core of $(1a'^2)(2a'^2)(3a'^2)(4a'^2)(5a'^2)(6a'^2)$, which is the Hartree-Fock representation of the inner 1s and 2s electrons. Unfortunately, the characteristic charge density corresponding to this core representation differs significantly for different spin and spatial couplings of $N + O_2$. The characteristic charge of the $(6a'^2)$ pair, for example, differs in calculations in $^2A'$ symmetry as compared with $^2A''$ or $^4A'$ symmetry. Thus only a frozen inner shell (1s electrons) appears to be possible for this system. This smaller frozen core representation results in a great increase in the CI size, from 3048 to 28503 for $^2A'$ symmetry and from 3000 to 28125 for $^2A''$ symmetry. The calculations must therefore be carried out on a CRAY computer and the necessary code modifications for running this problem on the DNA access machines at LANL have been made. The calculations are carried out in C_s symmetry since we need to simultaneously examine the $N + O_2$ reaction path on nineteen surfaces in $^2A'$ and $^2A''$ symmetry and on twelve surfaces in $^4A'$ and $^4A''$ symmetry.

The results of our initial studies of the long range $N + O_2$ behavior are summarized in Table 19. We find that two of the states correlating to $N[^2P] + O_2[X^3\Sigma_g^-]$, $^2A' X$ and $^2A'' IX$, exhibit long range repulsion and thus should correlate adiabatically to $NO[a^4\Pi] + O[^3P]$ and $NO[X^2\Pi] + O[^1S]$ respectively. This leaves only the $^2A'' VIII$ surface correlating to $NO[X^2\Pi] + O[^1D]$. For the quartet surfaces which adiabatically correlate to $NO[a^4\Pi] + O[^3P]$, no vibrationally excited ground state $NO[X^2\Pi]$ is predicted. Detailed calculations of these quartet surfaces are in progress.

The statistical branching in the $N + O_2$ reaction can be partially analyzed in terms of these calculated potential energy surfaces. In Table 17, which lists the $N^*[^2P] + O_2$ reaction surfaces, we see that only the third reaction, which yields $NO[X^2\Pi] + O[^1D]$, is exothermic enough to yield NO with any significant degree of vibrational excitation. The reaction surfaces for $N^*[^2D] + O_2$ are listed in Table 18. Three surfaces represent closed (endothermic) channels for low energy collisions and are non-reactive for air chemistry. Six surfaces produce ground state NO with nearly 4 eV internal (rovibrational) energy and one surface produces NO with less than 2 eV internal energy. Thus, of the 16 potential surfaces governing the $N[^2D] + O_2$ and $N[^2P] + O_2$ reactions, we find the following:

1. 3 are non-reactive (endothermic)
2. 6 lead to electronically excited products with the result that the NO that is produced is not rovibrational excited.
3. 7 lead to the production of ground state NO with significant (3-4 eV) rovibrational excitation.

Further, 60% of all collisions involving $N[{}^2D]$ atoms should produce NO with significant internal excitation but only 1/6 of all collisions involving $N[{}^2P]$ atoms appear to lead to rovibrationally excited NO molecules. Non-adiabatic behavior at closer internuclear separations could modify these relative branching ratios but will not change the conclusion that $\sim 1/2$ of all collisions of $N[{}^2D, {}^2P] + O_2$ lead to NO with little or no rovibrational excitation. Detailed studies of these reaction surfaces are required to further analyze the branching rates in this system.

SECTION 5

RECOMMENDATIONS

Previous studies of the electronic structure and energy levels of the uranium/oxygen system have been undertaken by UTRC and reported in DNA-TR-82-159 (Reference 85), DNA-TR-85-156 (Reference 86), DNA-TR-88-12 (Reference 87) and the present technical report for Contract DNA001-88-0032. In these studies the focus was on estimating the LWIR radiation characteristics and the efficiency of solar pumping of the allowed electronic transitions in this system which fall in the visible wavelength region. An examination of the thermodynamics and kinetics of the uranium/oxygen system shows that U^+ and UO^+ are terminal ions, and therefore potentially important radiators at high altitudes, whereas UO_2^+ is more important at low altitudes where there is significant O_2 concentration. Further studies of the uranium/oxygen system are outlined below. In addition, suggested studies of dielectronic recombination and kinetic branching in atmospheric reactions producing radiating NO molecules are described.

5.1 URANIUM/OXYGEN.

The calculations of the electronic structure of the uranium oxide ions have been performed with neglect of the spin-orbit interaction term, optimizing the relativistic density functional SCF wavefunctions for the particular ion. Spin-orbit interaction is then introduced as a perturbation through configurational mixing. This same approach has been used by Krauss and Stevens (Reference 89), with a full *ab initio* treatment of the valence electrons, using ℓ -dependent relativistic effective core potentials. Either approach allows for polarization and charge transfer from the ligand oxygen atoms to the central uranium ion.

A different approach for rare earth metal oxides has been described by Dulick (Reference 105) which is based on a crystal field model. Application of this method to the UO and UO^+ ground states (Reference 106) yields a significantly different energy ordering for the Ω coupled states than is found in the full molecular treatments of the systems described above. The application of the crystal field model to lanthanide monoxides, however, appears to yield the known experimental electronic assignments (Reference 107). An examination of the composition of the predicted Ω states for UO^+ , based on this crystal field model, indicates a significant mixing of electronic states of the uranium ion of small ℓ -value. These efforts are not found in the molecular treatments, whose compositions are dominated by the tightly coupled $5f$ states. Further studies of these differences in approach are indicated; however, since all methods are either based on or predict a large ionic character in the UO^+ and UO_2^+ ions, our conclusion of strong LWIR emission should not be altered. The crystal field model has not been utilized for describing electronic transitions or the absorption/emission characteristics in either the IR or visible wavelength regions.

Our suggested studies include the further examination of low-lying electronic states in UO^+ and UO_2^+ . These studies will primarily cover the IR, visible and UV excitation wavelengths ($< \sim 5$ eV) in order to more accurately define the radiation emission strengths. A new density functional computer code, has been developed in collaboration with Professor F. E. Harris (University of Utah), and would be utilized to carry out these suggested studies. This new code yields a more accurate representation of the electron density in the valence region between atomic centers. This region has previously been described by a constant (muffin-tin) potential which can lead to inaccuracies in describing polarization effects. We feel that this new code would also permit a more critical evaluation of the crystal field model, as applied to the uranium/oxygen system.

Our increase in the data base for the uranium/oxygen system will include radiation f-numbers, characteristic absorption/emission wavelengths and calculated density of states for U^{+n} , UO^{+n} , UO_2^{+n} ($n = 0,1,2$). These studies would be aided by a parallel experimental program on the spectroscopy of electronic states of UO and/or UO^+ . A suggested collaborator is Professor Michael Heaven at Emory University.

5.2 DIELECTRONIC RECOMBINATION.

In addition to our suggested calculations of the structure and radiative properties of uranium/oxygen species, further analysis of the importance of dielectronic recombination processes should be carried out. A preliminary study of the important dissociative recombination states of U° , U^+ and U^{++} has been described above under Section 4. Several highly excited configurations for U° have been identified which indicate that $e + \text{U}^+$ may be an important charge neutralization process, but a more extensive study is required to determine the density of states accessible to dielectronic recombination under conditions up to perhaps 5000°K .

A corresponding DR process is possible for $e + \text{UO}^+$. At the present time, only the optically connected excited states of UO^+ have been studied. The ground molecular orbital configuration for UO^+ is:

$$^4\text{I}[1\sigma^2 2\sigma^2 3\sigma^2 4\sigma^2 1\pi^4 2\pi^4 : 3\pi 1\phi 1\delta] \quad (114)$$

where the last three molecular orbits are nearly pure f-orbitals centered on uranium. Excitation processes that need to be examined, all in a molecular framework, are: $f^2 \rightarrow d^2$, $f^2 \rightarrow s^2$, $f^2 \rightarrow sd$, $f^2 \rightarrow p^2$, $f^2 \rightarrow sp$, and $f^2 \rightarrow pd$. Additional excitations from the core 2π level will be examined but it is expected that these levels are too tightly bound for the electron energy range of interest.

These studies of dielectronic recombination contribute to our understanding of the kinetics of charge neutralization following nuclear bursts. In particular, the role of dielectronic recombination as a mechanism for removal of electrons is uncertain at present and, if found to be important, must be included in the chemistry kinetics in the NORSE code.

5.3 NO/NO⁺ FORMATION.

Under this Contract, DNA001-88-C-0032, a study of the atmospheric reactions $O + N_2$ and $N + O_2$ which yield vibrationally excited NO molecules was initiated. This study was in response to the requirement defined by Gilmore (Reference 108) for a more accurate analysis of the $N[{}^2D] + O_2$ and $N[{}^2P] + O_2$ reactions which are modeled in the NORSE calculation of NO chemiluminescence. Since the $N[{}^2P] + O_2$ reaction can yield $N[{}^2D] + O_2$ as products, as well as vibrationally excited NO, there is a large uncertainty in the kinetic branching. If vibrationally hot NO is strongly favored as the product channel, high IR emission at $9\mu m$ and $4.5\mu m$ is predicted. Our initial studies of the kinetics of the $N[{}^2P] + O_2$ reaction suggest that only 1/6 of all collisions involving $N[{}^2P]$ atoms appear to lead to rovibrationally excited NO molecules. Thus the present atmospheric codes predict too much excitation for the NO product of this reaction.

In a closely related problem, a strong radiator in the IR following a nuclear burst is vibrationally excited NO^+ , with emission near $4.3\mu m$. An examination of the ion-molecule reaction surface for $O + N_2^+$, $O_2^+ + N$, and $O^+ + N_2$ should be carried out to establish the overall product correlations for this system. If required, detailed quantum mechanical studies of the pertinent reaction surfaces should be examined. A similar study of the $O^+ + N_2 \rightarrow NO^+ + N$ reaction has been previously carried out for DNA by UTRC under AFGL Contract F19628-80-C-0209 (Reference 109). All of these studies of atmospheric molecules have the objective of increasing the fundamental data base of the reaction kinetics in order to provide useful input for chemiluminescence modeling in the various atmospheric codes.

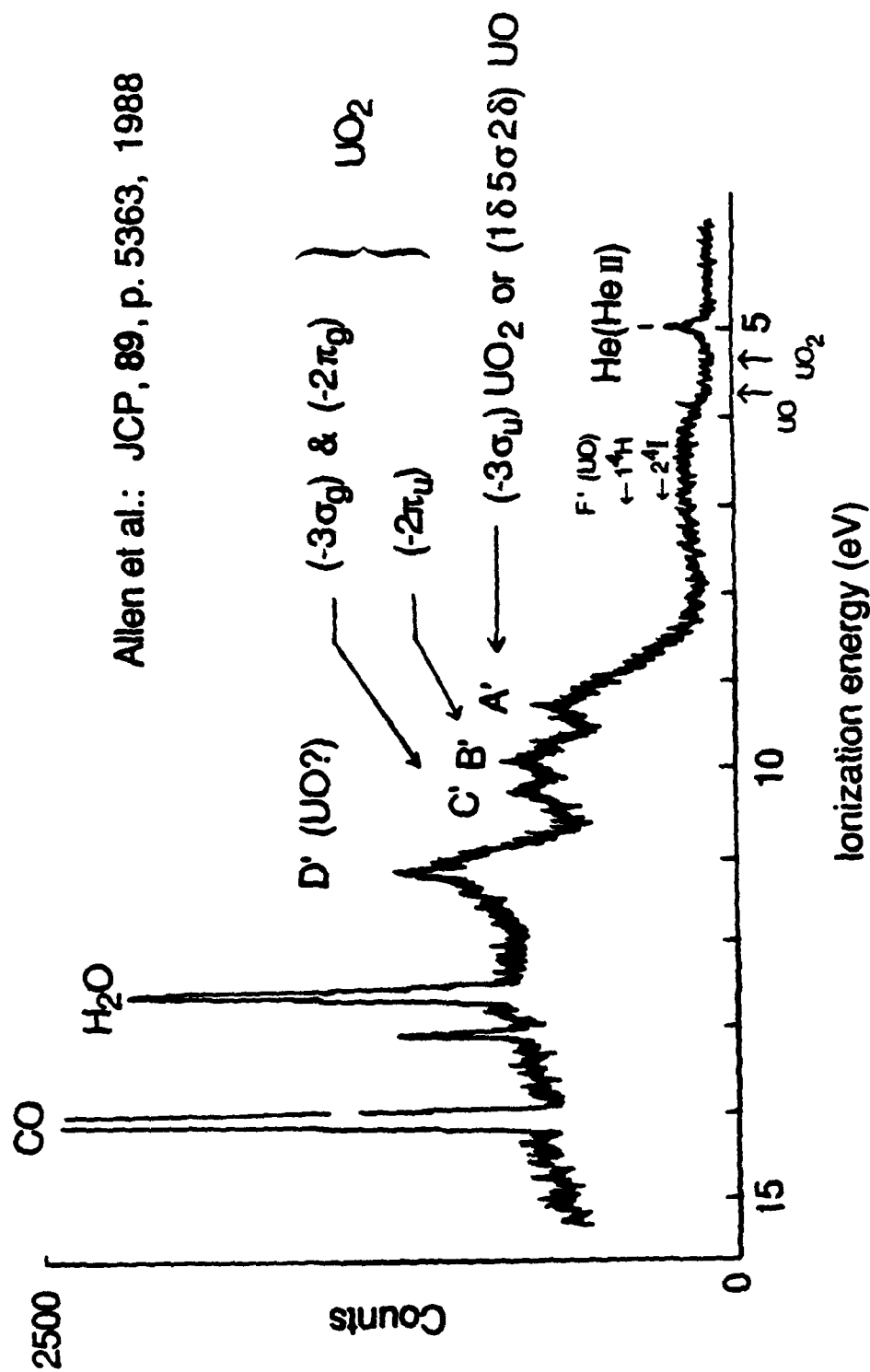
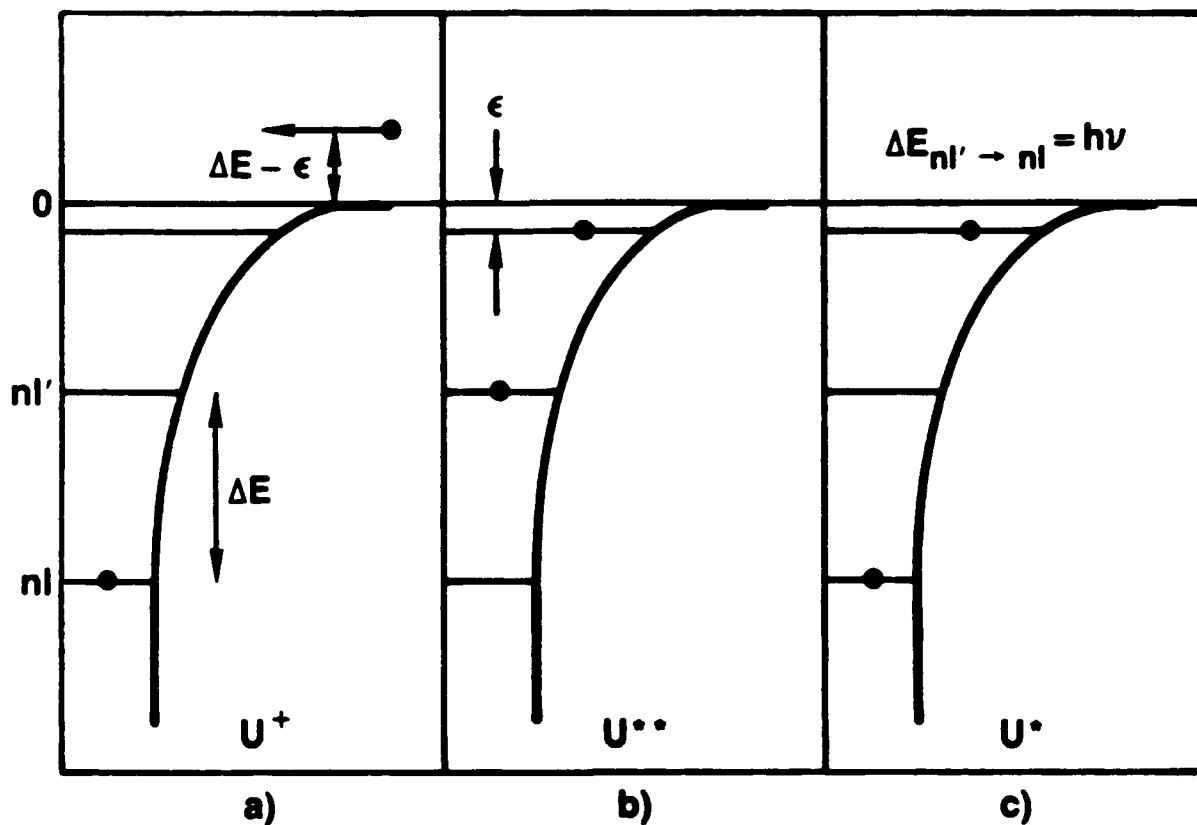


Figure 2. He I photoelectron spectrum of the vapor above an equimolar $\text{UO}_2(\text{s})/\text{U}(\text{s})$ mixture heated to 2250 ± 30 K.



- a) Incoming electron has energy less than $E_{nl'} - E_{nl}$.
- b) Incoming electron + KE in Coulomb field excites an electron from $nl \rightarrow nl'$ and incident electron is trapped in a highly excited state.
- c) Doubly excited state radiates ($nl' \rightarrow nl$) resulting in a stable excited state lying below the ionization threshold.

Figure 3. Dielectronic recombination.

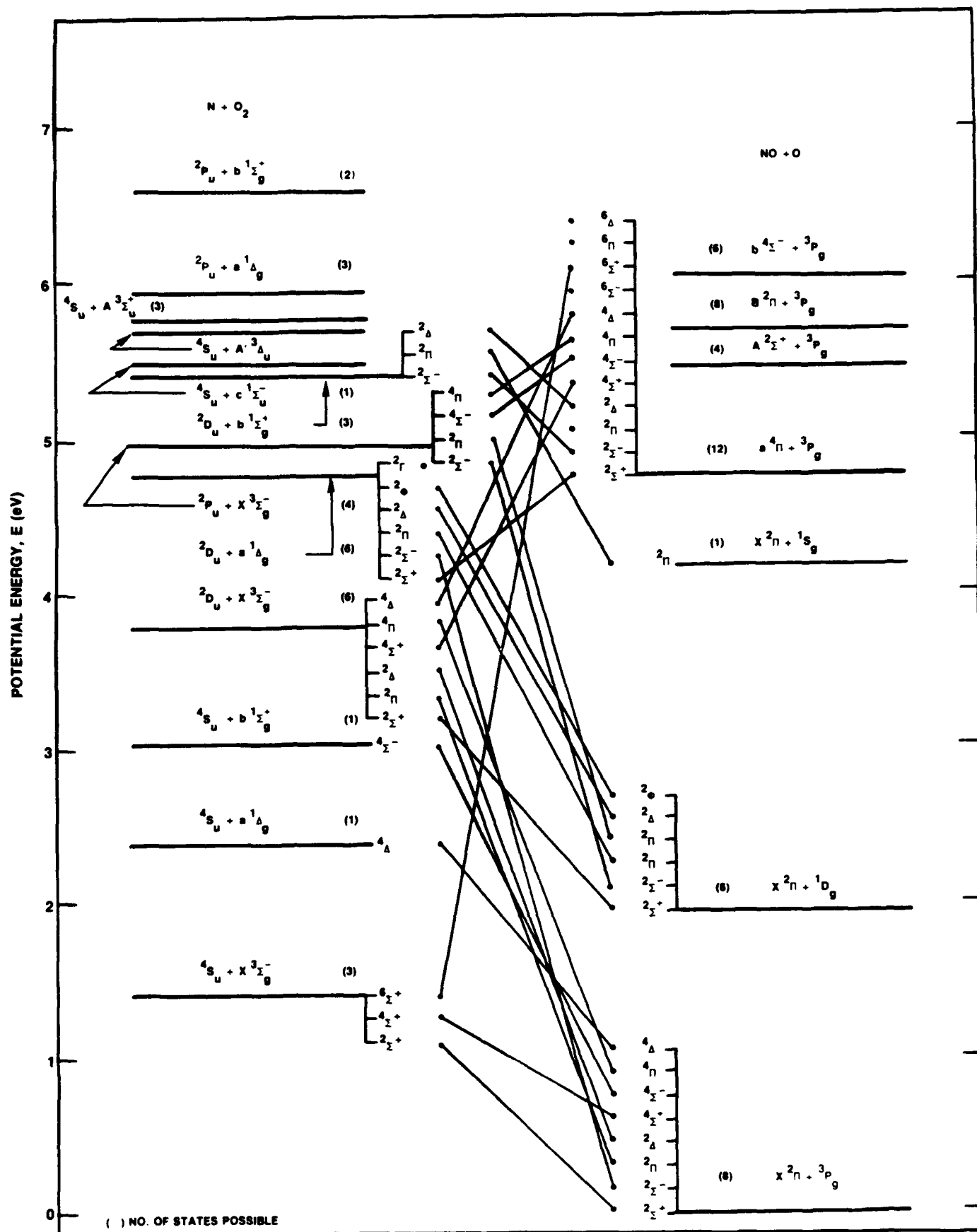


Figure 4. Molecular correlation diagram for low-lying states of NO_2 in $C_{\infty v}$ symmetry.

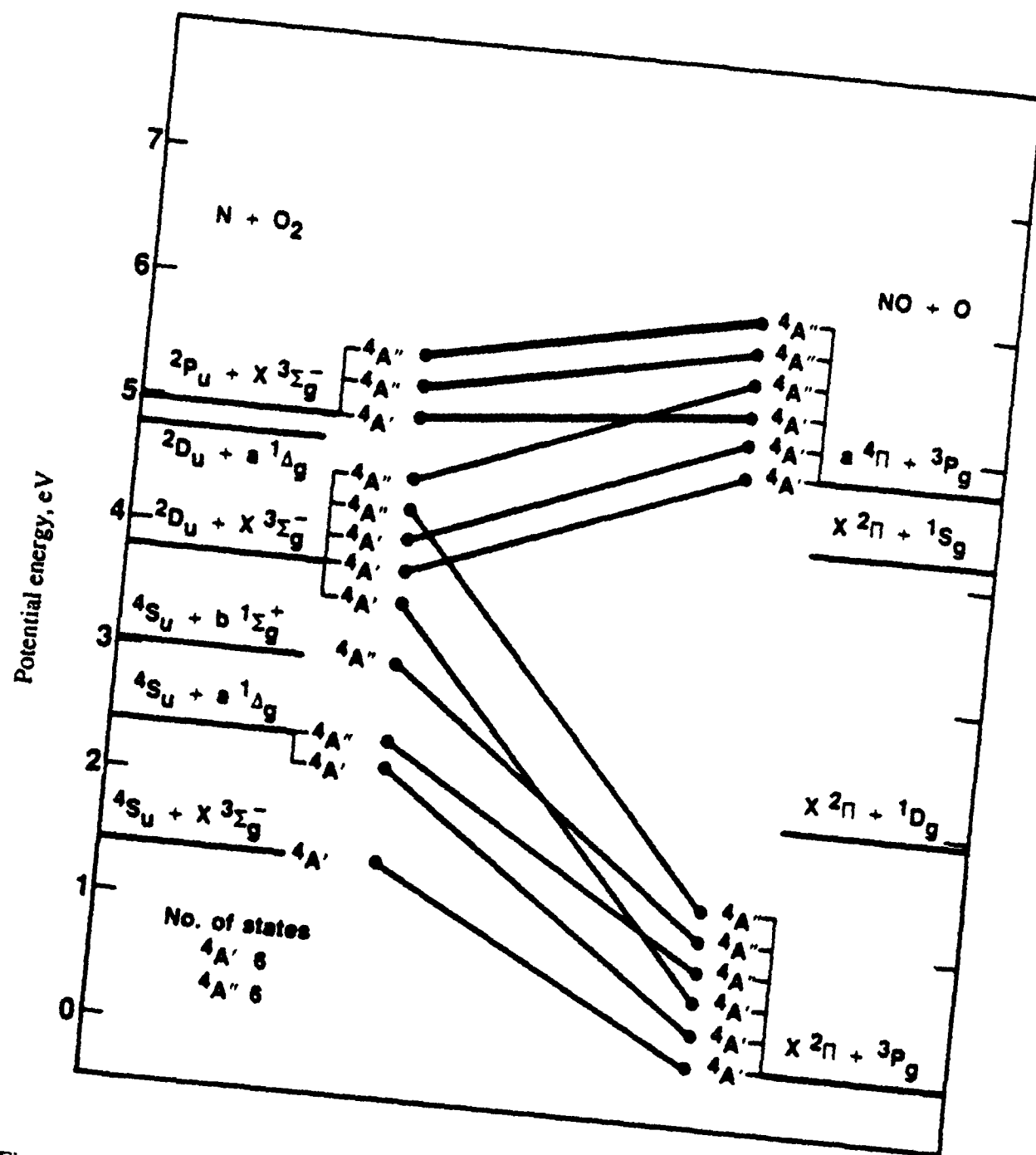


Figure 7. Molecular correlation diagram for low-lying quartet states of NO_2 in C_s symmetry.

Table 1. Calculated oscillator strengths $f_{(v'v')}$ for the $14j - 14K$ transition of UO^{+} .

v'/v''	0	1	2	3	4	5	6	7	8
0	*2.20-03 **0.654	1.36-03 0.694	3.99-04 0.739	6.94-05 0.790	5.21-06 0.849	6.11-08 0.916	8.29-13 0.994	5.34-10 1.086	2.10-09 1.195
1	1.54-03 0.622	3.49-04 0.658	1.33-03 0.698	6.50-04 0.744	1.48-04 0.795	1.41-05 0.854	6.94-08 0.921	3.28-08 1.00	9.54-10 1.092
2	4.54-04 0.592	1.35-03 0.625	3.66-07 0.661	1.09-03 0.701	8.69-04 0.747	2.29-04 0.798	2.30-05 0.857	3.84-08 0.924	1.47-07 1.003
3	8.93-05 0.563	8.13-04 0.593	8.13-04 0.625	1.44-04 0.661	7.52-04 0.702	1.04-03 0.747	3.25-04 0.798	3.45-05 0.856	7.60-08 0.923
4	1.95-05 0.537	2.86-04 0.564	9.24-04 0.593	3.20-04 0.625	3.85-04 0.661	4.26-04 0.701	1.15-03 0.746	4.45-04 0.797	5.51-05 0.854
5	6.61-06 0.513	8.96-05 0.538	4.88-04 0.564	7.89-04 0.593	5.30-05 0.626	5.51-04 0.661	1.68-04 0.701	1.16-03 0.746	5.96-04 0.796
6	2.97-06 0.492	3.14-05 0.514	2.03-04 0.539	6.23-04 0.565	5.36-04 0.595	3.72-06 0.627	6.04-04 0.662	2.06-05 0.702	1.04-03 0.746
7	1.20-06 0.473	1.27-05 0.494	8.26-05 0.516	3.38-04 0.540	6.66-04 0.567	2.88-04 0.596	7.97-05 0.628	5.56-04 0.664	1.20-05 0.703
8	3.07-07 0.455	4.98-06 0.475	3.38-05 0.495	1.58-04 0.518	4.61-04 0.542	6.21-04 0.569	1.18-04 0.598	1.85-04 0.630	4.42-04 0.665

* oscillator strengths
** wavelength, microns

Table 2. Calculated oscillator strengths $f_{(v'v'')}$ for the $141 - 34\text{H}$ transition of UO^+ .

v'/v''	0	1	2	3	4	5	6	7	8
0	*5.61-03 **0.438	8.53-03 0.456	6.05-03 0.475	2.78-03 0.495	9.76-04 0.518	2.77-04 0.542	5.99-05 0.568	8.13-06 0.598	3.47-07 0.629
1	7.97-03 0.425	1.74-03 0.442	9.45-04 0.460	4.85-03 0.479	4.81-03 0.500	2.57-03 0.523	9.12-04 0.547	2.08-04 0.574	2.42-05 0.603
2	6.70-03 0.412	6.20-04 0.428	4.78-03 0.444	5.94-04 0.462	1.47-03 0.482	4.39-03 0.503	3.56-03 0.525	1.54-03 0.550	3.82-04 0.576
3	3.94-03 0.399	4.14-03 0.413	7.76-04 0.429	2.49-03 0.446	2.56-03 0.464	7.01-05 0.483	3.13-03 0.504	4.11-03 0.527	2.20-03 0.551
4	1.92-03 0.387	5.37-03 0.401	8.63-04 0.415	2.67-03 0.431	3.95-04 0.448	3.08-03 0.465	1.93-04 0.484	1.86-03 0.506	4.17-03 0.528
5	7.52-04 0.375	3.95-03 0.388	4.14-03 0.402	8.68-07 0.417	2.95-03 0.432	2.09-05 0.449	2.50-03 0.467	7.76-04 0.486	9.73-04 0.507
6	2.09-04 0.365	1.92-03 0.377	4.87-03 0.390	2.44-03 0.404	4.48-04 0.418	2.21-03 0.434	4.25-04 0.451	1.69-03 0.469	1.27-03 0.488
7	3.13-05 0.355	5.96-04 0.367	3.01-03 0.379	4.89-03 0.392	1.18-03 0.406	1.08-03 0.420	1.38-03 0.436	9.05-04 0.453	1.03-03 0.471
8	6.89-07 0.346	9.54-05 0.357	1.07-03 0.369	3.80-02 0.381	4.44-03 0.394	4.37-04 0.408	1.52-03 0.422	7.47-04 0.438	1.25-03 0.455

* oscillator strengths
 ** wavelength, microns

Table 3. Calculated oscillator strengths $f_{(v'v')}$ for the $1^4I - 2^4H$ transition of UO^{+} .

v'/v''	0	1	2	3	4	5	6	7	8
0	*4.21-03 **0.683	3.45-05 0.727	2.63-05 0.776	7.62-08 0.833	4.45-07 0.898	1.01-08 0.973	5.13-09 1.062	1.51-09 1.167	2.25-13 1.295
1	3.22-05 0.634	4.18-03 0.672	4.23-05 0.714	7.22-05 0.762	8.58-08 0.816	1.84-06 0.877	6.54-08 0.949	2.10-08 1.032	9.17-09 1.131
2	4.19-05 0.593	3.21-05 0.626	4.16-03 0.662	2.39-05 0.703	1.29-04 0.749	4.48-09 0.800	4.57-06 0.859	2.61-07 0.927	4.91-08 1.006
3	1.10-06 0.557	1.04-04 0.587	1.58-05 0.619	4.13-03 0.654	1.39-06 0.693	1.80-04 0.738	9.85-07 0.787	8.37-06 0.844	9.02-07 0.909
4	1.66-07 0.527	1.32-06 0.553	1.75-04 0.581	1.18-06 0.613	4.08-03 0.647	1.74-05 0.685	2.01-04 0.728	5.78-06 0.776	1.16-05 0.83
5	5.69-09 0.501	3.40-07 0.524	2.35-07 0.550	2.43-04 0.577	6.44-06 0.608	3.96-03 0.641	1.10-04 0.679	1.79-04 0.720	1.58-05 0.767
6	4.96-09 0.478	7.59-08 0.499	2.89-07 0.522	6.40-07 0.547	3.00-04 0.574	4.28-05 0.604	3.77-03 0.637	2.85-04 0.674	1.23-04 0.714
7	1.08-09 0.458	3.73-08 0.477	2.80-07 0.498	4.21-08 0.521	5.94-06 0.545	3.37-04 0.572	1.14-04 0.602	3.50-03 0.634	5.17-04 0.670
8	1.10-10 0.440	1.98-09 0.457	1.39-07 0.477	5.52-07 0.497	1.45-07 0.520	1.72-05 0.544	3.54-04 0.571	2.19-04 0.60	3.18-03 0.632

* oscillator strengths
** wavelength, microns

Table 4. Calculated oscillator strengths $f_{(v'v'')}$ for the $141 - 14H$ transition of UO^{+} .

v'/v''	0	1	2	3	4	5	6	7	8
0	*2.73-06 **8.580	9.38-09 35.608	0. -	0. -	0. -	0. -	0. -	0. -	0. -
1	7.14-08 5.099	2.32-06 9.290	3.49-08 50.644	0. -	0. -	0. -	0. -	0. -	0. -
2	3.38-11 3.610	3.61-07 5.304	1.84-06 9.938	4.43-08 75.241	0. -	0. -	0. -	0. -	0. -
3	1.07-09 2.767	6.79-09 3.664	6.62-07 5.406	1.53-06 10.239	4.69-08 91.987	0. -	0. -	0. -	0. -
4	1.62-09 2.227	2.22-09 2.773	3.55-08 3.667	8.17-07 5.394	1.42-06 10.144	5.72-08 81.079	0. -	0. -	0. -
5	1.04-10 1.858	3.69-09 2.223	2.99-09 2.763	7.82-08 3.641	8.16-07 5.323	1.48-06 9.841	7.13-08 62.820	0. -	0. -
6	2.34-11 1.596	2.24-10 1.859	5.04-09 2.222	2.27-09 2.757	1.22-07 3.624	7.15-07 5.272	1.59-06 9.616	7.91-08 53.063	0. -
7	2.25-11 1.408	9.66-11 1.608	2.43-10 1.873	4.54-09 2.239	8.30-10 2.780	1.56-07 3.656	6.05-07 5.324	1.60-06 9.740	7.72-08 55.332
8	2.07-12 1.270	1.03-10 1.431	3.09-10 1.637	3.12-10 1.910	1.66-09 2.289	7.54-10 2.852	1.66-07 3.774	5.96-07 5.562	1.37-06 10.504

* oscillator strengths
 ** wavelength, microns

Table 5. Calculated oscillator strengths $f_{(v'v'')}$ for the $1^4I - 2^4I$ transition of UO^{+} .

v'/v''	0	1	2	3	4	5	6	7	8
0	*3.55-03 **0.782	1.59-04 0.840	1.35-05 0.907	5.99-07 0.985	1.18-08 1.077	1.15-09 1.187	7.30-10 1.322	3.42-09 1.489	8.56-09 1.704
1	1.99-04 0.733	3.26-03 0.784	2.27-04 0.842	2.93-05 0.909	1.32-06 0.986	3.24-08 1.078	5.49-08 1.188	4.09-08 1.322	1.92-08 1.488
2	4.56-08 0.690	3.13-04 0.735	3.10-03 0.786	2.36-04 0.844	4.61-05 0.911	5.70-06 0.988	4.89-07 1.080	3.37-07 1.189	3.44-07 1.322
3	4.10-07 0.654	6.41-07 0.694	3.70-04 0.739	2.87-03 0.790	3.29-04 0.848	7.77-05 0.915	1.87-05 0.993	4.21-06 1.084	1.65-06 1.194
4	7.24-11 0.621	1.98-06 0.657	8.25-07 0.698	5.71-04 0.743	2.36-03 0.794	4.64-04 0.853	1.48-04 0.920	4.82-05 0.998	1.75-05 1.090
5	9.91-11 0.593	3.59-09 0.626	1.48-06 0.662	4.51-10 0.703	9.58-04 0.749	1.70-03 0.800	5.25-04 0.859	2.34-04 0.927	8.95-05 1.006
6	5.15-10 0.568	2.07-07 0.598	9.61-10 0.631	9.35-07 0.668	1.27-06 0.709	1.43-03 0.755	1.17-03 0.807	4.64-04 0.867	2.81-04 0.935
7	1.25-08 0.544	3.57-11 0.572	4.16-07 0.602	1.73-11 0.635	1.88-06 0.672	2.50-06 0.714	1.79-03 0.760	8.54-04 0.813	3.74-04 0.873
8	2.17-10 0.522	4.69-09 0.547	1.34-08 0.575	2.09-07 0.605	3.71-08 0.639	6.09-06 0.676	2.47-06 0.718	2.01-03 0.765	6.72-04 0.818

* oscillator strength
** wavelength, microns

Table 6. Calculated oscillator strengths $f_{(v'v'')}$ for the $1^4I - 1^6H$ transition of UO^{+} .

v'/v''	0	1	2	3	4	5	6	7	8
0	*1.35-03 **0.480	1.66-03 0.501	1.22-03 0.524	6.43-04 0.550	2.75-04 0.577	1.05-04 0.607	3.67-05 0.641	1.09-05 0.678	2.42-06 0.719
1	2.01-03 0.468	2.56-04 0.488	1.18-04 0.509	7.02-04 0.533	8.82-04 0.559	6.45-04 0.587	3.46-04 0.619	1.49-04 0.653	5.17-05 0.691
2	1.66-03 0.456	3.81-04 0.475	8.11-04 0.495	1.72-04 0.518	6.50-05 0.542	4.66-04 0.569	6.32-04 0.598	4.91-04 0.630	2.77-04 0.666
3	6.98-04 0.445	1.50-03 0.463	2.33-05 0.482	4.04-04 0.504	5.10-04 0.527	5.34-05 0.552	1.06-04 0.579	4.39-04 0.609	5.46-04 0.642
4	1.64-04 0.434	1.40-03 0.451	7.36-04 0.470	3.70-04 0.490	3.51-05 0.512	4.75-04 0.535	2.84-04 0.561	7.65-07 0.589	1.89-04 0.620
5	1.17-05 0.423	5.30-04 0.440	1.61-03 0.458	1.49-04 0.477	5.25-04 0.497	3.81-05 0.519	2.47-04 0.544	4.15-04 0.570	8.03-05 0.599
6	2.08-07 0.413	7.16-05 0.429	9.69-04 0.446	1.34-03 0.464	1.96-06 0.483	3.93-04 0.504	2.10-04 0.527	5.59-05 0.551	3.80-04 0.578
7	1.00-06 0.403	4.21-07 0.418	2.27-04 0.434	1.33-03 0.451	8.17-04 0.470	1.28-04 0.489	1.70-04 0.511	3.53-04 0.534	7.63-07 0.559
8	2.51-07 0.394	2.70-06 0.408	1.16-05 0.423	4.77-04 0.440	1.45-03 0.457	3.19-04 0.476	2.87-04 0.496	1.93-05 0.518	3.64-04 0.542

* oscillator strength
** wavelength, microns

Table 7. Calculated oscillator strengths $f(v'v'')$ for the $14I - 34I$ transition of UO^{+} .

v'/v''	0	1	2	3	4	5	6	7	8
0	*2.10-07 **0.340	1.98-06 0.351	8.93-06 0.362	2.55-05 0.374	5.23-05 0.386	8.20-05 0.400	1.03-04 0.414	1.05-04 0.429	8.91-05 0.445
1	1.31-06 0.333	9.68-06 0.343	3.23-05 0.354	6.31-05 0.365	7.81-05 0.377	6.00-05 0.390	2.33-05 0.403	7.51-07 0.417	9.63-06 0.433
2	4.73-06 0.327	2.73-05 0.336	6.64-05 0.347	8.33-05 0.357	4.96-05 0.369	5.79-06 0.381	7.90-06 0.394	4.07-05 0.408	4.94-05 0.422
3	1.20-05 0.320	5.06-05 0.329	7.98-05 0.339	4.75-05 0.349	2.00-06 0.360	2.00-05 0.372	5.21-05 0.384	2.90-05 0.397	1.93-07 0.410
4	2.35-05 0.313	6.83-05 0.322	6.00-05 0.331	6.74-06 0.341	1.56-05 0.351	4.96-05 0.362	2.01-05 0.374	1.92-06 0.386	3.42-05 0.399
5	3.39-05 0.307	6.61-05 0.315	2.66-05 0.324	1.79-06 0.334	3.61-05 0.344	2.37-05 0.354	4.97-07 0.365	2.81-05 0.377	2.31-05 0.389
6	4.94-05 0.302	6.21-05 0.310	6.96-06 0.319	1.65-05 0.328	3.48-05 0.337	2.08-06 0.347	1.84-05 0.358	2.75-05 0.369	5.25-07 0.381
7	6.74-05 0.297	4.79-05 0.305	5.87-08 0.313	3.17-05 0.322	1.54-05 0.331	4.99-06 0.341	2.93-05 0.351	4.82-06 0.362	1.19-05 0.373
8	8.20-05 0.292	2.80-05 0.300	7.80-06 0.308	3.21-05 0.317	1.12-06 0.326	1.99-05 0.335	1.61-05 0.345	2.18-06 0.355	2.40-05 0.366

* oscillator strength
** wavelength, microns

Table 8. Calculated oscillator strengths $f_{(v'v')}$ for the $1^4H - 2^4I$ transition of UO^{+} .

v'/v''	0	1	2	3	4	5	6	7	8
0	*2.83-03 **0.860	2.79-04 0.923	3.33-05 0.998	7.19-06 1.090	1.80-06 1.205	2.12-07 1.350	3.79-10 1.532	2.18-09 1.758	3.43-10 2.034
1	3.65-04 0.802	2.03-03 0.856	6.19-04 0.920	1.05-04 0.997	1.92-05 1.093	3.97-06 1.211	6.37-07 1.355	6.24-08 1.529	1.55-09 1.734
2	9.71-06 0.751	8.63-04 0.798	1.29-03 0.854	7.74-04 0.920	1.72-04 1.000	3.65-05 1.099	9.06-06 1.216	1.58-06 1.355	3.06-07 1.513
3	1.52-06 0.708	5.69-05 0.750	1.14-03 0.798	7.28-04 0.856	8.46-04 0.925	2.65-04 1.008	6.42-05 1.107	2.10-05 1.220	5.21-06 1.347
4	1.98-07 0.670	3.95-06 0.707	1.49-04 0.750	1.32-03 0.801	3.16-04 0.862	7.48-04 0.933	3.76-04 1.017	1.10-04 1.111	4.40-05 1.216
5	4.99-08 0.637	8.74-07 0.671	1.23-05 0.710	2.82-04 0.755	1.44-03 0.808	9.38-05 0.871	5.08-04 0.943	4.35-04 1.024	1.65-04 1.112
6	5.90-09 0.608	3.68-10 0.639	1.14-06 0.674	1.73-05 0.714	4.04-04 0.762	1.56-03 0.817	2.14-05 0.881	2.75-04 0.951	4.01-04 1.026
7	2.44-08 0.581	7.55-08 0.609	1.60-07 0.641	6.25-09 0.677	8.93-06 0.720	4.64-04 0.770	1.67-03 0.826	4.19-06 0.887	1.49-04 0.952
8	1.70-09 0.556	5.13-09 0.582	6.62-07 0.610	1.91-06 0.644	4.04-06 0.682	5.74-07 0.726	4.91-04 0.776	1.70-03 0.830	1.87-06 0.887

* oscillator strength
** wavelength, microns

Table 9. Calculated oscillator strengths $f_{(v'v'')}$ for the $1^4H - 2^4H$ transition of UO^{+} .

v'/v''	0	1	2	3	4	5	6	7	8
0	*3.63-03 **0.742	1.14-05 0.788	3.41-05 0.842	1.94-06 0.907	6.01-07 0.985	1.25-07 1.080	7.50-09 1.193	7.43-09 1.326	1.94-11 1.477
1	4.34-06 0.685	3.48-03 0.724	2.05-04 0.769	4.60-05 0.823	9.64-06 0.887	1.11-06 0.963	5.33-07 1.052	8.61-09 1.154	3.44-08 1.267
2	5.54-05 0.637	1.22-04 0.672	3.02-03 0.709	5.66-04 0.755	3.13-05 0.808	2.13-05 0.871	1.17-06 0.944	1.38-06 1.025	5.49-11 1.113
3	2.90-06 0.597	1.63-04 0.626	2.84-04 0.660	2.46-03 0.699	9.16-04 0.744	1.02-05 0.797	3.37-05 0.858	4.82-07 0.924	2.86-06 0.995
4	2.99-07 0.562	2.36-05 0.588	2.87-04 0.618	3.95-04 0.652	2.01-03 0.691	1.16-03 0.737	6.84-10 0.788	4.36-05 0.843	1.87-07 0.902
5	9.46-08 0.532	2.45-06 0.556	6.24-05 0.582	3.77-04 0.612	4.64-04 0.646	1.70-03 0.686	1.28-03 0.730	1.73-05 0.778	4.31-05 0.827
6	1.15-09 0.506	3.11-07 0.527	5.36-06 0.551	9.67-05 0.578	4.25-04 0.609	5.27-04 0.644	1.45-03 0.682	1.35-03 0.724	8.71-05 0.766
7	2.24-09 0.484	2.68-09 0.503	1.32-07 0.524	5.07-06 0.549	1.13-04 0.576	4.56-04 0.607	6.08-04 0.642	1.14-03 0.678	1.43-03 0.716
8	7.74-10 0.463	4.33-08 0.482	1.58-07 0.501	1.36-07 0.523	2.32-06 0.548	1.18-04 0.576	5.05-04 0.607	7.02-04 0.639	6.85-04 0.673

* oscillator strength
** wavelength, microns

Table 10. Calculated oscillator strengths $f_{(v'v')}$ for the $1^4H - 1^4K$ transition of UO^{+} .

v'/v''	0	1	2	3	4	5	6	7	8
0	2.49-03 0.708	1.18-03 0.750	1.07-04 0.799	8.12-07 0.857	4.40-08 0.926	5.64-08 1.010	5.93-08 1.108	2.66-10 1.222	1.93-09 1.349
1	1.13-03 0.671	1.15-03 0.708	1.36-03 0.751	1.74-04 0.802	5.49-06 0.863	1.54-07 0.935	2.51-07 1.019	1.59-07 1.114	4.97-10 1.219
2	2.85-04 0.636	1.06-03 0.670	6.81-04 0.708	1.48-03 0.753	2.78-04 0.806	1.91-05 0.869	1.98-06 0.941	7.29-07 1.021	1.08-07 1.108
3	4.95-05 0.603	3.83-04 0.633	1.06-03 0.667	2.92-04 0.707	1.50-03 0.754	4.52-04 0.808	5.35-05 0.870	6.53-06 0.939	7.17-07 1.012
4	7.41-06 0.573	1.06-04 0.600	4.75-04 0.630	1.02-03 0.666	3.96-05 0.707	1.33-03 0.755	6.78-04 0.809	1.13-04 0.867	9.25-06 0.930
5	1.58-06 0.546	2.24-05 0.571	1.73-04 0.598	5.77-04 0.630	8.41-04 0.667	2.42-05 0.709	1.02-03 0.756	9.22-04 0.807	1.72-04 0.861
6	5.65-07 0.522	4.89-06 0.545	4.91-05 0.570	2.57-04 0.598	6.90-04 0.632	5.18-04 0.669	1.91-04 0.711	7.39-04 0.756	1.12-03 0.803
7	1.97-07 0.501	1.50-06 0.521	1.15-05 0.544	9.73-05 0.570	3.63-04 0.600	7.57-04 0.634	2.00-04 0.672	3.17-04 0.712	5.95-04 0.754
8	3.66-08 0.481	4.64-07 0.500	3.24-06 0.521	2.62-05 0.545	1.68-04 0.573	4.80-04 0.603	7.02-04 0.637	3.63-05 0.673	3.21-04 0.710

* oscillator strength
 ** wavelength, microns

Table 11. Calculated oscillator strengths $f_{(v'v'')}$ for the $1^4H - 1^6H$ transition of UO^{+} .

v'/v''	0	1	2	3	4	5	6	7	8
0	*1.76-03 **0.508	2.05-03 0.530	9.07-04 0.554	2.58-04 0.581	8.70-05 0.612	4.05-05 0.647	1.99-05 0.686	7.62-06 0.728	1.40-06 0.772
1	1.96-03 0.494	1.38-05 0.515	7.37-04 0.537	1.03-03 0.563	6.01-04 0.592	3.25-04 0.625	1.91-04 0.661	1.04-04 0.700	3.47-05 0.740
2	1.28-03 0.481	9.93-04 0.500	5.28-04 0.521	2.05-05 0.545	4.44-04 0.573	5.41-04 0.604	4.74-04 0.638	3.78-04 0.674	2.13-04 0.711
3	5.53-04 0.469	1.43-03 0.487	2.79-04 0.507	7.35-04 0.530	1.61-04 0.556	4.62-05 0.585	3.05-04 0.616	5.30-04 0.650	5.55-04 0.684
4	8.78-05 0.457	7.57-04 0.474	1.55-03 0.493	1.40-06 0.515	4.47-04 0.539	4.53-04 0.566	2.94-05 0.596	1.05-04 0.627	4.66-04 0.659
5	2.50-06 0.445	1.64-04 0.462	1.08-03 0.480	1.30-03 0.500	1.29-04 0.523	9.53-05 0.548	4.58-04 0.576	1.45-04 0.605	3.19-05 0.635
6	2.14-06 0.434	5.79-06 0.449	2.52-04 0.466	1.49-03 0.486	7.34-04 0.507	3.35-04 0.531	2.90-06 0.557	2.97-04 0.585	2.15-04 0.612
7	2.44-06 0.423	4.71-06 0.438	1.08-05 0.454	4.30-04 0.472	1.76-03 0.492	1.95-04 0.515	3.43-04 0.539	8.36-05 0.565	1.76-04 0.591
8	5.53-07 0.413	6.57-06 0.427	5.82-06 0.442	2.49-05 0.459	7.82-04 0.479	1.58-03 0.500	5.26-07 0.523	1.99-04 0.547	1.52-04 0.571

* oscillator strength
** wavelength, microns

Table 12. Calculated oscillator strengths $f_{(v'v')}$ for the $1^4H - 3^4H$ transition of UO^+ .

v'/v''	0	1	2	3	4	5	6	7	8
0	*7.31-03 **0.462	1.02-02 0.480	4.04-03 0.499	8.66-04 0.521	2.13-04 0.546	7.59-05 0.574	2.62-05 0.604	5.68-06 0.637	1.27-07 0.669
1	7.62-03 0.448	1.48-04 0.464	5.03-03 0.482	5.90-03 0.503	2.45-03 0.526	8.82-04 0.552	3.55-04 0.580	1.11-04 0.610	1.06-05 0.640
2	5.20-03 0.433	2.67-03 0.448	3.10-03 0.465	7.42-04 0.484	4.57-03 0.506	3.50-03 0.530	1.74-03 0.556	7.48-04 0.583	1.66-04 0.610
3	2.78-03 0.419	4.57-03 0.433	3.28-04 0.449	4.62-03 0.466	1.28-04 0.486	2.27-03 0.508	3.87-03 0.532	2.69-03 0.557	1.06-03 0.582
4	1.27-03 0.405	3.74-03 0.419	3.48-03 0.433	1.22-04 0.450	3.61-03 0.468	1.36-03 0.489	7.00-04 0.511	3.84-03 0.533	3.40-03 0.556
5	4.39-04 0.393	2.12-03 0.405	4.20-03 0.419	2.30-03 0.434	1.07-03 0.452	1.69-03 0.471	2.18-03 0.491	1.86-04 0.512	4.06-03 0.533
6	9.12-05 0.381	7.71-04 0.393	2.79-03 0.406	4.54-03 0.420	1.17-03 0.436	2.04-03 0.454	4.20-04 .473	2.04-03 0.493	1.29-04 0.512
7	5.36-06 0.370	1.39-04 0.382	1.07-03 0.394	3.41-03 0.407	4.63-03 0.423	3.38-04 0.439	2.36-03 0.457	3.55-05 0.475	1.62-03 0.493
8	8.92-07 0.361	3.59-06 0.371	1.75-04 0.383	1.39-03 0.395	4.05-03 0.410	4.26-03 0.425	7.88-06 0.442	2.08-03 0.459	4.45-07 0.476

* oscillator strength
 ** wavelength, microns

Table 13. Calculated oscillator strengths $f_{(v'v'')}$ for the $14\text{H} - 34\text{I}$ transition of UO^{+} .

v'/v''	0	1	2	3	4	5	6	7	8
0	*7.55-07 **0.354	8.06-06 0.365	2.82-05 0.376	5.43-05 0.388	7.68-05 0.402	9.61-05 0.417	1.16-04 0.432	1.31-04 0.449	1.12-04 0.465
1	3.94-06 1.346	3.15-05 0.356	7.72-05 0.367	9.30-05 0.379	6.94-05 0.392	3.34-05 0.406	5.73-06 0.421	4.19-06 0.436	5.00-05 0.452
2	1.21-05 0.340	7.14-05 0.349	1.16-04 0.359	7.13-05 0.370	1.24-05 0.383	2.24-06 0.396	2.89-05 0.411	5.38-05 0.425	3.50-05 0.440
3	2.58-05 0.332	1.02-04 0.341	8.46-05 0.351	7.55-06 0.361	1.58-05 0.373	5.36-05 0.386	4.30-05 0.400	4.73-06 0.414	1.73-05 0.427
4	4.29-05 0.325	1.03-04 0.333	2.67-05 0.342	1.21-05 0.353	6.35-05 0.364	3.91-05 0.376	6.57-07 0.389	2.18-05 0.402	3.73-05 0.415
5	5.43-05 0.318	7.51-05 0.326	8.03-07 0.335	4.38-05 0.345	4.42-05 0.356	1.27-06 0.367	1.92-05 0.380	3.09-05 0.392	1.15-06 0.404
6	7.13-05 0.313	5.27-05 0.321	5.78-06 0.329	5.50-05 0.338	1.11-05 0.349	1.19-05 0.360	3.81-05 0.372	7.68-06 0.383	1.13-05 0.396
7	8.88-05 0.307	2.73-05 0.315	2.56-05 0.323	3.75-05 0.332	9.66-07 0.342	3.80-05 0.353	1.98-05 0.364	2.55-06 0.376	2.50-05 0.387
8	1.00-04 0.303	8.07-06 0.310	4.20-05 0.318	1.19-05 0.327	1.85-05 0.336	3.43-05 0.347	5.02-07 0.358	2.06-05 0.369	1.13-05 0.380

* oscillator strength
** wavelength, microns

Table 14. Energetics of dielectronic recombination.

$e + U^+$	$\epsilon \text{ (cm}^{-1}\text{)}$	U^*	$\epsilon \text{ (cm}^{-1}\text{)}$
$e + [5f_{5/2}^3 7s^2]$	0.	$[5f_{5/2}^3 7s 7p_{1/2} 7p_{3/2}]$	-0.
		$[5f_{5/2}^2 7s^2 7p_{3/2} 6d_{5/2}]$	116.
		$[5f_{5/2}^3 7s 7p_{3/2}^2]$	6154.
		$[5f_{5/2}^3 7s 6d_{3/2} n\ell]$	9589. - $E_{n\ell}$
		$[5f_{5/2}^3 7s 6d_{5/2} n\ell]$	14071. - $E_{n\ell}$
		$[5f_{5/2}^2 7s^2 6d_{3/2} n\ell]$	19924. - $E_{n\ell}$
$e + U^{++}$	$\epsilon \text{ (cm}^{-1}\text{)}$	$[U^+]^*$	$\epsilon \text{ (cm}^{-1}\text{)}$
$e + [5f_{5/2}^3 7s]$	0.	$[5f_{5/2}^2 7s 7p_{3/2}^2]$	2711.
		$[5f_{5/2}^3 6d_{3/2} n\ell]$	4117. - $E_{n\ell}$
		$[5f_{5/2}^3 6d_{5/2} n\ell]$	9345. - $E_{n\ell}$
		$[5f_{5/2}^2 7s 6d_{3/2} n\ell]$	24660. - $E_{n\ell}$
		$[5f_{5/2}^2 6d_{3/2}^2 n\ell]$	24722. - $E_{n\ell}$
$e + [5f_{5/2}^3 6d_{3/2}]$	4117.	$[5f_{5/2}^3 6d_{5/2} n\ell]$	5228. - $E_{n\ell}$
		$[5f_{5/2}^2 7s 6d_{3/2} n\ell]$	20543. - $E_{n\ell}$
		$[5f_{5/2}^2 6d_{3/2}^2 n\ell]$	20604. - $E_{n\ell}$

Table 15. $e + U^+$ dielectronic recombination rate (preliminary data).

T (K)	α (cm ³ /sec)	
	$5f^3 7s 7p^2$	$5f^2 7s^2 7p 6d$
300	5.9×10^{-11}	1.6×10^{-23}
1000	1.4×10^{-11}	2.4×10^{-15}
10000	5.1×10^{-13}	2.2×10^{-13}
20000	1.8×10^{-13}	3.4×10^{-13}

Table 16. Molecular correlation diagram for N + O₂.

Reactants	Energy (eV)	States	Point Group
N(⁴ S _u) + O ₂ (X ³ Σ _g ⁻)	1.401	2,4,6Σ ⁺ 2,4,6B ₁ 2,4,6A'	C _{∞v} C _{2v} C _s
N(⁴ S _u) + O ₂ (a ¹ Δ _g)	2.383	⁴ Δ ⁴ A ₂ , ⁴ B ₁ ⁴ A'', ⁴ A'	C _{∞v} C _{2v} C _s
N(⁴ S _u) + O ₂ (b ¹ Σ _g ⁺)	3.037	⁴ Σ ⁻ ⁴ A ₂ ⁴ A''	C _{∞v} C _{2v} C _s
N(² D _u) + O ₂ (X ³ Σ _g ⁻)	3.785	2,4Σ ⁺ , 2,4Π, 2,4Δ 2,4B ₁ (2), 2,4B ₂ , 2,4A ₂ , 2,4A ₁ , 2,4A'' (2), 2,4A' (3)	C _{∞v} C _{2v} C _s
N(² D _u) + O ₂ (a ¹ Δ _g)	4.766	2Σ ⁺ , 2Σ ⁻ , 2Π, 2Δ, 2Φ, 2Γ 2A ₁ (2), 2A ₂ (3), 2B ₁ (3), 2B ₂ (2), 2A' (5), 2A'' (5)	C _{∞v} C _{2v} C _s
N(² P _u) + O ₂ (X ³ Σ _g ⁻)	4.977	2,4Σ ⁻ , 2,4Π 2,4A ₁ , 2,4A ₂ , 2,4B ₂ 2,4A', 2,4A'' (2)	C _{∞v} C _{2v} C _s
N(² D _u) + O ₂ (b ¹ Σ _g ⁺)	5.420	2Σ ⁻ , 2Π, 2Δ 2A ₁ , 2A ₂ (2), 2B ₁ , 2B ₂ 2A' (2), 2A'' (3)	C _{∞v} C _{2v} C _s
N(⁴ S _u) + O ₂ (c ¹ Σ _u ⁻)	5.499	⁴ Σ ⁺ ⁴ A ₁ ⁴ A'	C _{∞v} C _{2v} C _s
N(⁴ S _u) + O ₂ (A' ³ Δ _u)	5.701	2,4,6Δ 2,4,6A ₁ , 2,4,6B ₂ 2,4,6A', 2,4,6A''	C _{∞v} C _{2v} C _s
N(⁴ S _u) + O ₂ (A ³ Σ _u ⁺)	5.789	2,4,6Σ ⁻ 2,4,6B ₂ 2,4,6A''	C _{∞v} C _{2v} C _s

Table 16. Molecular correlation diagram for N + O₂. (Concluded)

Reactants	Energy (eV)	States	Point Group
N(³ P _u) + O ₂ (a ¹ Δ _g)	5.958	² Π, ² Δ, ² Φ ² A ₁ (2), ² A ₂ , ² B ₁ , ² B ₂ (2) ² A' (3), ² A" (3)	C _{∞v} C _{2v} C _s
N(² P _u) + O ₂ (b ¹ Σ _g ⁺)	6.612	² Σ ⁺ , ² Π ² A ₁ , ² B ₁ , ² B ₂ ² A' (2), ² A"	C _{∞v} C _{2v} C _s
Products	Energy (eV)	States	Point Group
NO(² Π) + O(³ P _g)	0	^{2,4} Σ ⁺ , ^{2,4} Σ ⁻ , ^{2,4} Π, ^{2,4} Δ ^{2,4} A' (3), ^{2,4} A" (3)	C _{∞v} C _s
NO(² Π) + O(¹ D _g)	1.967	² Σ ⁺ , ² Σ ⁻ , ² Π(2), ² Δ, ² Φ ² A' (5), ² A" (5)	C _{∞v} C _s
NO(² Π) + O(¹ S _g)	4.189	² Π ² A', ² A"	C _{∞v} C _s
NO(a ⁴ Π) + O(³ P _g)	4.765	^{2,4,6} Σ ⁺ , ^{2,4,6} Σ ⁻ , ^{2,4,6} Π, ^{2,4,6} Δ ^{2,4,6} A' (3), ^{2,4,6} A" (3)	C _{∞v} C _s
NO(A ² Σ ⁺) + O(³ P _g)	5.450	^{2,4} Σ ⁻ , ^{2,4} Π ^{2,4} A', ^{2,4} A" (2)	C _{∞v} C _s
NO(B ² Π) + O(³ P _g)	5.693	^{2,4} Σ ⁺ , ^{2,4} Σ ⁻ , ^{2,4} Π, ^{2,4} Δ ^{2,4} A' (3), ^{2,4} A" (3)	C _{∞v} C _s
NO(b ⁴ Σ ⁻) + O(³ P _g)	6.0344	^{2,4,6} Σ ⁺ , ^{2,4,6} Π ^{2,4,6} A' (2), ^{2,4,6} A"	C _{∞v} C _s

Table 17. Adiabatic reaction surfaces arising from $N(^2P) + O_2$.

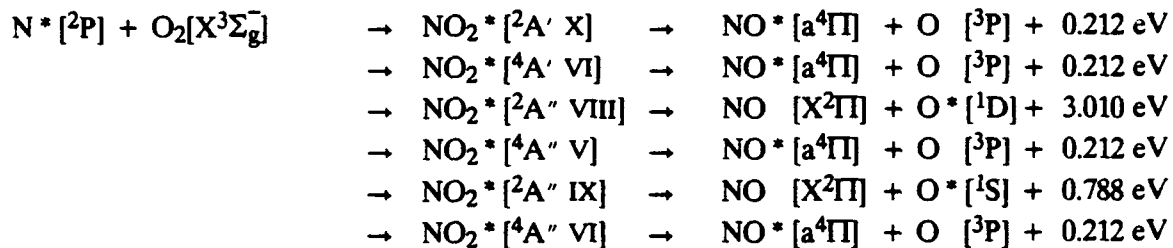


Table 18. Adiabatic reaction surfaces arising from $N(^2D) + O_2$.

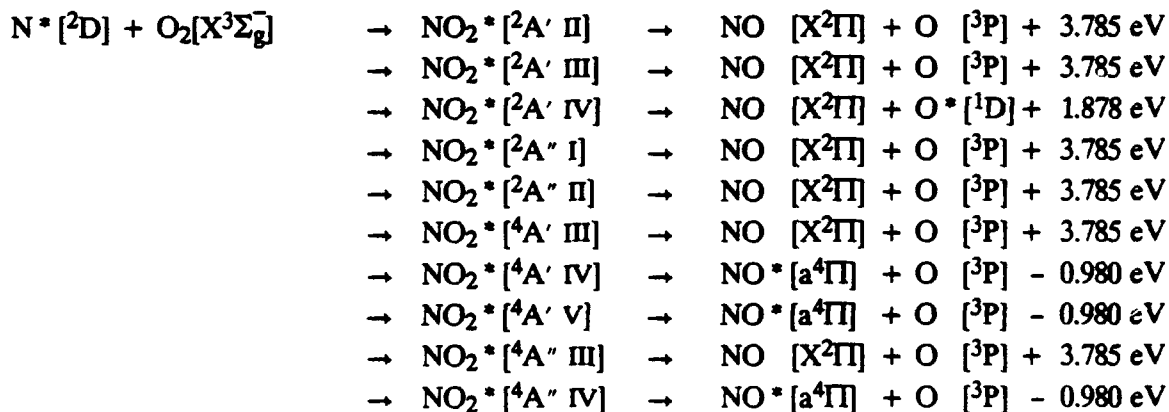


Table 19. Minimum energy long range interaction potentials for
N + O₂ in C_s symmetry.

$^2A'$	R = 4.0 bohrs ^a	R = 3.0 bohrs	Long Range Character
$^4S_u + X^3\Sigma_g^-$	-201.4657103	-201.4657669	a
$^2D_u + X^3\Sigma_g^-$	-201.3423547	-201.3428036	a
	-201.3423540	-201.342542	r
	-201.3423535	-201.3415228	r
$^2D_u + a^1\Delta_g$	-201.3045858	-201.3051402	a
	-201.3045827	-201.3048667	a
	-201.3045808	-201.3043220	r
	-201.3045790	-201.3041826	r
	-201.3045775	-201.3040453	r
$^2P_u + X^3\Sigma_g^-$	-201.2994959	-201.2988189	r
<hr/>			
$^2A''$			
$^2D_u + X^3\Sigma_g^-$	-201.3423546	-201.3427958	a
	-201.3423536	-201.3420978	r
$^2D_u + a^1\Delta_g$	-201.3045845	-201.3051136	a
	-201.3045830	-201.3048777	a
	-201.3045810	-201.3043588	r
	-201.3045790	-201.3041614	r
	-201.3045775	-201.3040561	a
$^2P_u + X^3\Sigma_g^-$	-201.2994986	-201.2999683	a
	-201.2994921	-201.2987603	r

^aR is measured from N to the center of the O₂ molecule, energy in hartrees.

SECTION 6
LIST OF REFERENCES

1. Harang, O., "AlO Resonant Spectrum for Upper Atmosphere Temperature Determination," AFCRL-66-314, Environmental Research Paper, No. 192, 1966.
2. Churchill, D. R. and R. E. Meyerott, "Spectral Absorption in Heated Air," Journal of Quantitative Spectroscopy and Radiative Transfer, 5, p. 69, 1965.
3. The Airglow and the Aurorae, edited by E. B. Armstrong and A. Dalgarno. Pergamon Press, New York, 1955.
4. Armstrong, B. H., R. R. Johnston and P. S. Kelly, "The Atomic Line Contribution to the Radiation Absorption Coefficient of Air," Journal of Quantitative Spectroscopy and Radiative Transfer, 5, p. 55, 1965.
5. Johnston, R. R., B. H. Armstrong and O. R. Platas, "The Photoionization Contribution to the Radiation Absorption Coefficient of Air," Journal of Quantitative Spectroscopy and Radiative Transfer, 5, p. 49, 1965.
6. Michels, H. H. and F. E. Harris, "Valence Configuration Interaction Calculations for Atomic Scattering," International Journal of Quantum Chemistry, IIS, p. 21, 1968.
7. Harris, F. E. and H. H. Michels, "Open-Shell Valence Configuration - Interaction Studies of Diatomic and Polyatomic Molecules," International Journal of Quantum Chemistry, IS, p. 329, 1967.
8. Michels, H. H., "Molecular Orbital Studies of the Ground and Low-Lying Excited States of the HeH⁺ Molecular Ion," Journal of Chemical Physics, 44, p. 3834, 1966.
9. Michels, H. H., "Ab Initio Calculation of the B²Σ⁺ - X²Σ⁺ Oscillator Strengths in AlO," Journal of Chemical Physics, 56, p. 665, 1971.
10. Michels, H. H., "Calculation of Electronic Wavefunctions," Final Report for AFOSR Contract F44620-74-C-0083, August 1975.
11. Michels, H. H., "Calculation of Potential Energy Curves for Metal Oxides and Halides," Final Report for AFOSR, Contract F44620-73-C-0077, May 1977.
12. Michels, H. H., "Theoretical Determination of Metal Oxide f-Numbers," Final Report for AFWL, Contract F29601-71-C-0119, Report AFWL-TR-74-239, May 1975.

13. Schaefer, F. E. and F. E. Harris, "*Ab Initio* Calculations of 62 Low-Lying States of the O₂ Molecule," Journal of Chemical Physics, **48**, p. 4946, 1968.
14. Michels, H. H. and F. E. Harris, "Predissociation Effects in the $A^2\Sigma^+$ State of the OH Radical," Chemical Physics Letters, **3**, p. 441, 1969.
15. Harris, F. E., "Open-Shell Orthogonal Molecular Orbital Theory," Journal of Chemical Physics, **46**, p. 2769, 1967.
16. Roothan, C.C. J. and P. S. Bagus, "Atomic Self-Consistent Field Calculations by the Expansion Method," Methods in Computational Physics, Edited by B. Alder, **2**, p. 47, 1963.
17. Givens, W., "Eigenvalue-Eigenvector Techniques," Oak Ridge Report Number ORNL 1574 (Physics).
18. Shavitt, I., C. F. Bender, A. Pipano and R. P. Hosteny, "The Iterative Calculation of Several of the Lowest or Highest Eigenvalues and Corresponding Eigenvectors of Very Large Symmetry Matrices," Journal of Computational Physics, **11**, p. 90, 1973.
19. Raffenetti, R. C., "A Simultaneous Coordinate Relaxation Algorithm for Large, Sparse Matrix Eigenvalue Problems," Journal of Computational Physics, **32**, p. 403, 1979.
20. Harris, F. E. and H. H. Michels, "The Evaluation of Molecular Integrals for Slater-Type Orbitals," Advances in Chemical Physics, **13**, p. 205, 1967.
21. Hehre, W. J., L. Radom, P. von R. Schleyer and J. A. Pople, "*Ab Initio* Molecular Orbital Theory," Wiley-Interscience, New York, 1986.
22. Dupuis, M., D. Spangler and J. J. Wendoloski, "GAMESS User's Guide," NRCC Software Catalog, Vol. 1, Program QG01, Lawrence Berkley Laboratory, 1980.
23. Davidson, E. R., "Natural Expansion of Exact Wavefunctions, III. The Helium Atom Ground State," Journal of Chemical Physics, **39**, p. 875, 1963.
24. Wahl, A. C., P. J. Bertoncini, G. Das And T. L. Gilbert, "Recent Progress Beyond the Hartree-Fock Method for Diatomic Molecules, The Method of Optimized Valence Configurations," International Journal of Quantum Chemistry, **15**, p. 123, 1967.
25. Ruedenberg, K., L. M. Cheung and S. T. Elbert, "MCSCF Optimization Through Combined Use of Natural Orbitals and the Brillouin - Levy - Berthier Theorem," International Journal of Quantum Chemistry, **16**, p. 1069, 1979.

26. Slater, J. C., Advances in Quantum Chemistry, 6, p. 1, 1972.
27. Löwdin, P. O., "Quantum Theory of Many-Particle Systems. I. Physical Interpretations by Means of Density Matrices, Natural Spin-Orbitals, and Convergence Problems in the Method of Configurational Interaction," Physical Review, 97, p. 1474, 1955.
28. Kohn, W. and L. Sham, "Self-Consistent Equations Including Exchange and Correlation Effects," Physical Review, 140A, p. 1133, 1965.
29. Slater, J. C., "A Simplification of the Hartree-Fock Method", Physical Review, 81, p. 385, 1951.
30. Schwarz, K., "Optimization of the Statistical Exchange Parameters α for the Free Atoms H Through Nb, " Physical Review, B5, p. 2466, 1972.
31. Beebe, N. H. F., "On the Transition State in the X_α Method," Chemical Physics Letters, 19, p. 290, 1973.
32. Schwarz, K. and J. W. D. Connolly, "Approximate Numerical Hartree-Fock Method for Molecular Calculations," Journal of Chemical Physics, 55, p. 4710, 1971.
33. Connolly, J. W. D.: unpublished results.
34. Slater, J. C., "Hellman-Feynman and Virial Theorems in the X_α Method," Journal of Chemical Physics, 57, p. 2389, 1972.
35. Michels, H. H., R. H. Hobbs and J. W. D. Connolly, "Optimized SCF- X_α Procedures for Heteropolar Molecules," Journal of Chemical Physics (to be published).
36. Rosch, Notker and Keith H. Johnson, "On the Use of Overlapping Spheres in the SCF- X_α Scattered-Wave Method," Chemical Physics Letters, 23, p. 149, 1973.
37. Dupuis, M., H. F. King, J. Rys and T. Takada, "HONDO Documentation. QCPE Software Catalog," Vol. 17, Indiana University, Department of Chemistry, 1985.
38. Amos, R. D. and J. E. Rice, "The Cambridge Analytic Derivatives Package Documentation, Issue 4.0," University Chemical Laboratory, Cambridge, England, 1988.
39. Dupuis, M., J. D. Watts, H. O. Villar and G. J. B. Hurst, "HONDO: Version 7.0 (1987) Documentation," IBM, Kingston, New York, 1988.

40. Lischka, H., R. Shepard, F. B. Brown and I. Shavitt, "New Implementation of the Graphical Unitary Group Approach for Multireference Direct Configuration Interaction Calculations," International Journal of Quantum Chemistry, Symposium #15, p. 91, 1981.
41. Ahlrichs, R., H. J. Böhm, C. Ehrhardt, P. Scharf, H. Schiffer, H. Lischka and M. Schindler, "Implementation of an Electronic Structure Program System on the Cyber 205," Journal of Computational Chemistry, 6, p. 200, 1985.
42. Shavitt, I., "Unitary Group Approach to Configuration Interaction Calculations of the Electronic Structure of Atoms and Molecules," Mathematical Frontiers in Computational Chemical Physics, Editor - D.G. Truhlar, Springer-Verlag, Berlin, 1988.
43. Pople, J. A. and R. K. Nesbet, "Self-Consistent Orbitals for Radicals," Journal of Chemical Physics, 22, p. 571, 1954.
44. Nesbet, R. K., "Approximate Methods in the Quantum Theory of Many-Fermion Systems," Reviews of Modern Physics, 33, p. 28, 1961.
45. Roothan, C. C. J. and P. S. Bagus, "Atomic Self-Consistent Field Calculations by the Expansion Method," Methods in Computational Physics, Edited by B. Alder, 2, p. 47, 1963.
46. Roothan, C. C. J., "New Developments in Molecular Orbital Theory," Reviews of Modern Physics, 23, p. 69, 1951.
47. Heitler, W., "The Quantum Theory of Radiation," 3rd Edition, Oxford University Press, 1953.
48. Nicholls, R. W. and A. L. Stewart, "Allowed Transitions," Atomic and Molecular Processes, D. R. Bates, Editor. Academic Press, 1962.
49. Penner, S. S., "Quantitative Molecular Spectroscopy and Gas Emissivities," Addison-Wesley Publishing Company, Inc., 1959.
50. Dennison, D. M., "The Rotation of Molecules," Physical Review, 28, p. 318, 1926.
51. Kronig, R. and I. Rabi, "The Symmetrical Top in the Undulatory Mechanics," Physical Review, 29, p. 262, 1927.
52. Rademacher, H. and F. Reiche, "Die Quantelung des symmetrischen Kreisel nach Schrödingers Undulationsmechanik," Zeitschrift für Physik, 41, p. 453, 1927.
53. Hönl, H. and F. London, "Intensities of Band Spectrum Lines," Zeitschrift für Physik, 33, p. 803, 1925.

54. Herzberg, G., "Spectra of Diatomic Molecules," 2nd Edition, Van Nostrand, 1950.
55. Fraser, P. A., "A Method of Determining the Electronic Transition Moment for Diatomic Molecules," Canadian Journal of Physics, 32, p. 515, 1954.
56. Breit, G., "The Effect of Retardation on the Interaction of Two Electrons," Physical Review, 34, p. 553, 1929; "The Fine Structure of He as a Test of the Spin Interactions of Two Electrons," 36, p. 383, 1930; "Dirac's Equation and the Spin-Spin Interactions of Two Electrons," 39, p. 616, 1932.
57. Bethe, H. A. and E. E. Salpeter, Quantum Mechanics of One- and Two-Electron Atoms. Academic Press, New York, 1957.
58. Hirschfelder, J. O., C. F. Curtiss and R. B. Bird, Molecular Theory of Gases and Liquids. John Wiley, New York, 1964.
59. Itoh, T., "Derivation of Nonrelativistic Hamiltonian for Electrons from Quantum Electrodynamics," Reviews of Modern Physics, 37, p. 159, 1965.
60. Kolos, W. and L. Wolniewicz, "Accurate Adiabatic Treatment of the Ground State of the Hydrogen Molecule," Journal of Chemical Physics, 41, p. 3663, 1964; "Accurate Computation of Vibronic Energies and Some Expectation Values for H₂, D₂, and T₂," 41, p. 3674, 1964; "Potential-Energy Curve for the $B^1\Sigma_u^+$ State of the Hydrogen Molecule," 45, p. 509, 1966.
61. Liberman, D., J. T. Waber, D. T. Cromer, "Self-Consistent Field Dirac-Slater Wave Functions for Atoms and Ions. I. Comparison with Previous Calculations," Physical Review, A137, p. 27, 1965.
62. Mann, J. B. and J. T. Waber, "SCF Relativistic Hartree-Fock Calculations on the Superheavy Elements 118-131," Journal of Chemical Physics, 53, p. 2397, 1970.
63. Grant, I. P., "Relativistic Calculation of Atomic Structures," Advances in Physics, 19, p. 747, 1970.
64. Cowan, R. D., "Atomic Self-Consistent-Field Calculations Using Statistical Approximations for Exchange and Correlation," Physical Review, 163, p. 54, 1967.
65. Desclaux, J. P., D. F. Mayers, and F. O'Brien, "Relativistic Atomic Wave Functions," Journal of Physics B, 4, p. 631, 1971.

66. Cowan, R. D. and D. C. Griffin, "Approximate Relativistic Corrections to Atomic Radial Wave Functions," Journal of the Optical Society of America, **66**, p. 1010, 1976.
67. Wood, J. H. and A. M. Boring, "Improved Pauli Hamiltonian for Local-Potential Problems," Physical Review B, **18**, p. 2701, 1978.
68. Boring, A. M. and J. H. Wood, "Relativistic Calculations of the Electronic Structure of UF_6 ," Journal of Chemical Physics, **71**, p. 32, 1979.
69. Wood, J. H., A. M. Boring and S. B. Woodruff, "Relativistic Electronic Structure of UO_2^{++} , UO_2^+ , UO_2 ," Journal of Chemical Physics, **74**, p. 5225, 1981.
70. Michels, H. H., R. H. Hobbs and J. W. D. Connolly, "Electronic Structure and Photoabsorption of the Hg_2^+ Dimer Ion," Chemical Physics Letters, **68**, p. 549, 1979.
71. Weeks, J. D., A. Hazi and S. A. Rice, Advances in Chemical Physics, **16**, p. 283, 1969.
72. Bardsley, J. N., Case Studies in Atomic Physics, **4**, p. 299, 1974.
73. Phillips, J. C. and L. Kleinman, "New Method for Calculating Wave Functions in Crystals and Molecules," Physical Review, **116**, p. 287, 1959.
74. Hazi, A. U. and S. A. Rice, "Pseudopotential Theory of Atomic and Molecular Rydberg States," Journal of Chemical Physics, **45**, p. 3004, 1966.
75. Tully, J. C., "Many-Electron Pseudopotential Formalism for Atomic and Molecular Excited-State Calculations," Physical Review, **181**, p. 7, 1969.
76. Melius, C. F., B. D. Olafson and W. A. Goddard III, "Fe and Ni *Ab Initio* Effective Potentials for Use in Molecular Calculations," Chemical Physics Letters, **28**, p. 457, 1974.
77. Szasz, L. and G. McGinn, "Atomic and Molecular Calculations with the Pseudopotential Method. II. Exact Pseudopotentials for Li, Na, K, Rb, Be^+ , Mg^+ , Ca^+ , Al^{++} , Cu and Zn^+ ," Journal of Chemical Physics, **47**, p. 3495, 1967; "Atomic and Molecular Calculations with the Pseudopotential Method III: The Theory of Li_2 , Na_2 , K_2 , LiH, NaH and KH; Pseudopotential Theory of Atoms and Molecules. II. Hylleraas-Type Correlated Pair Functions for Atoms with Two Valence Electrons," **56**, p. 1019, 1972.
78. Kahn, L. R., P. Baybutt and D. G. Truhlar, "*Ab Initio* Effective Core Potentials: Reduction of All-Electron Molecular Structure Calculations to Calculations Involving Only Valence Electrons," Journal of Chemical Physics, **65**, p. 3826, 1976.

79. Lee, Y. S., W. C. Ermler and K. S. Pitzer, "Ab Initio Effective Core Potentials Including Relativistic Effects. I. Formalism and Applications to the Xe and Au Atoms," Journal of Chemical Physics, 67, p. 5861, 1977.
80. Courant, R. and D. Hilbert, Methods of Mathematical Physics, Interscience, New York, 1961.
81. Froese-Fischer, C., Comp. Phys. Comm. 1, p. 151, 1969.
82. Kahn, L. R., P. J. Hay and R. D. Cowan, "Relativistic Effects in Ab Initio Effective Core Potentials for Molecular Calculations. Applications to the Uranium Atom," Journal of Chemical Physics, 68, p. 2386, 1978.
83. Desclaux, J. P., Atomic Data and Nuclear Tables, 12, p. 311, 1973.
84. Krauss, M. O., private communication.
85. Michels, H. H. and R. H. Hobbs, "Theoretical Study of the Radiative and Kinetic Properties of Selected Metal Oxides and Air Molecules," Final Report for DNA Contract DNA001-82-C-0015, DNA-TR-82-159, July 1983.
86. Michels, H. H. and R. H. Hobbs, "Theoretical Study of the Radiative and Kinetic Properties of Selected Metal Oxides and Air Molecules," Final Report for DNA Contract DNA001-83-C-0044, DNA-TR-85-156, May 1985.
87. Michels, H. H., "Theoretical Study of the Radiative and Kinetic Properties of Selected Metal Oxides and Air Molecules," Final Report for DNA Contract DNA001-85-C-0120, DNA-TR-88-12, March 1988.
88. Hulburt, H. M. and J. O. Hirschfelder, "Potential Energy Functions for Diatomic Molecules," Journal of Chemical Physics, 9, p. 61, 1941.
89. Krauss, M. O. and W. S. Stevens, "The Electronic Structure and Spectra of UO^+ ," Chemical Physics Letters, 99, p. 417, 1983.
90. Heaven, M. C., J. Nicolai, S. J. Riley and E. K. Parks, "Rotationally Resolved Electronic Spectra for Uranium Monoxide," Chemical Physics Letters, 119, p. 229, 1985.
91. Kaledin, L. A., A. N. Kulikov, A. I. Kobylanskii, E. A. Shenyavskaya and L. V. Gurvich, "Relative Position of a Group of Low-Lying States for the UO Molecule," Zhurnal Fizicheskoi Khimii, 61, N5, p. 1374, 1987.

92. Dulick, M., private communication.
93. McGlynn, S. P. and J. K. Smith, "Electronic Structure, Spectra, and Magnetic Properties of Actinyl Ions. II. Neptunyl and the Ground States of Other Actinyls," Journal of Molecular Spectroscopy, **6**, p. 188, 1961.
94. Hay, private communication.
95. Badger, R. M., "The Relation Between the Internuclear Distances and the Force Constants of Molecules of its Application to Polyatomic Molecules," Journal of Chemical Physics, **3**, p. 710, 1935.
96. Allen, G. C., E. J. Baerends, P. Vernooijs, J. M. Dyke, A. M. Ellis, M. Feher and A. Morris, "High Temperature Photoelectron Spectroscopy: A Study of U, UO and UO₂," Journal of Chemical Physics, **89**, p. 5363, 1988.
97. Heaven, M. C., J. Nicolai, S. J. Riley and E. K. Parks, "Rotationally Resolved Electronic Spectra for Uranium Monoxide," Chemical Physics Letters, **119**, p. 229, 1985.
98. Kaledin, L. A., A. N. Kulikov, A. I. Kobylanskii, E. A. Shenyavskaya and L. V. Gurvich, "The Relative Positions of the Low-Lying States of the Uranium Monoxide (UO) Molecule," Russian Journal of Physical Chemistry, **61**, p. 712, 1987 - translated from Zhurnal Fizicheskoi Khimii, **61**, p. 1374, 1987.
99. Piper, L. G., M. E. Donahue and W. T. Rawlins, "Rate Coefficients for N(²D) Reactions," Journal of Physical Chemistry, **91**, p. 3883, 1987.
100. Piper, L.G., "The Rate Coefficient for Quenching N(²D) by O(³P)," Journal of Chemical Physics, **91**, p. 3516, 1989.
101. Donovan, R. J. and D. Husain, "Recent Advances in the Chemistry of Electronically Excited Atoms," Chemical Reviews, **70**, p. 489, 1970.
102. Schofield, K., "Critically Evaluated Rate Constants for Gaseous Reactions of Several Electronically Excited Species," Journal of Physical Chemical Reference Data, **8**, p. 723, 1979.
103. Gilmore, F., "Recommended Revision of the NORSE Calculation of NO Chemiluminescence from N(²P) + O₂," RDA Technical Note, November 1986.
104. Dupuis, M., D. Spangler and J. J. Wendoloski, GAMESS User's Guide, Lawrence Berkeley Laboratory, 1980.

105. Dulick, M., Ph.D. Thesis, Massachusetts Institute of Technology, 1982.
106. Michels, H. H., private communication.
107. Dulick, M., E. Murad and R. F. Barrow, "Thermochemical Properties of the Rare Earth Monoxides," Journal of Chemical Physics, 85, p. 385, 1986.
108. Gilmore, F., "Recommended Revision of the NORSE Calculation of NO Chemiluminescence from $N(^2P) + O_2$," RDA Technical Note dated November 17, 1986.
109. Michels, H. H., "Theoretical Research Investigation for Air Molecular Calculations," Final Report for AFGL Contract F19628-80-C-0209, AFGL-TR-81-0151, April 1981.

DISTRIBUTION LIST

DNA-TR-91-189

DEPARTMENT OF DEFENSE

ASSISTANT TO THE SECRETARY OF DEFENSE
ATTN: EXECUTIVE ASSISTANT

DEFENSE NUCLEAR AGENCY
ATTN: PRPD R YOHO
ATTN: RAAE K SCHWARTZ
ATTN: RAAE B PRASAD
ATTN: RAAE D RIGGIN
ATTN: RAAE L WITTWER
ATTN: RAAE S BERGGREN
ATTN: RAAE J MEYERS
2 CYS ATTN: TITL

DEFENSE TECHNICAL INFORMATION CENTER
2 CYS ATTN: DTIC/FDAB

FIELD COMMAND DEFENSE NUCLEAR AGENCY
ATTN: FCTT
2 CYS ATTN: W SUMMA

STRATEGIC AND THEATER NUCLEAR FORCES
ATTN: DR E SEVIN

THE JOINT STAFF
ATTN: JKCS

DEPARTMENT OF THE ARMY

U S ARMY RESEARCH OFFICE
ATTN: R MACE

DEPARTMENT OF THE NAVY

NAVAL RESEARCH LABORATORY
ATTN: CODE 2627
ATTN: CODE 4104 H HECKATHORN

DEPARTMENT OF THE AIR FORCE

AIR FORCE OFFICE OF SCIENTIFIC RSCH
ATTN: AFOSR/NC
ATTN: AFOSR/NP

AIR FORCE PHILLIPS LABORATORY
ATTN: OP A GIANETTI
ATTN: OP D PAULSEN
ATTN: OP W BLUMBERG

DEPARTMENT OF ENERGY

LAWRENCE LIVERMORE NATIONAL LAB
ATTN: L-84 A GROSSMAN
ATTN: L-84 G SIMONSON

LOS ALAMOS NATIONAL LABORATORY
ATTN: REPORT LIBRARY

SANDIA NATIONAL LABORATORIES
ATTN: DIV 9014 R BACKSTROM
ATTN: ORG 9110 W D BROWN
ATTN: TECH LIB 3141
ATTN: 2000 G T CHENEY

OTHER GOVERNMENT

CENTRAL INTELLIGENCE AGENCY
ATTN: OSWR/NED
ATTN: OSWR/SSD FOR L BERG

DEPARTMENT OF DEFENSE CONTRACTORS

BERKELEY RSCH ASSOCIATES, INC
ATTN: J WORKMAN
ATTN: S BRECHT

GENERAL RESEARCH CORP INC
ATTN: J EOLL

INSTITUTE FOR DEFENSE ANALYSES
ATTN: E BAUER

KAMAN SCIENCES CORP
ATTN: DASAC
ATTN: E CONRAD
ATTN: G DITTBERNER

KAMAN SCIENCES CORPORATION
ATTN: B GAMBILL
5 CYS ATTN: DASAC
ATTN: R RUTHERFORD

MISSION RESEARCH CORP
ATTN: W WHITE

MISSION RESEARCH CORP
2 CYS ATTN: TECH LIBRARY

PACIFIC-SIERRA RESEARCH CORP
ATTN: H BRODE

PHOTOMETRICS, INC
ATTN: I L KOFSKY

PHOTON RESEARCH ASSOCIATES
ATTN: D BURWELL

SCIENCE APPLICATIONS INTL CORP
ATTN: D SACHS

SRI INTERNATIONAL
ATTN: W CHESNUT

TELEDYNE BROWN ENGINEERING
ATTN: P SHELTON
ATTN: N PASSINO

UNITED TECHNOLOGIES RESEARCH CTR
4 CYS ATTN: H MICHELS

VISIDYNE, INC
ATTN: J CARPENTER
ATTN: J DEVORE
ATTN: J JORDANO